Table of Contents

1. Abbreviations

2-ATA
2-aminoterphtallic acid

BDTCA
2-(3-methylbutoxy)-2H-1,3-benzodithiole-5-carboxylic acid

BDTCA-Bn
benzyl 2-(3-methylbutoxy)-2H-1,3-benzodithiole-5-carboxylate

BDTCA-EtOH
2-hydroxyethyl 2-(3-methylbutoxy)-2H-1,3-benzodithiole-5-carboxylate

BDTCA-Me
methyl 2-methoxy-2H-1,3-benzodithiole-5-carboxylate

DClSB
1,2-dichlorosulfonylbenzene

DClSBA
3,4-bis(chlorsulfonyl)benzoic acid

DClSBA-Bn
benzyl 3,4-bis(chlorsulfonyl)benzoate

DClSBA-EtOH
2-hydroxyetyl 3,4-bis(chlorsulfonyl)benzoate

DClSBA-Me
methyl 3,4-bis(chlorsulfonyl)benzoate

DMT
dimethyl terphthalate

DSI
benzene-1,2-disulfonimide

DSI-PABA-Bn
4-[2-benzyloxycarbonyl]-N-(p-[2-benzyloxycarbonyl]phenyl)benzene-1,2-disulfonimide

DSI-PABA-EtOH
4-[2-hydroxyethoxycarbonyl]-N-(p-[4-hydroxyethoxycarbonyl]phenyl)benzene-1,2-disulfonimide

DSI-PABA-Me
4-[2-methoxycarbonyl]-N-(p-[2-methoxycarbonyl]phenyl)benzene-1,2-disulfonimide

PABA
p-aminobenzoic acid

PABA-Bn
benzyl p-aminobenzoate

PABA-EtOH
2-hydroxyetyl p-aminobenzoate

PABA-Me
methyl p-aminobenzoate

PET
polyethylene terphthalate

Poly(DSI - TPA)
poly(4-[2-ethoxycarbonyl]-N-(p-{4-ethoxycarbonyl}phenyl)benzene-1,2-disulfonimide benzene-1,4-dicarboxylate)

PI-TPA
poly(4-[2-ethoxycarbonyl]-N-(p-{4-ethoxycarbonyl}phenyl)phthalimide benzene-1,4-dicarboxylate)

TPA
terphthaloyl chloride

2. Computational Section

2.1 Quantum Mechanics

Density functional theory (DFT) calculations were performed using the ORCA 6.0 software package [20]. Initial geometries of DSI-PABA-Me and DSI-PABA-EtOH were pre-optimised with the MMFF94 force field [21]. These structures were subsequently refined by full geometry optimisation using the B3LYP functional with the def2-SVP basis set. The optimised conformers were analysed to evaluate key structural features (Table S5, Table S7).

For DSI-PABA-Me, vibrational frequency calculations were carried out at the same level of theory at 293 K to obtain animated vibrational modes and simulated FTIR spectra (Figure S9b). Band broadening was applied to the calculated spectra, and vibrational assignments were made by correlating the animated normal modes with the corresponding FTIR absorptions.

2.2 Molecular Dynamics

Molecular dynamics (MD) simulations of poly(DSI-TPA), the homologous polyimide (PI-TPA), and poly(ethylene terephthalate) (PET) were performed using OpenMM [22] with the OPLS-AA force field [43] parameters and 1.14 × CM1A atomic charges. All force-field parameters were assigned via LigParGen [24]. Parameters for the ethylene linkage were derived from model dimers.
The suitability of the OPLS-AA parameters was verified by comparing vibrational modes of DSI-PABA-Me calculated using DFT (B3LYP level of theory, 293 K) with those obtained from the MD Hessian. The DFT spectrum correlated well with the experimental IR data; the average deviation between DFT and MD frequencies was 43 cm^{-1}, while the key DSI vibrational modes were represented adequately by the MD calculations.
A poly(DSI-TPA) chain with a polymerisation degree of 12 was built from the DSI-PABA-Me and dimethyl terephthalate monomer geometries optimized at the B3LYP level by linking through terminal methyl groups. The geometry of the linking bond was optimized using the DSI-TPA dimer. In constructing the polymer, all possible orientations of the DSI fragment were considered with equal probability, resulting in a random-copolymer configuration. The PI-TPA (degree of polymerisation = 12) and PET (degree of polymerisation = 34, to achieve similar chain length) models were prepared in an analogous way from their respective monomers.
Sample preparation for T_g estimation followed an adapted procedure from Refs. [25, 26]. Each single polymer chain was first modeled for 10 ns at 600 K under constant volume to obtain a folded conformation (Figure S1a). A cubic box (20 × 20 × 20 nm^3) containing 28 folded chains was then packed using Packmol [27] (Figure S1a).

Each polymer sample was equilibrated through the following steps:

1. Compression at 600 K with pressure increasing from 50 to 300 bar in 50 bar increments, simulated for 2 ns per step (12 ns total per polymer).

2. Relaxation at 150 bar for 5 ns, followed by 1 bar for 5 ns (10 ns total per polymer).

3. Annealing at 1 bar, with three cooling/heating cycles between 600 and 300 K (step = 50 K; 2 ns per step, 36 ns total per polymer).

4. High-temperature equilibration at 600 K for 700 ns.

Three statistically independent configurations were extracted from the equilibrated trajectory at 500, 600, and 700 ns. Each configuration was cooled from 600 K to 290 K at 1 bar in 10 K steps, simulating 4 ns at each temperature. Density values were recorded at the end of each step. The glass-transition temperatures were determined from the density-temperature curves by fitting linear regressions in the 290–330 K and 540–580 K for PET and in the 290–340 K and 540–590 K ranges for poly(DSI-TPA) and PI-TPA and identifying their intersection (Figure S1b). The densities of the three samples per polymer were averaged to obtain final temperature-density curves for T_g calculation (Figure S1b).

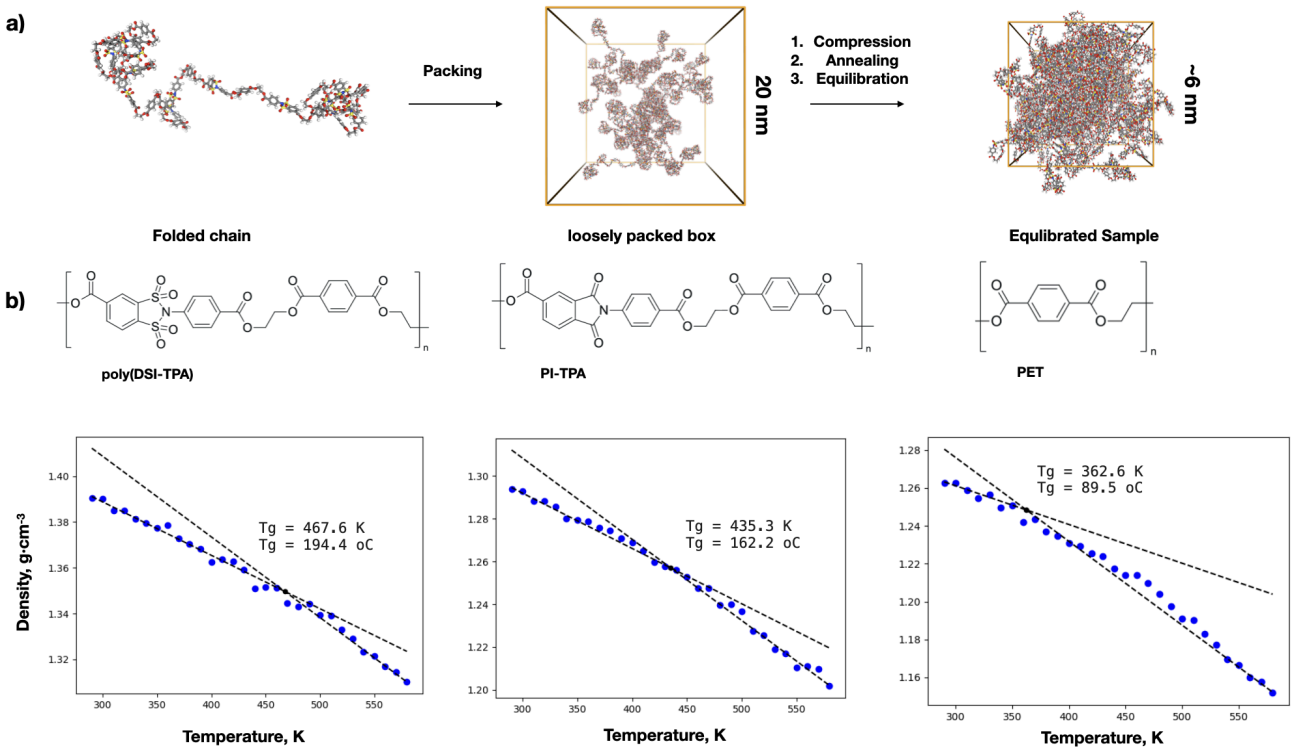

Figure S1.1 (a) Schematic representation of the preparation and equilibration of polymer samples, shown for on the example of poly(DSI-TPA); (b) averaged temperature-density curve plots for poly(DSI-TPA), PI-TPA and PET with the fitted linear regressions and marked glass transition temperatures.

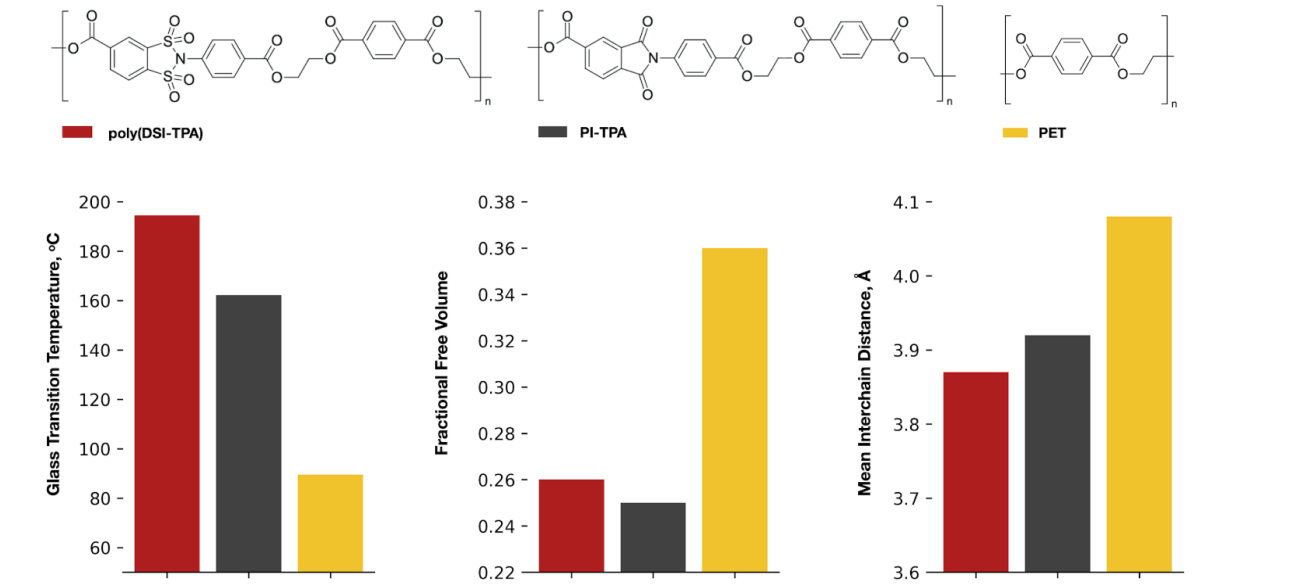

Figure S1.2 Comparison of the glass-transition temperature (°C), fractional free volume (290 K), and mean interchain distance (290 K, Å) of poly(DSI-TPA), PI-TPA and PET samples, obtained from molecular dynamics simulations.

The FFV was calculated using equilibrated configurations at 290 K and 1 bar. For each polymer, three 1.5 nm cubic sub-boxes centered within the simulation cell were extracted. The van der Waals volume of atoms within the sub-box of each sample was computed and averaged. FFV was then obtained as:

$$FFV = \frac{V_{box} - V_{vdW}}{V_{box}}$$

Where, V_{box} - volume of the bounding box (15 × 15 × 15 Å) $Å^3$, V_{vdW} - total van der Waals volume of the atoms inside the bounding box $Å^3$.

The average interchain distance in the amorphous polymer samples was estimated from the atomic coordinates of configurations equilibrated at 290 K. For every heavy atom, the shortest distance to any atom belonging to another chain was determined within a 10 Å cutoff. The resulting set of nearest-neighbour distances was averaged over all atoms to obtain the mean interchain distance per sample, which were then averaged over 3 samples within each polymer subset.

3. Experimental Section

3.1 Materials and Methods

3.1.1 Reagents

All reagents were obtained from Sigma-Aldrich or Thermo Fisher Scientific and were of reagent grade, unless stated otherwise.

3.1.2 NMR

The NMR spectra were recorded on Bruker Avance III 400 and Bruker Avance III 600 NMR spectrometers (AV400 and AV600 correspondingly). Spectra were analysed using Topspin (v4.4.1).

3.1.3 FTIR

Infrared spectra were recorded on a Thermo Scientific Nicolet is5 with an ATR attachment FTIR spectrometer in the range 500 - 4000 cm^{-1}.

3.1.4 Single-crystal X-ray Diffraction

SXD measurements were made using an Agilent Oxford Diffraction SuperNova equipped with a microfocus Cu Kα X-ray source and a Rigaku Arc100 hybrid pixel detector. A single crystal was selected under a polarising microscope and mounted onto a nylon loop with the aid of Fomblin® oil before mounting on the diffractometer (Figure S3, Figure S6). Total collection time was around 7 hr 30 min for a full sphere of data to a resolution of 0.84 Å. Data were collected using 0.5° scan frames in ω and reduced using the CrysAlis^{Pro} software package (version 1.171.43.144a from Rigaku Oxford Diffraction). The structures were solved using intrinsic phasing by ShelXT and refined by least-squares using ShelXL 2014 within the Olex2 program suite. The position and anisotropic displacement factors were refined freely for the non-hydrogen atoms. Molecular and crystal structures (Figures S4, Figure S7 and Figure S8) are illustrated with the program Mercury from CCDC with thermal ellipsoids (excluding H atoms) shown at 50% probability.

3.1.5 Elemental Analysis

Elemental (C,H,N,S) analysis was provided by the Elemental analysis service at London Metropolitan University. Samples were weighed using Mettler Toledo high precision scale and analysed using ThermoFlash 2000.

3.2 Synthetic Procedures and Characterisation

3.2.1 BDTCA

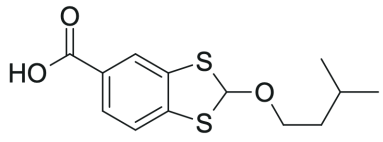

3-Methylbutyl nitrite (6.55 mmol, 0.881 ml), 3-methylbutan-1-ol (5.50 mmol, 0.5945 ml), and carbon disulfide (CS_2; 166.6 mmol, 10 ml) were dissolved in 1,2-dichloroethane (200 ml) and heated to reflux (82 °C). A solution of 2-aminoterephthalic acid (2-ATA; 5.50 mmol, 1.00 g) in tetrahydrofuran (THF, 100 ml) was added dropwise to the refluxing mixture over 30 minutes. After completion of the addition, the reaction was stirred at reflux for an additional 4 hours.

The solvents were removed under reduced pressure using a rotary evaporator, and the resulting residue was triturated with hexane (75–120 ml) to yield a yellow amorphous powder. The solid was dried under vacuum at room temperature for 72 hours to afford 1.44 g of 2-(3-methylbutoxy)-2H-1,3-benzodithiole-5-carboxylic acid (BDTCA, 1.44 g, ~98% purity by NMR, 5.00 mmol), corresponding to an isolated yield of 90.9%.

^{1}H NMR (600 MHz, [D_6]DMSO, ppm): δ =13.15 (s, 1H), 7.99 (d, J=1.2 Hz, 1H), 7.70 (dd, J=1.4, 8.2 Hz, 1H), 7.60 (d, J=8.2 Hz, 1H), 7.12 (s, 1H), 3.41 (t, J=6.3 Hz, 2H), 1.60–1.52 (m, 1H), 1.36–1.31 (m, 2H), 0.81 (d, J=6.7 Hz, 6H); ^{13}C NMR (151 MHz, [D_6]DMSO, ppm): δ =167.0 (s), 142.1 (s), 137.2 (s), 128.8 (s), 127.1 (s), 123.0 (s), 122.4 (s), 90.7 (s), 63.6 (s), 37.6 (s), 24.9 (s), 22.7 (s).

3.2.2 BDTCA-Me

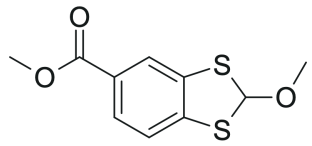

BDTCA (1.40 g, ~98% purity by NMR, 4.92 mmol) was dissolved in methanol (150 ml), and sulfuric acid (10–15 drops, approx. 0.03–0.05 ml) was added. The reaction mixture was refluxed for 8 hours, then cooled to room temperature and divided into two equal portions.

Each portion was poured into ethyl acetate (200 ml), washed sequentially with water (1 × 200 ml, then 2 × 100 ml), 0.1 M aqueous Na_2CO_3 (100 mL), and finally with water (100 mL). The organic phase (top layer) was separated, dried over anhydrous $MgSO_4$, filtered, and concentrated under reduced pressure. The resulting residue was dried under vacuum at room temperature for 48 hours to afford methyl 2-methoxy-2H-1,3-benzodithiole-5-carboxylate (BDTCA-Me) as a clear orange-brown oil (0.45 g, ~98% purity by NMR, 1.82 mmol). The isolated yields were 37.0% based on BDTCA and 33.1% based on 2-ATA.

^{1}H NMR (400 MHz, [D_6]DMSO, ppm): δ =8.03 (d, J=1.5 Hz, 1H), 7.72 (q, J=3.3 Hz, 1H), 7.64 (d, J=8.2 Hz, 1H), 7.15 (s, 1H), 3.84 (s, 3H), 3.15 (s, 3H); ^{13}C NMR (151 MHz, [D_6]DMSO, ppm): δ =166.0 (s), 142.6 (s), 137.4 (s), 127.6 (s), 126.9 (s), 122.9 (s), 122.6 (s), 91.8 (s), 53.0 (s), 52.7 (s).

Reaction Monitoring via NMR

Aliquots were taken from the reaction mixture every 4 hours, concentrated under reduced pressure using a rotary evaporator, dissolved in DMSO-d_6, and analyzed by ^{1}H NMR spectroscopy to monitor reaction progress. Key signals corresponding to the methyl groups of the ether (H-10) and ester (H-8) functionalities, as well as the carboxylic acid proton, were tracked. The integral values were normalized relative to the H-10 signal.

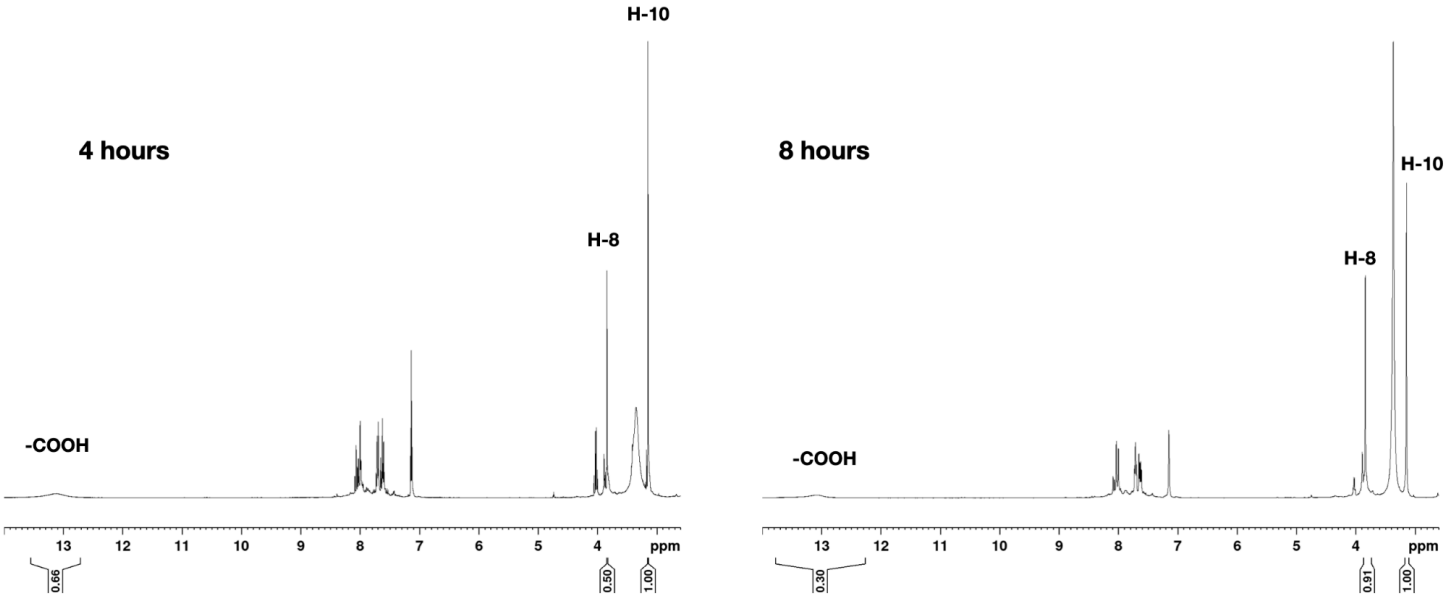

Figure S2. NMR spectra after 4 and 8 hours of the reaction (DMSO-d_6, 600 MHz).

Table S1. Relative areas of the selected peaks on the ^{1}H NMR spectrum after 4 and 8 hours of the reaction.

Time, h	H-10 (3.13 ppm, ether)	H-8 (3.83 ppm, ester)	-COOH Proton 13.15 ppm
4	1.00	0.50	0.66
8	1.00	0.91	0.30

The observed increase in the H-15 methyl signal and concurrent decrease in the carboxylic acid proton signal indicate progressive esterification over the monitored time interval. Notably, the consistently higher integral values for H-10 at earlier time points suggest that substitution at the intersulfur carbon proceeds more rapidly than ester formation.

DMT Polymorph Crystal Structure

Previously the crystal structure of dimethylterephthallate was reported as orthorhombic (refcode DMTPAL in the Cambridge Crystallographic Database [28]), while this new form is triclinic with two distinct crystallographic molecules within the unit cell.

Table S2a. Crystal data and structure refinement for dimethyl terephthalate at 150 K.

Identification code	exp_858
Empirical formula	$C_{10}H_{10}O_{40}$
Formula weight	194.18
Temperature / K	150
Crystal system	triclinic
Space group	$P\bar{1}$
a / Å	3.84270(10)
b / Å	10.7309(4)
c / Å	11.2638(5)
α / °	77.306(4)
β / °	84.190(3)
γ / °	89.289(3)
Volume / Å^3	450.77(3)
Z	2
ρ_{calc} / g cm^{-3}	1.431
μ / mm^{-1}	0.941
F(000)	204.0
Crystal size / mm^3	0.281 × 0.091 × 0.019
Radiation	Cu Kα (λ = 1.54184 Å)
2θ range for data collection / °	8.088 to 156.802
Index ranges	$-4 \le h \le 4$, $-13 \le k \le 13$, $-14 \le l \le 14$
Reflections collected	9019
Independent reflections	1876 [R_{int} = 0.0530, R_{sigma} = 0.0428]
Data/restraints/parameters	1876/0/163
Goodness-of-fit on F^2	1.029
Final *R* indexes [$I \ge 2\sigma(I)$]	R_1 = 0.0421, wR_2 = 0.1131
Final *R* indexes [all data]	R_1 = 0.0537, wR_2 = 0.1215
Largest diff. peak/hole / e Å^{-3}	0.23/−0.21

Table S2b. Fractional atomic coordinates and equivalent isotropic displacement parameters for dimethyl terephthalate at 150 K. U_{eq} is defined as ⅓ of the trace of the orthogonalised U_{ij} tensor.

Atom	***x***	***y***	***z***	***U*(eq) / Å²**
O(1A)	0.9068(3)	0.72828(9)	0.36416(9)	0.0344(3)
O(2A)	0.6513(3)	0.67134(10)	0.55659(10)	0.0434(3)
C(1A)	0.8974(4)	1.03743(13)	0.60848(13)	0.0272(3)
C(2A)	0.8109(4)	0.91612(13)	0.59637(13)	0.0277(3)
C(3A)	0.9131(4)	0.87853(12)	0.48747(12)	0.0263(3)
C(4A)	0.8086(4)	0.74858(13)	0.47585(13)	0.0288(3)
C(5A)	0.8085(5)	0.60584(15)	0.34258(17)	0.0387(4)
O(1B)	0.2253(3)	0.74728(9)	0.86302(9)	0.0349(3)
O(2B)	0.3377(3)	0.65382(10)	1.05344(10)	0.0413(3)
C(1B)	0.4541(4)	1.10687(13)	0.90772(13)	0.0279(3)
C(2B)	0.3697(4)	0.98648(13)	0.89279(13)	0.0269(3)
C(3B)	0.4142(3)	0.87933(12)	0.98532(12)	0.0254(3)
C(4B)	0.3232(4)	0.74808(13)	0.97320(13)	0.0283(3)
C(5B)	0.1289(5)	0.62358(15)	0.84321(17)	0.0382(4)
H(1A)	0.829(4)	1.0637(15)	0.6837(15)	0.030(4)
H(2A)	0.671(4)	0.8583(15)	0.6627(14)	0.030(4)
H(5AA)	0.890(6)	0.6097(19)	0.2590(20)	0.058(3)
H(5AB)	0.920(6)	0.5380(20)	0.3953(18)	0.058(3)
H(5AC)	0.554(6)	0.5982(19)	0.3526(18)	0.058(3)
H(1B)	0.420(4)	1.1835(16)	0.8434(15)	0.034(4)
H(2B)	0.273(4)	0.9785(15)	0.8189(16)	0.036(4)
H(5BA)	−0.062(5)	0.5888(19)	0.9013(18)	0.051(3)
H(5BB)	0.072(5)	0.6404(18)	0.7605(18)	0.051(3)
H(5BC)	0.332(5)	0.5649(19)	0.8529(17)	0.051(3)

Table S2c. Anisotropic displacement parameters for dimethyl terephthalate at 150 K. The anisotropic displacement factor exponent has the form: $-2\pi^2[h^2a^{*2}U_{11}+2hka^*b^*U_{12}+\ldots]$.

Atom	U_{11} / Å²	U_{22} / Å²	U_{33} / Å²	U_{23} / Å²	U_{13} / Å²	U_{12} / Å²
O(1A)	0.0440(7)	0.0282(5)	0.0324(6)	−0.0090(4)	−0.0043(5)	−0.0041(4)
O(2A)	0.0536(8)	0.0308(6)	0.0434(7)	−0.0075(5)	0.0068(5)	−0.0099(5)
C(1A)	0.0260(8)	0.0299(7)	0.0257(7)	−0.0062(5)	−0.0027(5)	0.0011(6)
C(2A)	0.0254(8)	0.0283(7)	0.0270(7)	−0.0014(5)	−0.0016(5)	−0.0011(5)
C(3A)	0.0238(8)	0.0253(7)	0.0292(7)	−0.0037(5)	−0.0056(5)	0.0019(5)
C(4A)	0.0274(8)	0.0274(7)	0.0309(7)	−0.0042(5)	−0.0049(6)	0.0013(6)
C(5A)	0.0476(11)	0.0291(8)	0.0421(9)	−0.0115(7)	−0.0100(8)	−0.0015(7)
O(1B)	0.0455(7)	0.0277(5)	0.0336(6)	−0.0096(4)	−0.0072(5)	−0.0052(4)
O(2B)	0.0586(8)	0.0257(6)	0.0389(6)	−0.0034(5)	−0.0095(5)	−0.0048(5)
C(1B)	0.0284(8)	0.0272(7)	0.0272(7)	−0.0036(5)	−0.0029(6)	0.0010(5)
C(2B)	0.0250(8)	0.0310(7)	0.0252(7)	−0.0071(5)	−0.0037(5)	0.0005(6)
C(3B)	0.0214(7)	0.0268(7)	0.0279(7)	−0.0076(5)	0.0011(5)	−0.0003(5)
C(4B)	0.0258(8)	0.0285(7)	0.0302(7)	−0.0071(6)	−0.0001(6)	−0.0001(5)
C(5B)	0.0444(10)	0.0311(8)	0.0429(9)	−0.0143(7)	−0.0076(7)	−0.0058(7)

Table S2d. Selected bond lengths for dimethyl terephthalate at 150 K.

Atom	— Atom	Length / Å	Atom	— Atom	Length / Å
Cl(1)	— S(1)	1.877(3)	O(2)	— C(1)	1.304(5)
Cl(2)	— S(2)	1.973(5)	C(1)	— C(2)	1.483(6)
O(1A)	— C(4A)	1.3397(17)	O(1B)	— C(4B)	1.3345(17)
O(1A)	— C(5A)	1.4489(18)	O(1B)	— C(5B)	1.4520(17)
O(2A)	— C(4A)	1.2039(17)	O(2B)	— C(4B)	1.2042(18)
C(1A)	— C(2A)	1.386(2)	C(1B)	— C(2B)	1.385(2)
C(1A)	— C(3A)[1]	1.3930(19)	C(1B)	— C(3B)[2]	1.3905(19)
C(2A)	— C(3A)	1.392(2)	C(2B)	— C(3B)	1.394(2)
C(3A)	— C(1A)[1]	1.3930(19)	C(3B)	— C(1B)[2]	1.3905(19)
C(3A)	— C(4A)	1.4924(19)	C(3B)	— C(4B)	1.4936(19)

[1]2−*x*, 2−*y*, 1−*z*; [2]1−*x*, 2−*y*, 2−*z*

Table S2e. Selected bond angles for dimethyl terephthalate at 150 K.

Atom	— Atom	— Atom	Angle / °	Atom	— Atom	— Atom	Angle / °
C(4A)	— O(1A)	— C(5A)	116.24(12)	C(4B)	— O(1B)	— C(5B)	116.06(12)
C(2A)	— C(1A)	— C(3A)[1]	120.35(13)	C(2B)	— C(1B)	— C(3B)[2]	119.98(13)
C(1A)	— C(2A)	— C(3A)	119.70(13)	C(1B)	— C(2B)	— C(3B)	120.03(13)
C(1A)[1]	— C(3A)	— C(4A)	121.49(12)	C(1B)[2]	— C(3B)	— C(2B)	119.99(13)
C(2A)	— C(3A)	— C(1A)[1]	119.95(13)	C(1B)[2]	— C(3B)	— C(4B)	118.36(12)
C(2A)	— C(3A)	— C(4A)	118.55(12)	C(2B)	— C(3B)	— C(4B)	121.65(13)
O(1A)	— C(4A)	— C(3A)	112.02(12)	O(1B)	— C(4B)	— C(3B)	112.20(12)
O(2A)	— C(4A)	— O(1A)	123.77(13)	O(2B)	— C(4B)	— O(1B)	123.91(13)
O(2A)	— C(4A)	— C(3A)	124.21(13)	O(2B)	— C(4B)	— C(3B)	123.89(13)

[1]2−*x*, 2−*y*, 1−*z*; [2]1−*x*, 2−*y*, 2−*z*

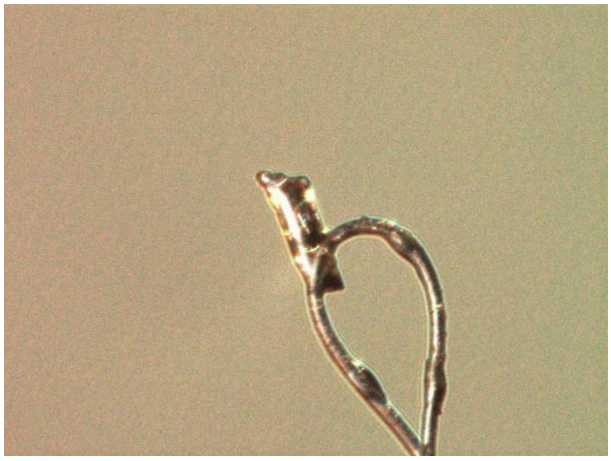

Figure S3. Photograph of a crystal of DMT mounted on a nylon loop *in situ* on the single-crystal diffractometer.

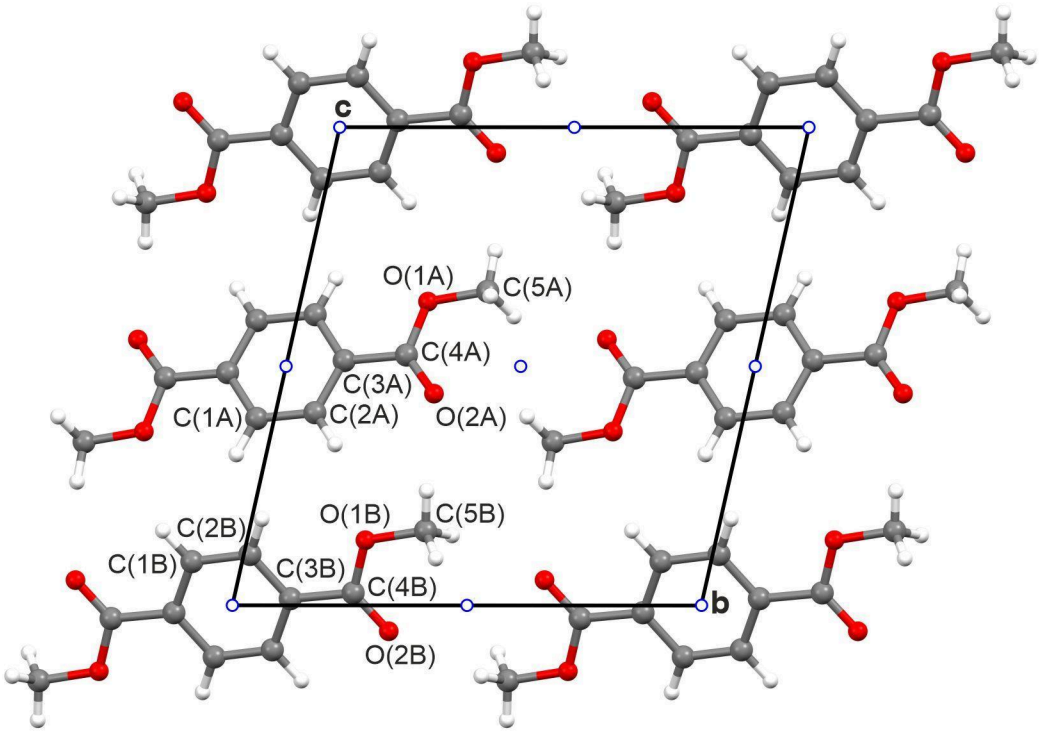

Figure S4. Crystal structure of the new polymorph of dimethyl terephthalate viewed down **a** showing the atom labels as used in the tables of the crystallographic structure. Centres of inversion symmetry are shown by open blue circles, which generate the other half of each of the two crystallographic dimethyl terephthalate molecules A and B, so that the structure has Z = 2, and $Z' = ½ + ½$. By contrast the previously reported polymorph (CCDC refcode DMTPAL) is orthorhombic, space group *Pbca*, with Z = 4, and $Z' = ½$.

3.2.3 BDTCA-Bn

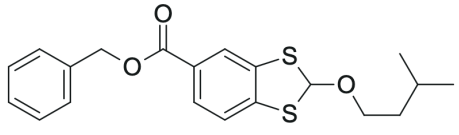

Step 1 – Preparation of BDTCA sodium salt:

BDTCA (1.222 g, ~98% purity by NMR, 4.30 mmol) was dissolved in a sodium hydroxide solution in methanol (17.2 ml, 0.01 g/mL NaOH) and stirred for 5–10 minutes in a 250 mL flask. The solvent was removed under reduced pressure using a rotary evaporator, and the resulting residue was dried under vacuum at 60 °C for 2 hours to afford BDTCA sodium salt.

Step 2 – Benzylation:

The crude BDTCA sodium salt was thoroughly dispersed in dimethylformamide (DMF, 30 mL), and benzyl chloride (0.5440 ml, 3.91 mmol) was added. The mixture was heated at 110 °C under vigorous stirring for 1.5 hours.

After cooling to room temperature, the reaction mixture was poured into water (300 mL), leading to precipitation of the ester. The resulting suspension was washed twice with ethyl acetate (2 × 150 ml); the combined organic layers were washed sequentially with 0.1 M Na_2CO_3 (100 ml), 0.5 M HCl (100 ml), and water (100 ml). The organic phase was dried over anhydrous $MgSO_4$, filtered, and concentrated under reduced pressure. The residue was dried under vacuum to afford
benzyl 2-(3-methylbutoxy)-2H-1,3-benzodithiole-5-carboxylate (BDTCA-Bn) as an orange amorphous solid (0.94 g, 2.51 mmol, ~90% purity by NMR), corresponding to an isolated yield of 52.6% based on BDTCA and 47.8% based on 2-ATA.

^{1}H NMR (400 MHz, [D_6]DMSO, ppm): δ =8.06 (d, J=1.4 Hz, 1H), 7.75 (dd, J=1.6, 8.2 Hz, 1H), 7.64 (d, J=8.2 Hz, 1H), 7.44–7.34 (m, 5H), 7.14 (s, 1H), 5.34 (s, 2H), 3.42–3.37 (m, 2H), 1.61–1.50 (m, 1H), 1.37–1.28 (m, 2H), 0.80 (d, J=6.6 Hz, 6H); ^{13}C NMR (101 MHz, [D_6]DMSO, ppm): δ =165.4 (s), 142.9 (s), 137.6 (s), 136.5 (s), 129.0 (s), 128.6 (s), 128.5 (s), 127.5 (s), 127.0 (s), 122.9 (s), 122.6 (s), 90.8 (s), 66.7 (s), 63.6 (s), 37.6 (s), 24.9 (s), 22.7 (s).

3.2.4 DClSBA

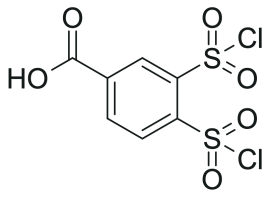

Oxidation with gaseous chlorine (Cl_2)

BDTCA (1.40 g, ~98% purity by NMR, 4.92 mmol) was dispersed in a mixture of tert-butanol (25 ml), dichloromethane (20 mL), and water (5 ml), and the suspension was cooled to 0-5 °C in an ice bath. Chlorine gas, generated in situ by the oxidation of hydrochloric acid with potassium permanganate, was bubbled through the reaction mixture while maintaining the temperature at 0-5 °C. After 1 hour, the BDTCA precipitate was no longer visible indicating completeness of the reaction.

The reaction mixture was then poured into dichloromethane (DCM, 100 ml) and washed with water (3 × 100 ml). The organic phase was separated, dried over anhydrous $MgSO_4$, filtered, and concentrated under reduced pressure. To expedite drying, hexane (approx. 150 ml) was added to the viscous residue and removed on a rotary evaporator. The crude product was redissolved in chloroform (50 ml), filtered through a cotton plug, and reconcentrated under reduced pressure (aided again by hexane addition). The resulting residue was dried in vacuo at room temperature for 72 hours to afford 3,4-bis(chlorsulfonyl)benzoic acid (DClSBA) as an oily yellow-white crystalline solid (1.30 g, ~90 wt% purity by NMR, 3.67 mmol), corresponding to a yield of 74.5% based on BDTCA and 67.7% based on 2-ATA

Oxidation with hydrogen peroxide and thionyl chloride (H_2O_2/$SOCl_2$)

BDTCA (1.40 g, ~98% purity by NMR, 4.92 mmol) was thoroughly dispersed in acetonitrile (60 ml) and the mixture was cooled to 0-5 °C in an ice bath with a reflux condenser mounted. Under vigorous stirring, hydrogen peroxide (29.5 mmol, 6.2 ml, 30% w/w) was added dropwise, followed by dropwise addition of thionyl chloride (10.3 mmol, 1.5 ml), taking care to prevent boiling due to the highly exothermic nature of the reaction (caution: vigorous gas evolution may occur). The reaction mixture was stirred for 5 minutes in the ice bath, then allowed to warm to room temperature and stirred for an additional 30 minutes.

DClSBA was isolated from the reaction mixture following the same work-up procedure as used in the gaseous chlorine oxidation method, affording 1.23 g of product (~90 wt% purity by NMR, 3.47 mmol), corresponding to a yield of 70.5% based on BDTCA and 64.1% based on 2-ATA

Rf = 0.32 (EtAc / MeOH 9:1 + 2 vol% Acetic acid); ^{1}H NMR (600 MHz, $CDCl_3$, ppm): δ = 9.01 (d, J=1.5 Hz, 1H), 8.60 (dd, J=1.6, 8.2 Hz, 1H), 8.51 (d, J=8.2 Hz, 1H); ^{1}H NMR (400 MHz, [D_6]DMSO, ppm): δ =14.44 (s, 1H), 8.55 (d, J=1.6 Hz, 1H), 8.12 (d, J=8.1 Hz, 1H), 8.06 (q, J=3.2 Hz, 1H); ^{13}C NMR (101 MHz, [D_6]DMSO, ppm): δ =165.8 (s), 144.3 (s), 141.8 (s), 137.1 (s), 136.7 (s), 133.5 (s), 132.8 (s); IR (cm^{-1}): ν = 860 (C-H bending - 1,2,4 substituted), 1179 and 1388 (S=O stretching), 1704 (C=O stretching carboxylic acid dimer); elemental analysis calcd (%) for $C_7H_4Cl_2O_6S_2$: C 26.34, H 1.25, N 0.00, S 20.09; found: C 26.74, H 1.84, N 0.00, S 19.96.

DClSBA FTIR spectrum

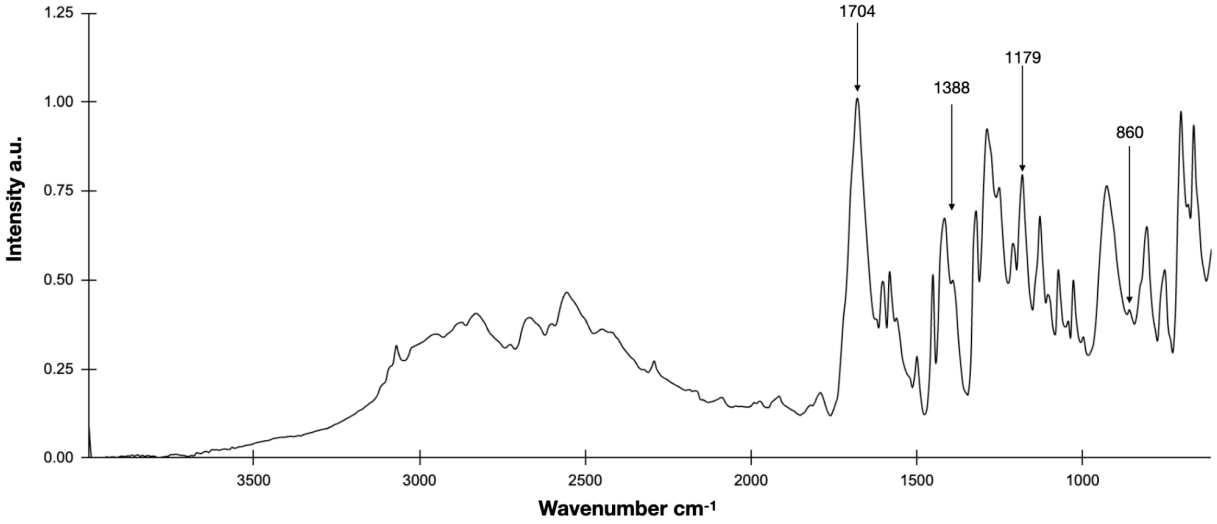

Figure S5. FTIR spectrum of DClSBA; 1704 cm^{-1} (C=O, stretching carboxylic acid dimer); 1388 and 1179 cm^{-1} (S=O stretching in sulfonyl chloride); 860 cm^{-1} (C-H bending - 1,2,4 substituted)

DClSBA Crystal Structure

In an attempt to characterise its molecular structure by the means of SXD, crystals of DClSBA were initially grown from THF, but the dataset was of poor quality. DClSBA was subsequently crystallized from *p*-xylene to avoid solvent disorder as seen with solvents such as THF and toluene. The molecules of DClSBA are arranged in planes with planes of solvent molecules interlayered between them (see Figure S8). Disorder of the chlorosulfonyl groups leads to additional solvent disorder, which was not modelled. As is common for organic acids, the molecules form dimers due to hydrogen bonding between the $–CO_2H$ groups of adjacent molecules within the crystallographic plane. The crystal structure reveals that the chlorosulfonyl groups in the 3 and 4 positions on the aromatic ring adopt a conformation to avoid steric interaction of the Cl atoms, with one above and the other below the plane of the ring. Given that the Cl atom of the chlorosulfonyl group in the 3-position can be either above or below the plane of the ring, this leads to disorder of this group in both the 3- and 4-position about the mirror plane in the crystal structure. The steric int

Table S3a. Crystal data and structure refinement for DClSBA.*p*-xylene at 130 K.

Identification code	exp_930
Empirical formula	$C_7H_4Cl_2O_6S_2.C_8H_{10}$
Formula weight	425.28
Temperature / K	130
Crystal system	orthorhombic
Space group	*Pbam*
a / Å	17.6722(4)
b / Å	14.9571(3)
c / Å	6.8177(3)
α / °	90
β / °	90
γ / °	90
Volume / $Å^3$	1802.09(10)
Z	4
ρ_{calc} / g cm^{-3}	1.568
μ / mm^{-1}	5.683
F(000)	872.0
Crystal size / mm^3	0.263 × 0.253 × 0.126
Radiation	Cu Kα (λ = 1.54184 Å)
2θ range for data collection / °	7.744 to 157.732
Index ranges	$-22 \le h \le 22$, $-18 \le k \le 18$, $-8 \le l \le 8$
Reflections collected	40469
Independent reflections	2078 [R_{int} = 0.0758, R_{sigma} = 0.0221]
Data/restraints/parameters	2078/3/123
Goodness-of-fit on F^2	1.099
Final *R* indexes [$I \ge 2\sigma(I)$]	R_1 = 0.0741, wR_2 = 0.2211
Final *R* indexes [all data]	R_1 = 0.0812, wR_2 = 0.2285
Largest diff. peak/hole / e $Å^{-3}$	0.48/−0.38

Table S3b. Fractional atomic coordinates and equivalent isotropic displacement parameters for DClSBA.*p*-xylene at 130 K. U_{eq} is defined as ⅓ of the trace of the orthogonalised U_{ij} tensor.

Atom	*x*	*y*	*z*	*U*(eq) / Å²
Cl(1)	0.18464(13)	0.6599(2)	0.7580(5)	0.1006(9)
Cl(2)	0.31096(17)	0.47817(19)	0.2243(7)	0.1286(14)
S(1)	0.21292(7)	0.68856(8)	½	0.0762(6)
S(2)	0.33565(7)	0.50562(8)	½	0.0851(7)
O(1)	0.5230(16)	0.8956(2)	½	0.0588(9)
O(2)	0.4052(17)	0.9494(2)	½	0.0571(9)
O(3)	0.1915(3)	0.6166(4)	0.3641(12)	0.0813(19)
O(4)	0.1844(2)	0.7759(3)	0.448(2)	0.089(6)
O(5)	0.2688(3)	0.4943(4)	0.6178(13)	0.104(3)
O(6)	0.4016(2)	0.4556(3)	0.5656(8)	0.069(2)
C(1)	0.4544(2)	0.8844(3)	½	0.0458(10)
C(2)	0.4209(2)	0.7935(3)	½	0.0496(11)
C(3)	0.3422(2)	0.7805(3)	½	0.0512(11)
C(4)	0.3130(2)	0.6950(3)	½	0.0534(11)
C(5)	0.3624(3)	0.6212(3)	½	0.0599(13)
C(6)	0.4400(2)	0.6343(3)	½	0.0646(15)
C(7)	0.4694(2)	0.7203(3)	½	0.0530(12)
H(2)	0.427(3)	1.000(2)	½	0.086
H(3)	0.3091	0.8305	½	0.061
H(6)	0.4732	0.5843	½	0.077
H(7)	0.5226	0.7292	½	0.064

Table S3c. Anisotropic displacement parameters for DClSBA.*p*-xylene at 130 K. The anisotropic displacement factor exponent has the form: $-2\pi^2[h^2a^{*2}U_{11}+2hka^*b^*U_{12}+\ldots]$.

Atom	U_{11} / Å²	U_{22} / Å²	U_{33} / Å²	U_{23} / Å²	U_{13} / Å²	U_{12} / Å²
Cl(1)	0.0524(11)	0.1064(19)	0.1430(3)	0.0054(18)	0.0381(14)	−0.0055(12)
Cl(2)	0.0951(18)	0.0753(15)	0.2150(4)	−0.0580(2)	0.0150(2)	−0.0144(13)
S(1)	0.0309(6)	0.0478(7)	0.1498(16)	0	0	−0.0006(4)
S(2)	0.0384(7)	0.0411(7)	0.1758(19)	0	0	−0.0025(4)
O(1)	0.0327(14)	0.0459(16)	0.098(3)	0	0	−0.0025(12)
O(2)	0.0384(15)	0.0400(16)	0.093(3)	0	0	−0.0020(12)
O(3)	0.036(2)	0.054(3)	0.153(6)	−0.006(4)	0.009(3)	−0.004(2)
O(4)	0.0343(18)	0.048(2)	0.185(17)	−0.005(4)	−0.003(4)	0.0085(16)
O(5)	0.051(3)	0.054(3)	0.206(8)	0.018(4)	0.042(4)	−0.004(2)
O(6)	0.043(2)	0.043(2)	0.120(7)	0.004(2)	0.010(2)	0.0007(16)
C(1)	0.0366(19)	0.042(2)	0.058(3)	0	0	0.0020(16)
C(2)	0.035(2)	0.041(2)	0.073(3)	0	0	0.0015(16)
C(3)	0.037(2)	0.045(2)	0.071(3)	0	0	0.0022(17)
C(4)	0.036(2)	0.044(2)	0.081(3)	0	0	−0.0025(17)
C(5)	0.037(2)	0.038(2)	0.105(4)	0	0	−0.0025(17)
C(6)	0.032(2)	0.042(2)	0.119(5)	0	0	0.0030(17)
C(7)	0.034(2)	0.041(2)	0.085(3)	0	0	0.0023(16)

Table S3d. Selected bond lengths for DClSBA.*p*-xylene at 130 K.

Atom	— Atom	Length / Å	Atom	— Atom	Length / Å
Cl(1)	— S(1)	1.877(3)	O(2)	— C(1)	1.304(5)
Cl(2)	— S(2)	1.973(5)	C(1)	— C(2)	1.483(6)
S(1)	— O(3)	1.469(6)	C(2)	— C(3)	1.404(6)
S(1)	— O(4)	1.446(5)	C(2)	— C(7)	1.390(6)
S(1)	— C(4)	1.772(5)	C(3)	— C(4)	1.378(6)
S(2)	— O(5)	1.437(6)	C(4)	— C(5)	1.408(6)
S(2)	— O(6)	1.457(4)	C(5)	— C(6)	1.385(6)
S(2)	— C(5)	1.793(5)	C(6)	— C(7)	1.388(6)
O(1)	— C(1)	1.222(5)			

Table S3e. Selected bond angles for DClSBA.*p*-xylene at 130 K.

Atom	— Atom	— Atom	Angle / °	Atom	— Atom	— Atom	Angle / °
O(3)	— S(1)	— Cl(1)	110.9(4)	O(5)	— S(2)	— C(5)	109.4(3)
O(3)	— S(1)	— C(4)	107.3(2)	O(6)	— S(2)	— Cl(2)	111.3(2)
O(4)	— S(1)	— Cl(1)	110.1(5)	O(6)	— S(2)	— C(5)	106.4(2)
O(4)	— S(1)	— O(3)	114.6(6)	C(5)	— S(2)	— Cl(2)	105.07(10)
O(4)	— S(1)	— C(4)	107.3(2)	C(3)	— C(4)	— S(1)	115.2(3)
C(4)	— S(1)	— Cl(1)	106.16(9)	C(5)	— C(4)	— S(1)	125.1(3)
O(5)	— S(2)	— Cl(2)	109.1(4)	C(4)	— C(5)	— S(2)	126.3(3)
O(5)	— S(2)	— O(6)	115.2(4)	C(6)	— C(5)	— S(2)	113.5(3)

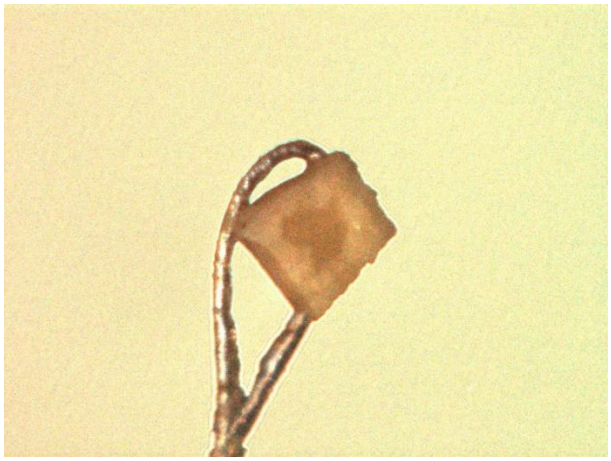

Figure S6. Photograph of a crystal of DClSBA mounted on a nylon loop in situ on the single-crystal diffractometer.

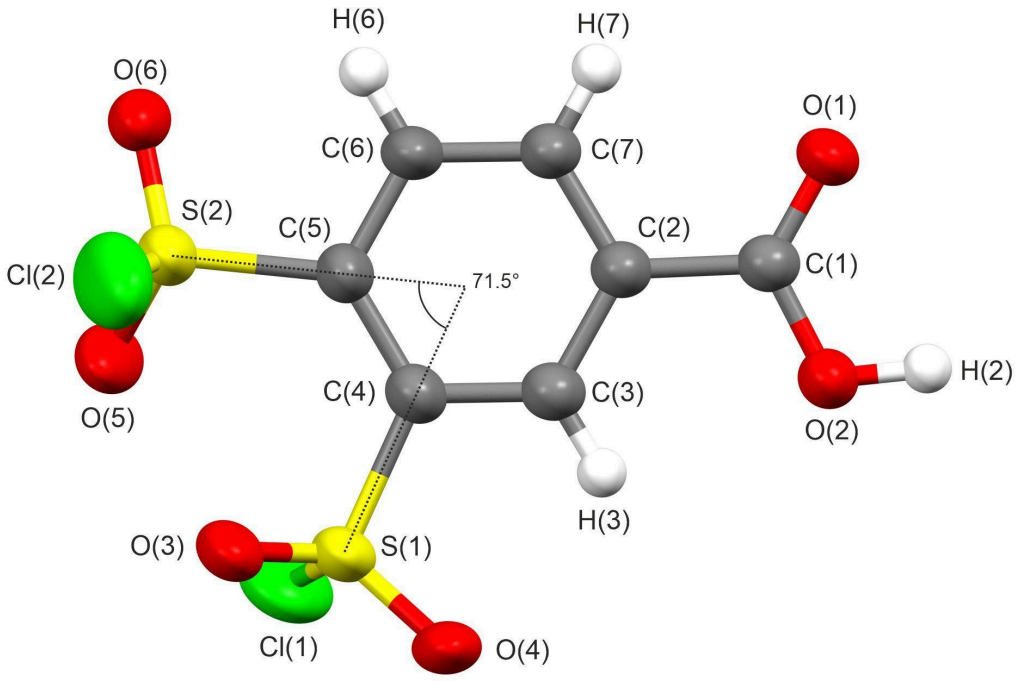

Figure S7. Molecular structure of DClSBA showing the atom labels as used in the tables of the crystallographic structure and the steric interaction between the chlorosulfonyl groups. Equivalent positions of the disordered chlorosulfonyl groups due to crystallographic mirror symmetry have been omitted.

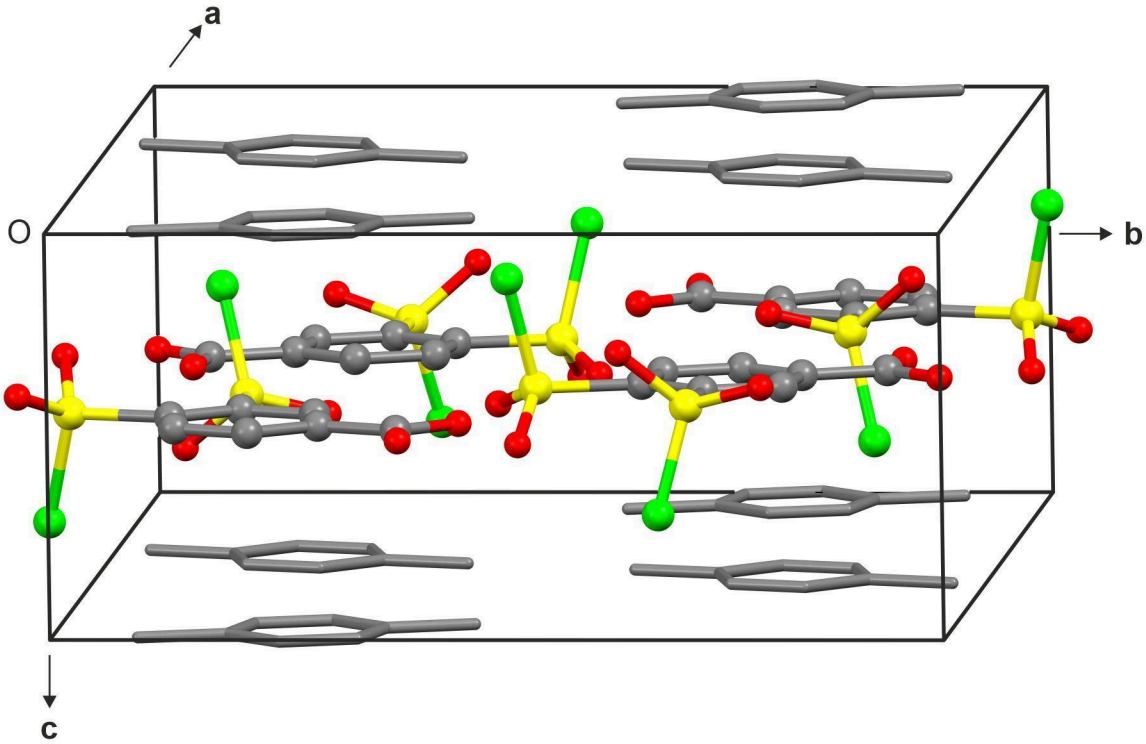

Figure S8. Crystallographic unit cell of DClSBA showing layers of DClSBA interspersed with layers of p-xylene. Equivalent positions of the chlorosulfonyl groups due to crystallographic mirror symmetry have been omitted randomly to reflect disorder. This disorder leads to disorder within the solvent layers too, and so for simplicity a single orientation of the p-xylene molecules is shown.

3.2.5 DClSBA-Me

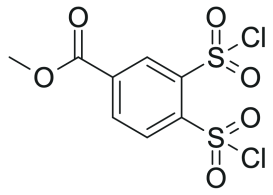

BDTCA-Me (0.45 g, ~98% purity by NMR, 1.82 mmol) was dispersed in tert-butanol (9 ml), dichloromethane (DCM, 8 ml), and water (2 ml), and the mixture was cooled to 0-5 °C in an ice bath. Chlorine gas, generated in situ by oxidation of hydrochloric acid with potassium permanganate, was bubbled through the reaction mixture for 1 hour while maintaining the temperature at 0-5 °C.

After completion, the reaction mixture was poured into dichloromethane (100 mL) and washed with 0.1 M Na_2CO_3(100 ml), followed by three additional washes with water (100 × 50 mL). The organic phase was separated, dried over anhydrous $MgSO_4$, filtered, and concentrated under reduced pressure. The residue was further dried in vacuo at room temperature for 72 hours to afford methyl-3,4-bis(chlorsulfonyl)benzoate (DClSBA-Me) as oily yellow-white crystalline solid (0.45 g, ~95 wt% purity by NMR, 1.28 mmol), corresponding to a 70.3 % yield based on BDTCA-Me and 23.5 % based on 2-ATA.

^{1}H NMR (400 MHz, $CDCl_3$, ppm): δ = 8.95 (d, J=1.7 Hz, 1H), 8.53 (dd, J=1.7, 8.2 Hz, 1H), 8.46 (d, J=8.2 Hz, 1H), 3.99 (s, 3H); ^{13}C NMR (101 MHz, $CDCl_3$, ppm): δ =162.9 (s), 143.9 (s), 141.7 (s), 137.1 (s), 136.6 (s), 133.0 (s), 132.7 (s), 53.7 (s).

3.2.6 DClSBA-Bn

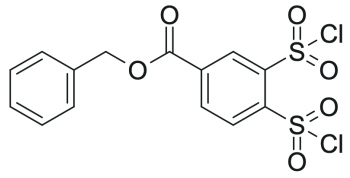

BDTCA-Bn (0.94 g, ~90% purity by NMR, 2.51 mmol) was oxidized following the procedure described for DClSBA-Me to afford benzyl 3,4-bis(chlorosulfonyl)benzoate (DClSBA-Bn) as a viscous yellow oil (0.69 g, ~92 wt% purity by NMR, 1.55 mmol) - 61.8% yield based on BDTCA-Bn and 28.2% overall yield based on the initially loaded 2-ATA.

^{1}H NMR (400 MHz, $CDCl_3$, ppm): δ =8.95 (d, J=1.7 Hz, 1H), 8.53 (dd, J=1.7, 8.3 Hz, 1H), 8.44 (d, J=8.2 Hz, 1H), 7.43–7.36 (m, 5H), 5.39 (s, 2H); ^{13}C NMR (101 MHz, $CDCl_3$, ppm): δ =162.4 (s), 143.9 (s), 141.7 (s), 137.3 (s), 136.7 (s), 134.5 (s), 133.1 (s), 132.7 (s), 129.1 (s), 128.9 (s), 128.8 (s), 128.7 (s), 68.7 (s).

3.2.7 DClSBA-EtOH

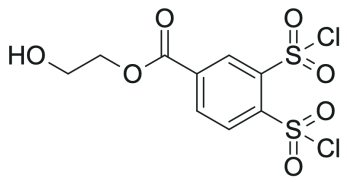

BDTCA-EtOH

Step 1 – Preparation of BDTCA sodium salt:

BDTCA (1.00 g, ~98% purity by NMR, 3.50 mmol) was dissolved in a sodium hydroxide solution in methanol (14.0 ml, 0.01 g/mL NaOH) and stirred for 5–10 minutes in a 250 ml flask. The solvent was removed under reduced pressure using a rotary evaporator, and the residue was dried under vacuum at 60 °C for 2 hours to afford BDTCA sodium salt.

Step 2 – Alkylation with 2-Chloroethanol:

The crude BDTCA sodium salt was thoroughly dispersed in 2-chloroethanol (20 ml), and the mixture was heated at 110 °C under vigorous stirring for 4 hours. After cooling to room temperature, the reaction mixture was filtered through a sintered glass funnel to remove precipitated NaCl. Excess 2-chloroethanol was then distilled off under vacuum at 110 °C. The resulting crude product, containing 2-hydroxyethyl 2-(3-methylbutoxy)-2H-1,3-benzodithiole-5-carboxylate (BDTCA-EtOH) was obtained as a viscous dark-red oily residue (1.10 g, crude).

DClSBA-EtOH

Crude BDTCA-EtOH (1.10 g) was oxidized following the procedure described for DClSBA-Me to afford 2-hydroxyetyl 3,4-bis(chlorsulfonyl)benzoate (DClSBA-EtOH) as a yellow oil (0.44 g, ~90% purity by NMR, 1.10 mmol) - overall yield of 20.0% based on 2-ATA.

^{1}H NMR (600 MHz, $CDCl_3$, ppm): δ =8.95 (d, J=1.4 Hz, 1H), 8.56 (dd, J=1.6, 8.2 Hz, 1H), 8.47 (d, J=8.3 Hz, 1H), 4.64 (t, J=5.6 Hz, 1H), 4.60–4.58 (m, 2H), 4.04–3.92 (m, 2H); ^{13}C NMR (151 MHz, $CDCl_3$, ppm): δ =162.8 (s), 144.0 (s), 141.7 (s), 137.1 (s), 136.8 (s), 133.1 (s), 132.7 (s), 68.2 (s), 60.8 (s).

3.2.8 PABA-Me

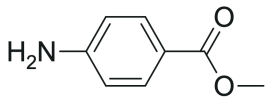

p-Aminobenzoic acid (4.00 g, 29.2 mmol) was dissolved in methanol (60 mL) under vigorous stirring. After complete dissolution, concentrated sulfuric acid (2.00 mL) was added dropwise with caution. The transient formation of an amino-sulfonate salt was observed as a precipitate. The reaction mixture was then heated under reflux for 2 hours.

After cooling to room temperature, the mixture was diluted with water (60 mL) and neutralized to pH 8–9 using saturated aqueous sodium carbonate. The product was extracted with dichloromethane (3 × 50 mL). The combined

organic layers were dried over anhydrous $MgSO_4$, filtered, and concentrated under reduced pressure to afford methyl p-aminobenzoate (PABA-Me) as a pale white-brown solid (1.4594 g, ~98 wt% purity by NMR, 9.43 mmol), corresponding to a 33.0% yield.

^{1}H NMR (600 MHz, [D_6]DMSO, ppm): δ =7.64 (td, J=2.2, 9.4 Hz, 2H), 6.57 (td, J=2.2, 9.4 Hz, 2H), 5.97 (s, 2H), 3.73(s, 3H); ^{13}C NMR (151 MHz, [D_6]DMSO, ppm): δ =166.8 (s), 154.0 (s), 131.5 (s), 116.2 (s), 113.1 (s), 51.6 (s).

3.2.9 PABA-Bn

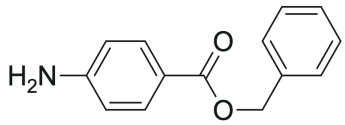

Step 1 – Preparation of sodium p-aminobenzoate:

p-Aminobenzoic acid (2.50 g, 18.2 mmol) was dissolved in a sodium hydroxide solution in methanol (72.9 mL, 0.01 g/mL NaOH) and stirred for 5-10 minutes in a 250 mL flask. The solvent was removed under reduced pressure using a rotary evaporator, and the resulting residue was dried under vacuum at 60 °C for 1–2 hours to afford sodium p-aminobenzoate PABA-Na.

Step 2 – Benzylation:

The crude PABA-Na was thoroughly dispersed in DMF (30 mL), followed by the addition of benzyl chloride (2.31 mL, 16.6 mmol). The reaction mixture was stirred vigorously at 110 °C under an air condenser for 1.5 hours. After cooling to room temperature, the mixture was poured into water (200 mL), resulting in precipitation of the ester product.

The resulting suspension was washed with ethyl acetate (2 × 100 mL). The combined organic layers were washed with 0.1 M Na_2CO_3 (100 mL) and water (100 mL), then dried over anhydrous $MgSO_4$. The organic phase was filtered and concentrated under reduced pressure. The residue was dried under vacuum at room temperature (Schlenk line) to afford benzyl p-aminobenzoate (PABA-Bn) as a pale white solid (3.34 g, ~94 wt% purity by NMR, 13.8 mmol), corresponding to a 75.8% yield.

^{1}H NMR (400 MHz, [D_6]DMSO, ppm): δ =7.68 (td, J=2.3, 9.3 Hz, 2H), 7.43–7.37 (m, 5H), 6.58 (td, J=2.2, 9.4 Hz, 2H), 6.01 (s, 2H), 5.25 (s, 2H); ^{13}C NMR (101 MHz, [D_6]DMSO, ppm): δ =166.2 (s), 154.1 (s), 137.3 (s), 131.7 (s), 128.9 (s), 128.3 (s), 128.2 (s), 116.1 (s), 113.2 (s), 65.5 (s).

3.2.10 PABA-EtOH

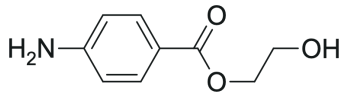

Step 1 – Preparation of PABA-Na:

p-Aminobenzoic acid (2.00 g, 14.6 mmol) was converted to its sodium salt (PABA-Na) following the same procedure as described for the preparation of benzyl p-aminobenzoate.

Step 2 – Alkylation with 2-Chloroethanol:

The resulting PABA-Na was thoroughly dispersed or dissolved in 2-chloroethanol (15 ml) and heated to 110 °C under an air condenser with vigorous stirring for 4 hours. After cooling to room temperature, the reaction mixture was filtered through a sintered glass funnel to remove precipitated NaCl. Excess 2-chloroethanol was then removed under vacuum at 110 °C.

The crude residue was cooled to room temperature, dissolved in ethyl acetate (100 ml), and washed sequentially with water (100 ml), 0.1 M aqueous Na_2CO_3 (100 ml), and again with water (100 ml). The organic layer was dried over anhydrous $MgSO_4$, filtered, and concentrated under reduced pressure. The product - initially a yellow to colorless oil - solidified upon standing and was dried under vacuum at room temperature overnight.

The crude solid was purified by flash chromatography using ethyl acetate as the eluent to afford 2-hydroxyethyl p-aminobenzoate (PABA-EtOH) as pale-brown crystalline solid (0.36 g, ~98 wt% purity by NMR, 1.99 mmol), corresponding to a 13.3% yield.

Rf = 0.74 (EtAc); ^{1}H NMR (600 MHz, [D_6]DMSO, ppm): δ =7.60 (d, J=8.5 Hz, 2H), 6.49 (d, J=8.6 Hz, 2H), 5.88 (s, 2H), 4.78 (t, J=5.6 Hz, 1H), 4.09 (t, J=5.1 Hz, 2H), 3.58 (q, J=5.2 Hz, 2H); ^{13}C NMR (151 MHz, [D_6]DMSO, ppm): δ =166.5 (s), 153.9 (s), 131.7 (s), 116.4 (s), 113.0 (s), 65.9 (s), 59.7(s).

3.2.11 DSI-PABA-Me

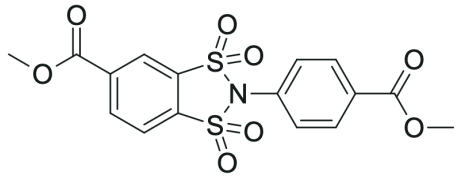

DClSBA-Me (0.45 g, ~95% purity by NMR, 1.28 mmol) was dissolved in 1,2-dichloroethane (DCE, 13.5 mL). A solution of methyl p-aminobenzoate (PABA-Me, 0.1940 g, 1.28 mmol) in DCE (4.5 mL) containing pyridine (0.250 mL, 3.0 mmol) was added under vigorous stirring. The reaction mixture was heated to 95–100 °C in an oil bath and refluxed overnight (24 h).

After cooling to room temperature, the mixture was poured into dichloromethane (DCM, 100 mL) and washed sequentially with 0.5 M HCl (3 × 50 mL) and water (3 × 50 mL). The organic phase was separated, dried over anhydrous $MgSO_4$, filtered, and concentrated under reduced pressure. The resulting residue was dried under vacuum at 100 °C for 30 minutes, followed by overnight drying at room temperature to yield 0.39 g of crude product.

Purification was carried out by flash chromatography using a gradient of hexane/ethyl acetate (96:4 → 8:2 → 0:1). This procedure afforded 4-[2-methoxycarbonyl]-N-(4-[2-methoxycarbonyl]phenyl)benzene-1,2-disulfonimide (DSI-PABA-Me) as an oily orange-brown solid (0.26 g, ~90 wt% purity by NMR, 0.57 mmol), corresponding to a 44.3% yield for this step and an overall yield of 10.4 % based on the initially loaded 2-ATA over four steps.

Rf = 0.76 (Hexane / EtAc 1:1); ^{1}H NMR (400 MHz, $CDCl_3$, ppm): δ =8.68 (dd, J=0.6, 1.4 Hz, 1H), 8.55 (dd, J=1.4, 8.2 Hz, 1H), 8.18 (td, J=2.1, 9.0 Hz, 2H), 8.13 (dd, J=0.5, 8.3 Hz, 1H), 7.68 (td, J=2.1, 9.0 Hz, 3H), 3.99 (s, 3H), 3.91 (s, 3H); ^{13}C NMR (151 MHz, $CDCl_3$, ppm): δ =165.8 (s), 163.3 (s), 138.0 (s), 135.9 (s), 135.7 (s), 133.2 (s), 131.9 (s), 131.5 (s), 131.2 (s), 129.0 (s), 124.0 (s), 123.0 (s), 53.6 (s), 52.7 (s); IR (cm^{-1}): ν = 572, 606, 693, 736, 924, 948, 1112, 1122, 1171, 1212, 1222-1248, 1288, 1344, 1355, 1435, 1462, 1606, 1700-1755, 2800 - 3200.

Note: Elemental analysis did not yield satisfactory results (expected: C 46.71%, H 3.16%, N 3.40%, S 15.59%; found: C 53.92%, H 5.58%, N 2.96%, S 6.61%). The compound is an oily and strongly hygroscopic material, which likely hampers accurate weighing and favors retention of moisture or volatile impurities. Moreover, the consistently low sulfur content suggests incomplete combustion under the applied conditions. Taken together, these factors may account for the observed discrepancies, despite the compound being thoroughly characterized by NMR, FTIR, and TLC [28]

DSI-PABA-Me FTIR Spectrum

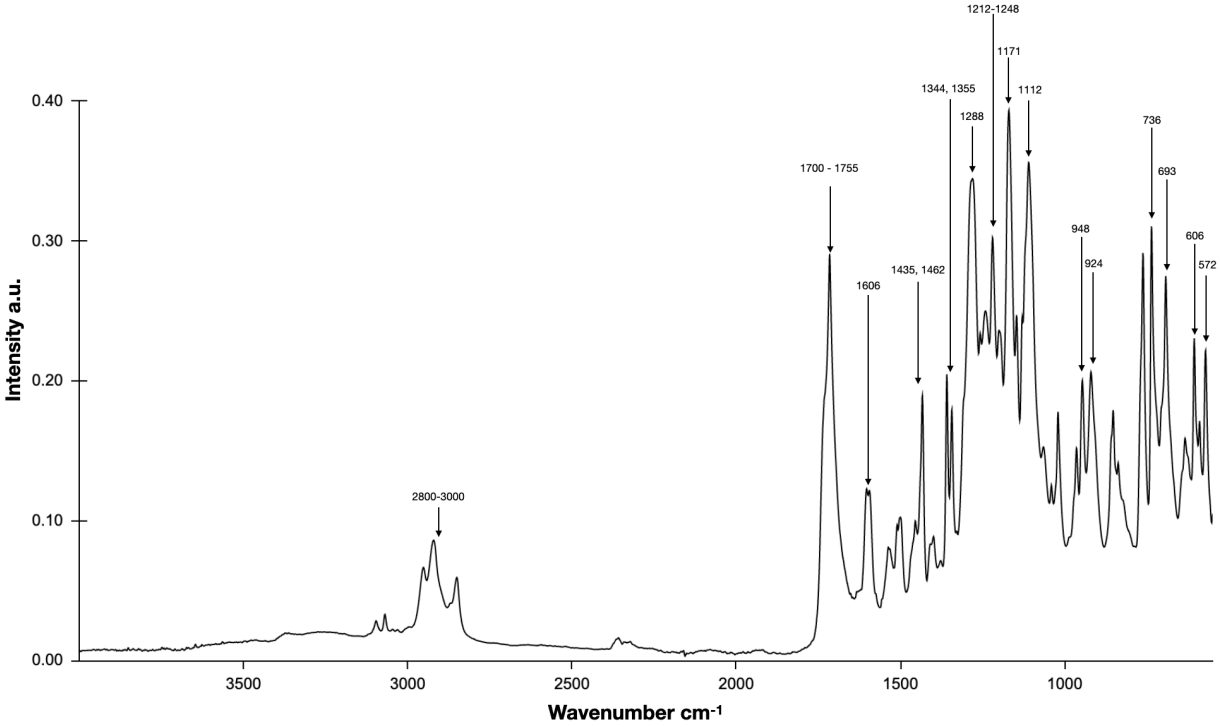

Figure S9a. Experimental FTIR spectrum of DSI-PABA-Me, detailed band assignments are provided in Table S4.

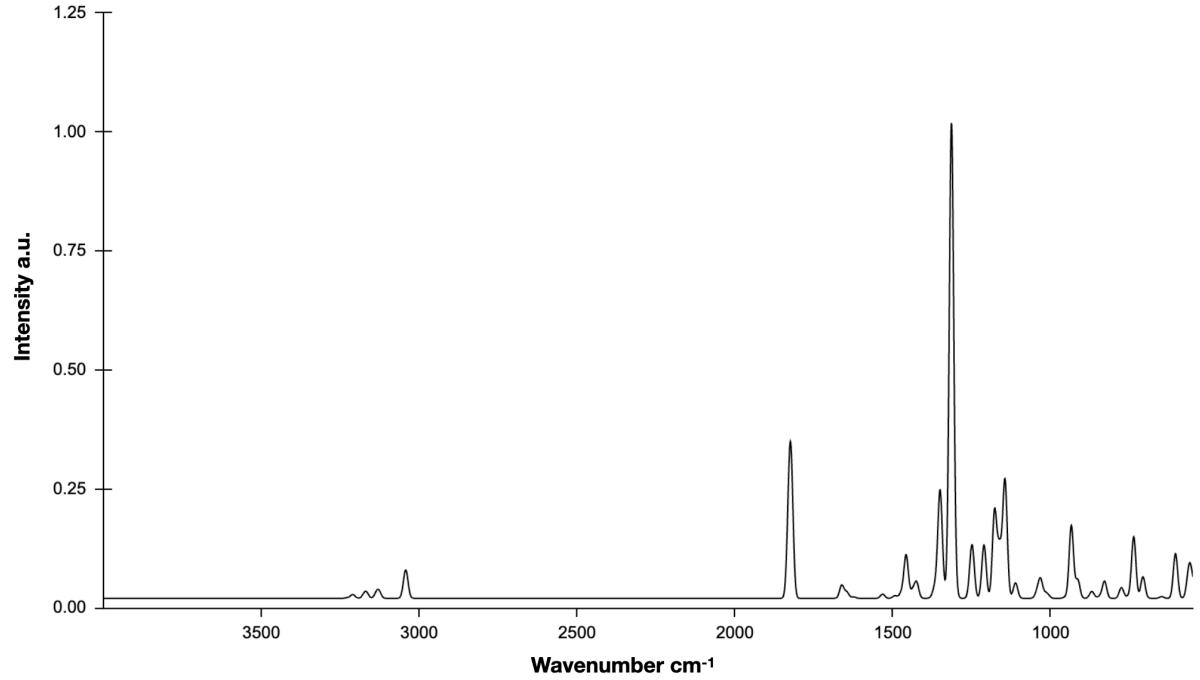

Figure S9b. FTIR spectrum of DSI-PABA-Me, modelled at B3LYP level of theory. Detailed band assignments are provided in Table S4.

Table S4. Assignment of key vibrational bands in the Modelled and Experimental FTIR spectra of DSI-PABA-Me.

Wavenumber Experimental, cm^{-1}	Wavenumber Modelled, cm-1	Assignment
572	564, 568	DSI - cycle deformations (bending and stretching)
606	605	DSI - cycle deformations (symmetric SO2 wagging)
693	708	N in cycle deformation (asymmetric stretch S-N-S)
736	737	N in cycle deformation (symmetric stretch S-N-S)
924	915	N in cycle deformation (rocking S-N-S)
948	935	N in cycle deformation (scissoring S-N-S)
1112	1144	SO_2 in DSI (SO_2 near carboxyl symmetric stretching, asymmetric to other SO2)
1122	1148	SO_2 in DSI (SO_2 further from carboxyl symmetric stretching, asymmetric to other SO_2)
1171	1175, 1178	SO_2 - cycle deformations (symmetric SO_2 and DSI cycle stretching)
1212	1211, 1212	Ester methyls wagging
1222-1248	1248, 1253	N in cycle deformation (N-C in PABA core stretching), and SO2 cycle deformations (C-S-N mutually asymmetric scissoring)
1288	1315	C-CO-O asymmetric stretchings
1344	1341	SO_2 vibrations (S-N-S twisting, SO_2 (O=S=O asymmetric) mutually asymmetric stretching)
1355	1351	SO_2 vibrations (S-N-S wagging, SO_2 (O=S=O asymmetric) mutually symmetric stretching)
1435	1455	Ester methyls rocking
1462	1459	Ester methyls scissoring
1606	1646, 1662	PABA-Me (1662) and DClSBA-Me (1646) benzene ring deformations
1700-1755	1822, 1829	C=O stretching in Ester groups
2800 - 3200	3041, 3045	H in Ester Methyls symmetric stretching

B3LYP-optimised geometry of DSI-PABA-Me

Table S5. Atomic coordinates (Å) of the optimised DSI-PABA-Me conformer. (Energy = -2068.346 Hartree)

Atom	x	y	z
H	0.9893749633	-1.174788863	2.270581258
C	0.5353159674	-0.7628242792	1.366808421
C	-0.7893855238	-0.3179884303	1.362692263
H	-1.38607185	-0.3674642212	2.274204819
C	-1.374787094	0.1868646069	0.1882947316
C	-0.6354155544	0.2556238384	-1.002511815
H	-1.10948762	0.6334851589	-1.910781134
C	0.6864360411	-0.1745660778	-0.9825597441
C	1.262877243	-0.6781888137	0.1813327001
S	1.76178348	-0.1229639652	-2.416729932
S	2.973485849	-1.195241056	0.03272481542
N	2.941612686	-1.185988643	-1.703707948
C	-2.799504834	0.6593225641	0.140352621
O	-3.324974251	1.101196047	-0.8527706398
O	-3.418065236	0.5329606511	1.323045215
C	-4.784222702	0.9567144687	1.374913584
H	-4.870967825	2.019630664	1.104059462
H	-5.1132943	0.7954938523	2.408561687
H	-5.398723468	0.3657678481	0.6790448843
O	1.146890814	-0.809615108	-3.543819952
O	2.304888372	1.222169362	-2.585141859
O	3.13105806	-2.572323562	0.4820788501
O	3.856843881	-0.1532339641	0.5479596711
C	4.191192096	-1.366916142	-2.387327889
C	5.121331761	-0.3199602111	-2.477887211
C	4.464452137	-2.620787609	-2.950500413
C	5.673545983	-2.830949422	-3.611082134
C	6.609158795	-1.788160271	-3.711071905
C	6.325878907	-0.5359836101	-3.144147126
H	4.889831095	0.6460473159	-2.028748484
H	3.721829138	-3.415196839	-2.859865985
H	5.899970961	-3.801921569	-4.052699427
H	7.068444907	0.2591307389	-3.23363745
C	7.923452093	-1.956857721	-4.408887334

O	8.754914823	-1.085552324	-4.51373731
O	8.083962838	-3.194475886	-4.912516924
C	9.310323856	-3.442560733	-5.600195005
H	9.26905039	-4.487527382	-5.932071667
H	10.17150374	-3.286073156	-4.932570071
H	9.415689381	-2.770077259	-6.465435623

3.2.12 DSI-PABA-Bn

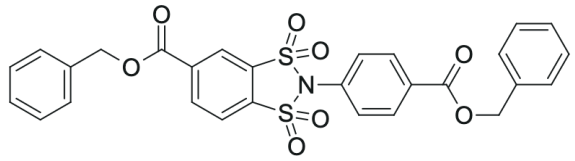

DClSBA-Bn (0.69 g, ~92 wt% purity by NMR, 1.55 mmol) was dissolved in 1,2-dichloroethane (DCE, 20 mL). A solution of benzyl p-aminobenzoate (PABA-Bn, 0.3525 g, 1.55 mmol) in DCE (10 mL) containing pyridine (0.30 mL, 3.72 mmol) was added under vigorous stirring. The reaction mixture was heated to 95–100 °C in an oil bath and refluxed for 4 hours.

After cooling to room temperature, the reaction mixture was poured into dichloromethane (DCM, 100 mL) and washed sequentially with 0.5 M HCl (2 × 50 mL) and water (1 × 50 mL). The organic phase was separated, dried over anhydrous $MgSO_4$, filtered, and concentrated under reduced pressure. The crude residue was further dried under vacuum at 100 °C for 30 minutes, followed by overnight drying at room temperature, yielding crude 4-[2-benzyloxycarbonyl]-N-(p-[2-benzyloxycarbonyl]phenyl)benzene-1,2-disulfonimide
(DSI-PABA-Bn) as an orange oily solid (0.64 g, ~45 wt% by NMR, 0.51 mmol), corresponding to a 32.94% yield for this step and an overall yield of 9.35 % based on the initially loaded 2-ATA over four steps.

^{1}H NMR (600 MHz, $CDCl_3$, ppm): δ =8.66 (s, 1H), 8.55 (d, J=8.6 Hz, 1H), 8.20 (d, J=8.7 Hz, 2H), 8.10 (d, J=8.7 Hz, 1H), 7.66 (d, J=8.4 Hz, 2H), 7.39–7.34 (m, 10H), 5.39 (s, 2H), 5.34 (s, 2H);

Note: A ^{13}C NMR spectrum was recorded but not attributed due to the moderate compound purity (~45 wt%). Hydrogenative deprotections were performed without prior isolation of the target DSI, since final purification was intended after the deprotection step.

3.2.13 DSI-PABA-EtOH

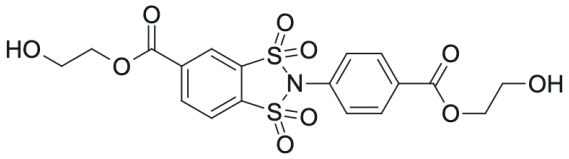

Freshly prepared and dried DClSBA-EtOH (0.41 g, ~90 % purity by NMR, 1.02 mmol) was dissolved in tetrahydrofuran (THF, 10 mL) and added in one portion to a stirred solution of PABA-EtOH (0.1841 g, 1.02 mmol) in THF (10 mL) containing pyridine (0.20 mL, 2.48 mmol). The mixture was diluted with 1,2-dichloroethane (DCE, 10 mL) and refluxed at 82 °C for 4 h, during which the separation of a red, oily fraction was observed. After cooling to room temperature, the reaction mixture was concentrated under reduced pressure. The crude residue was purified by flash column chromatography on silica gel, using ethyl acetate as the eluent. The product-containing fraction was concentrated, dissolved in ethyl acetate (10 mL), washed with 0.5 M HCl (10 mL), dried over anhydrous $MgSO_4$, filtered, and concentrated under reduced pressure. The resulting residue was dried under vacuum at room temperature for 72 h to afford

4-[2-hydroxyethoxycarbonyl]-N-(p-[4-hydroxyethoxycarbonyl]phenyl)benzene-1,2-disulfonimide (DSI-PABA-EtOH) as a brown–orange oily solid (0.06 g, ~85–90 wt % purity by NMR, 0.11 mmol), corresponding to a yield of 10.4 % for this step and an overall yield of 2.0 % over four synthetic steps from the initially loaded 2-ATA.

Rf = 0.68 (EtAc); ^{1}H NMR (400 MHz, [D_6]DMSO, ppm): δ =9.13 (d, J=1.0 Hz, 1H), 8.79 (d, J=8.3 Hz, 1H), 8.70 (dd, J=1.4, 8.3 Hz, 1H), 8.30 (td, J=2.2, 9.0 Hz, 2H), 7.80 (td, J=2.2, 8.9 Hz, 2H), 5.10 (t, J=6.3 Hz, 1H), 4.98 (t, J=5.7 Hz, 1H), 4.40–4.33 (m, 4H), 3.78–3.70 (m, 4H); ^{1}H NMR (400 MHz, [D_8]THF, ppm): δ =8.83 (d, J=1.0 Hz, 1H), 8.59 (dd, J=1.4, 8.3 Hz, 1H), 8.38 (d, J=8.3 Hz, 1H), 8.16 (td, J=2.2, 9.0 Hz, 2H), 7.64 (td, J=2.2, 8.9 Hz, 2H), 4.34 (t, J=5.0 Hz, 2H), 4.28 (t, J=5.0 Hz, 2H), 4.08 (t, J=6.3 Hz, 1H), 3.92 (t, J=5.7 Hz, 1H), 3.66–3.76 (m, 4H); ^{13}C NMR (101 MHz, [D_6]DMSO, ppm): δ =165.2 (s), 163.4 (s), 137.2 (s), 136.0 (s), 134.9 (s), 133.6 (s), 132.4 (s), 131.9 (s), 131.3 (s), 129.3 (s), 124.8 (s), 124.7 (s), 68.7 (s), 67.7 (s), 59.5 (s), 59.3 (s); IR (cm^{-1}): ν = 574, 608, 695, 736, 921, 946, 1075, 1124, 1151, 1172, 1212, 1216-1248, 1275, 1352-1360, 1606, 1700-1731, 2800 - 3200, 3100 - 3400.

During the formation of DSI-PABA-EtOH, an oily precipitate separated from the reaction mixture. Given the known insolubility of pyridinium hydrochloride in ethers such as THF, [30] the precipitate was hypothesized to consist mainly of pyridinium salts. NMR analysis of both the supernatant and precipitated phases confirmed that the oily phase predominantly contained pyridinium species, while the desired product was present in both phases. To investigate the impact of reaction heterogeneity on yield, several experiments were conducted using alternative solvents. Similar reactions performed in acetonitrile and DMF proceeded homogeneously but afforded significantly lower yields (~3% in acetonitrile; no product isolated from DMF). The reduced yield in acetonitrile was attributed to possible side reactions between the solvent and the chlorosulfonyl group.[31] In the case of DMF, the complete absence of isolated product was unexpected, but it may be explained by the formation of a catalytic complex between DMF and the chlorosulfonyl species,[32] potentially promoting an undesired reaction pathway over DSI formation, for reasons that remain unclear. These results suggest that polar, non-coordinating solvents could be more favourable for DSI formation, though further investigation is needed to support this conclusion.

Note: Elemental analysis was not performed, as homologous DSI-PABA-Me exhibited unreliable results under the applied conditions.

DSI-PABA-EtOH FTIR Spectrum

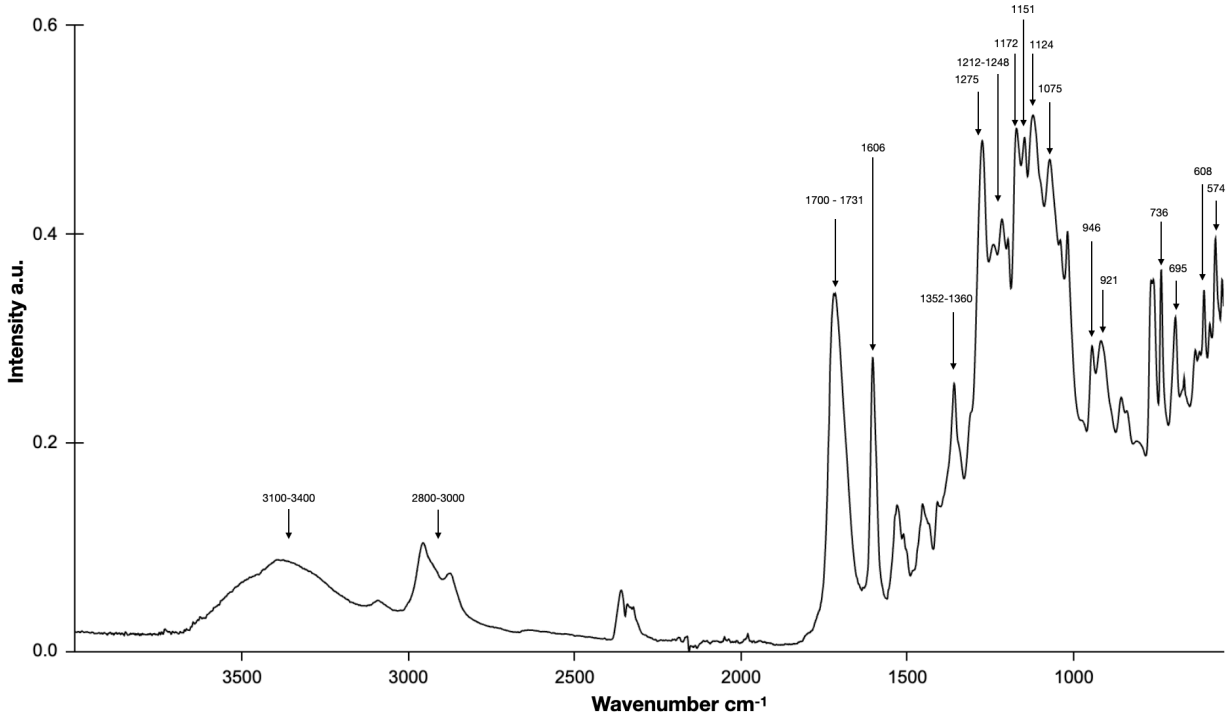

Figure S10. FTIR Spectrum of DSI-PABA-EtOH, detailed band assignments are provided in Table S6.

Table S6. Assignment of key vibrational bands in the FTIR spectrum of DSI-PABA-EtOH.

Wavenumber, cm^{-1}	Assignment
574	DSI - cycle deformations (bending and stretching)
608	DSI - cycle deformations (symmetric SO_2 wagging)
695	N in cycle deformation (asymmetric stretch S-N-S)
736	N in cycle deformation (symmetric stretch S-N-S)
921	N in cycle deformation (rocking S-N-S)
946	N in cycle deformation (scissoring S-N-S)
1075	C-O stretching in hydroxy-ethoxy fragment
1124	SO_2 in DSI (SO_2 near carboxyl symmetric stretching, asymmetric to other SO_2)
1151	SO_2 in DSI (SO_2 further from carboxyl symmetric stretching, asymmetric to other SO_2)
1172	SO_2 - cycle deformations (symmetric SO_2 and DSI cycle stretching)
1212	Ester methyls wagging
1216-1248	N in cycle deformation (N-C in PABA core stretching), and SO_2 cycle deformations (C-S-N mutually asymmetric scissoring)
1275	C-CO-O asymmetric stretchings
1352-1360	SO_2 vibrations (S-N-S twisting, SO_2 (O=S=O asymmetric) mutually asymmetric stretching)
1606	PABA-EtOH and DClSBA-EtOH benzene ring deformations
1700-1731	C=O stretching in Ester groups
2800 - 3200	C-H stretchings in the hydroxy(ethoxy fragment)
3100 - 3400	O-H stretchings

B3LYP-optimised geometry of DSI-PABA-EtOH

Table S7. Atomic coordinates (Å) of the optimised DSI-PABA-EtOH conformer. (Energy = -2297.109 Hartree)

Atom	x	y	z
H	0.954885	-1.223738	2.272441
C	0.504866	-0.816165	1.364652
C	-0.831785	-0.409568	1.34081
H	-1.443168	-0.484765	2.240712
C	-1.410399	0.088275	0.160046
C	-0.652591	0.189462	-1.01711
H	-1.121629	0.560939	-1.930542
C	0.680231	-0.203088	-0.977385
C	1.24952	-0.700642	0.192726
S	1.78029	-0.11258	-2.391831
S	2.976098	-1.167915	0.069316
N	2.967126	-1.156635	-1.666719
C	-2.848059	0.515499	0.089983
O	-3.367553	0.941796	-0.913976
O	-3.481552	0.359765	1.262855
C	-4.874848	0.712827	1.320187
C	-5.069859	2.202953	1.610544
H	-5.302127	0.112268	2.13484
H	-5.35759	0.439879	0.368903
O	1.202409	-0.801729	-3.536709
O	2.296662	1.245549	-2.537446
O	3.167014	-2.540742	0.518466
O	3.819639	-0.100061	0.597515
C	4.224242	-1.327158	-2.338107
C	5.14531	-0.271478	-2.42024
C	4.514385	-2.579059	-2.89709
C	5.732779	-2.779415	-3.543203
C	6.65998	-1.728214	-3.63406
C	6.358734	-0.477004	-3.073542
H	4.899404	0.692503	-1.974066
H	3.777812	-3.379782	-2.813433
H	5.97355	-3.748983	-3.980152
H	7.094974	0.324685	-3.155961
C	7.98532	-1.888354	-4.311879

O	8.8043	-1.004218	-4.41489
O	8.170231	-3.135385	-4.789278
C	9.417532	-3.418422	-5.438242
H	9.58768	-4.496876	-5.312009
H	10.224341	-2.858391	-4.939649
C	9.373459	-3.068398	-6.927279
O	-6.435386	2.498498	1.786633
H	-4.606229	2.802005	0.804248
H	-4.556511	2.458625	2.551809
H	-6.864803	2.502281	0.920886
O	10.56736	-3.458024	-7.568034
H	9.161536	-1.989036	-7.04662
H	8.550952	-3.623446	-7.406989
H	11.266357	-2.841797	-7.312019

3.2.14 Model Polycondensation

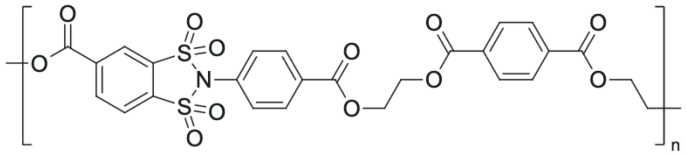

Approximately 3 mg of DSI-PABA-EtOH (additionally purified by preparative TLC using ethyl acetate as an eluent) was dried under vacuum at 40 °C for 48 hours, dissolved in 0.4 mL of THF-d_8, and transferred into a pressure-resistant NMR tube equipped with a PTFE valve, which had been pre-dried at 200 °C for 2 h. A solution of p-xylene in THF-d_8 (0.1708 g, c = 0.0227 $g \cdot g^{-1}$; total p-xylene 3.88 mg, 0.0365 mmol) was added as an internal reference. The precise amount of DSI-PABA-EtOH was determined by quantitative ^{1}H NMR (2.65 mg, 0.0056 mmol) using the p-xylene signal as an internal standard. Subsequently, terephthaloyl chloride (TPA, 4.4 mg, 0.0217 mmol, 4 equiv) and a solution of triethylamine in THF-d_8 (0.3 g, c = 0.0146 $g \cdot g^{-1}$; total TEA 4.38 mg, 0.0433 mmol) were added. The tube was degassed and filled with dry nitrogen.

The reaction mixture was maintained at room temperature for 24 h, after which the ^{1}H NMR spectrum was recorded.

The resonance at δ 8.25 ppm was assigned to aromatic protons of unreacted TPA (added in excess). The multiplet at δ 8.18 - 8.05 ppm is most plausibly attributed to mono-adducts of TPA formed with water and/or the diol, as indicated by HMBC correlations to carbons at δ ~165 ppm (carboxylic acid/ester C=O) and δ 161.1 ppm (acyl chloride C=O), which overlap with signals from the PABA aromatic ring (arising from both unreacted and esterified species). The overlapping resonances at δ 8.03 - 7.95 ppm can be assigned to terephthaloyl units incorporated into the target di-ester linkages, which is further supported by its correlation to carbons at δ 165.0 ppm (ester C=O) on the HMBC (Figure 4b). The signals at δ 7.66–7.61 ppm are attributed to PABA-ring protons, with overlapping contributions from the monomer and the esterified product. HMBC spectra further showed that the carbon signal adjacent to the DSI nitrogen remained at approximately δ 129 ppm, indicating that the DSI moiety remained chemically intact throughout the reaction. Despite employing a fourfold excess of TPA, the ^{1}H NMR data suggest a conversion of roughly 50%, most likely limited by residual water in the reaction mixture; the resonances of the esterified monomer appear slightly upfield and partially overlap with those of the unreacted diol.

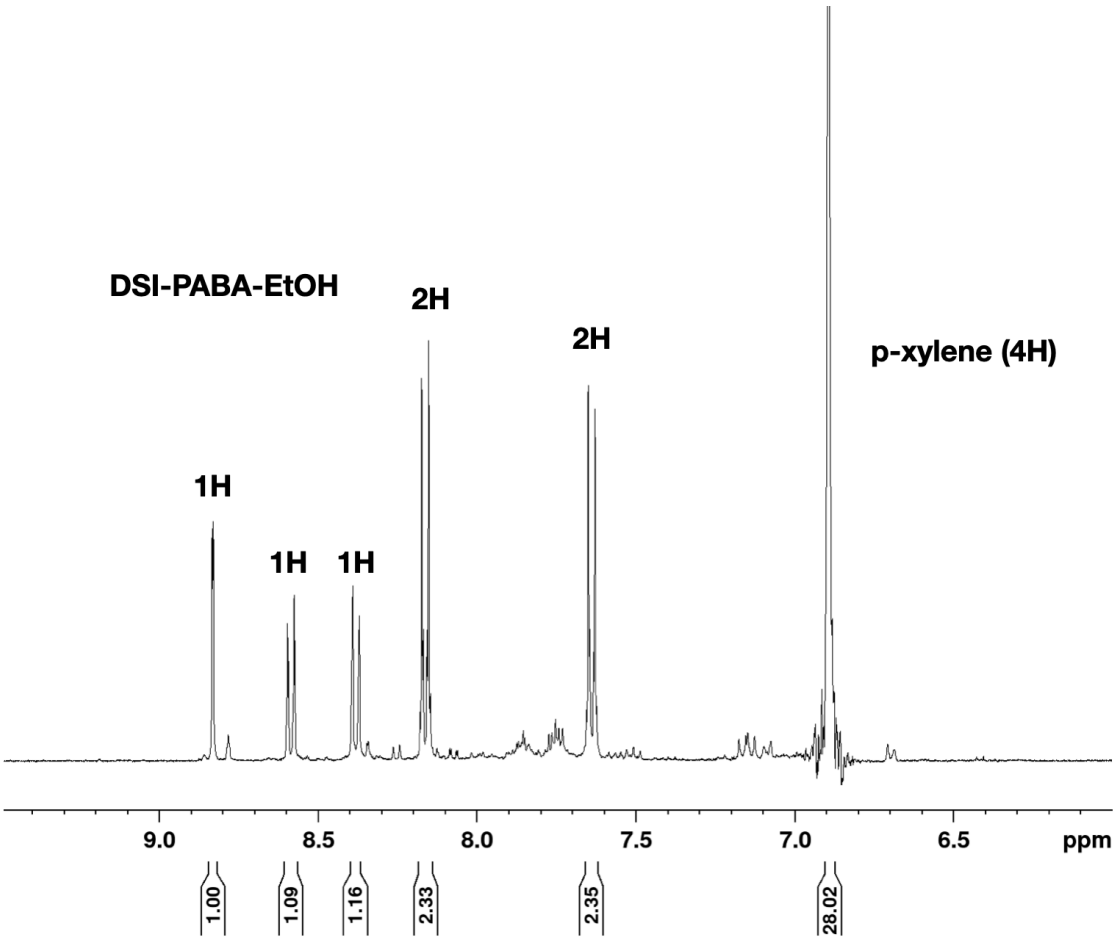

Figure S11. Integrated spectra of the DSI-PABA-EtOH (THF-d_8, 400 MHz) with p-xylene standard, used for quantitative NMR calculations.

4. References

[20] F. Neese, Comput Mol Sci 2011, 2, 73–78.
https://doi.org/10.1002/wcms.81

[21] T. A. Halgren, J. Comput. Chem. 1996, 17, 490–519.
https://doi.org/10.1002/(SICI)1096-987X(199604)17:5/6<490::AID-JCC1>3.0.CO;2-P

[22] P. Eastman, R. Galvelis, R. P. Peláez, C. R. A. Abreu, S. E. Farr, E. Gallicchio, A. Gorenko, M. M. Henry, F. Hu, J. Huang, A. Krämer, J. Michel, J. A. Mitchell, V. S. Pande, J. P. Rodrigues, J. Rodriguez-Guerra, A. C. Simmonett, S. Singh, J. Swails, P. Turner, Y. Wang, I. Zhang, J. D. Chodera, G. De Fabritiis, T. E. Markland, J. Phys. Chem. B 2023, 128, 109–116.
https://doi.org/10.1021/acs.jpcb.3c06662

[23] W. L. Jorgensen, D. S. Maxwell, J. Tirado-Rives, J. Am. Chem. Soc. 1996, 118, 11225–11236.
https://doi.org/10.1021/ja9621760

[24] L. S. Dodda, I. Cabeza de Vaca, J. Tirado-Rives, W. L. Jorgensen, Nucleic Acids Research 2017, 45, W331–W336.
https://doi.org/10.1093/nar/gkx312

[25] S. V. Lyulin, A. A. Gurtovenko, S. V. Larin, V. M. Nazarychev, A. V. Lyulin, Macromolecules 2013, 46, 6357–6363.
https://doi.org/10.1021/ma4011632

[26] S. V. Lyulin, S. V. Larin, A. A. Gurtovenko, V. M. Nazarychev, S. G. Falkovich, V. E. Yudin, V. M. Svetlichnyi, I. V. Gofman, A. V. Lyulin, 'Thermal properties of bulk polyimides: insights from computer modeling versus experiment' Soft Matter 2014, 10, 1224.
https://doi.org/10.1039/C3SM52521J

[27] L. Martínez, R. Andrade, E. G. Birgin, J. M. Martínez, 'PACKMOL: A package for building initial configurations for molecular dynamics simulations' J Comput Chem 2009, 30, 2157–2164.
https://doi.org/10.1002/jcc.21224

[28] F. Brisse and S. Pérez, Etudes conformationnelles de dérivés d'oligométhylène glycols et de composés apparentés. V. Structure cristalline et moléculaire du téréphtalate de méthyle, C10H10O4, Acta Crystallogr B Struct Sci, 1976, 32, 2110–2115.
https://doi.org/10.1107/S0567740876007218

[29] R. E. H. Kuveke, L. Barwise, Y. van Ingen, K. Vashisth, N. Roberts, S. S. Chitnis, J. L. Dutton, C. D. Martin, R. L. Melen, 'An International Study Evaluating Elemental Analysis' ACS Cent. Sci. 2022, 8, 855–863.
https://doi.org/10.1021/acscentsci.2c00325

[30]M. D. Taylor and L. R. Grant, Preparation of anhydrous pyridine hydrochloride, J. Chem. Educ., 1955, 32, 39.
https://doi.org/10.1021/ed032p39

[31] Y. Markushyna, M. Antonietti and A. Savateev, Synthesis of Sulfonyl Chlorides from Aryldiazonium Salts Mediated by a Heterogeneous Potassium Poly(heptazine imide) Photocatalyst, ACS Org. Inorg. Au, 2021, 2, 153–158.
https://doi.org/10.1021/acsorginorgau.1c00038

[32] J. D. Albright, E. Benz, A. E. Lanzilotti and L. Goldman, Reactions of sulphonyl chloride–NN-dimethylformamide complexes, Chem. Commun. (London), 1965, 0, 413–414.
https://doi.org/10.1039/C19650000413

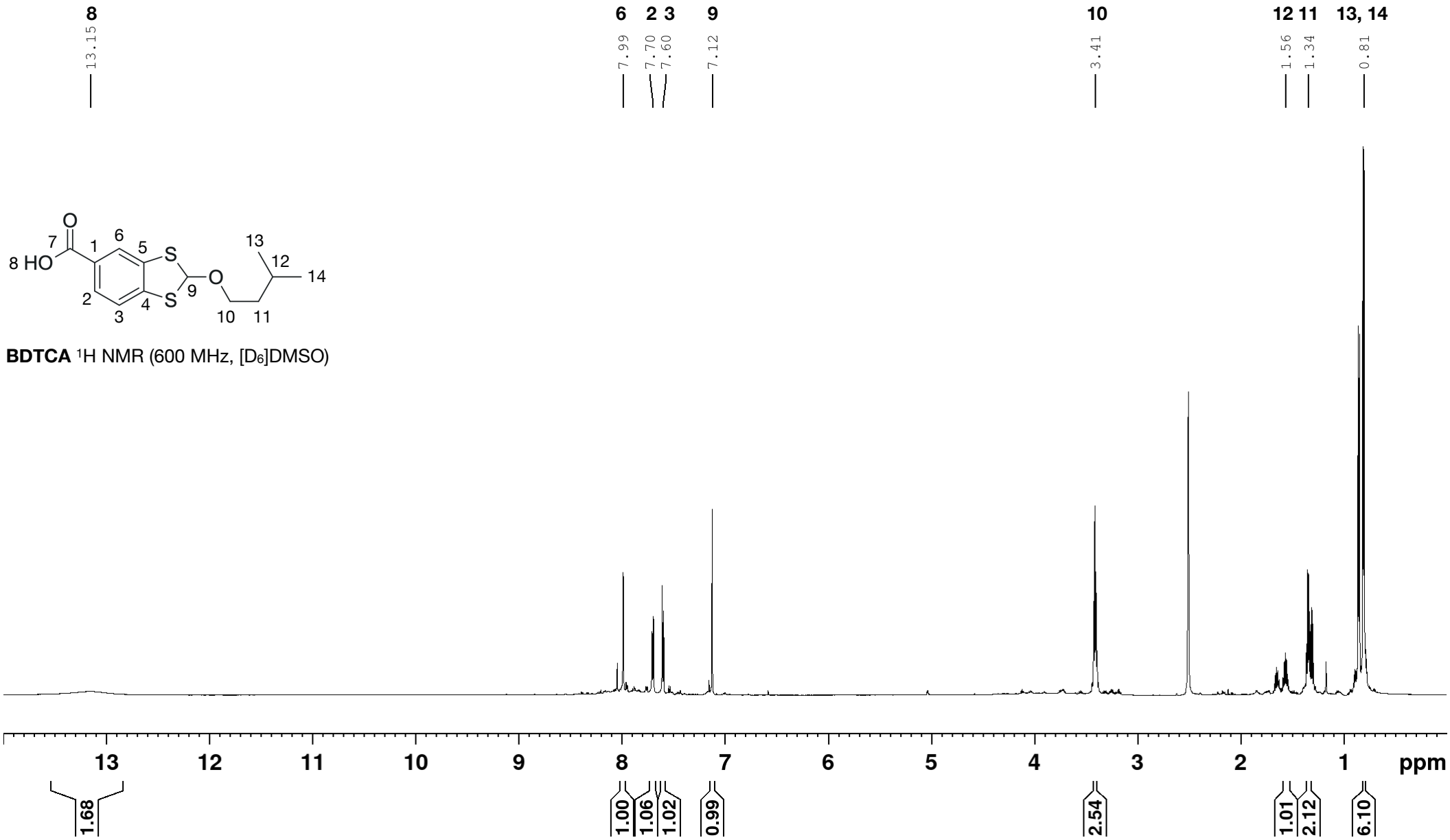

BDTCA ^{1}H NMR (600 MHz, [D$_6$]DMSO)

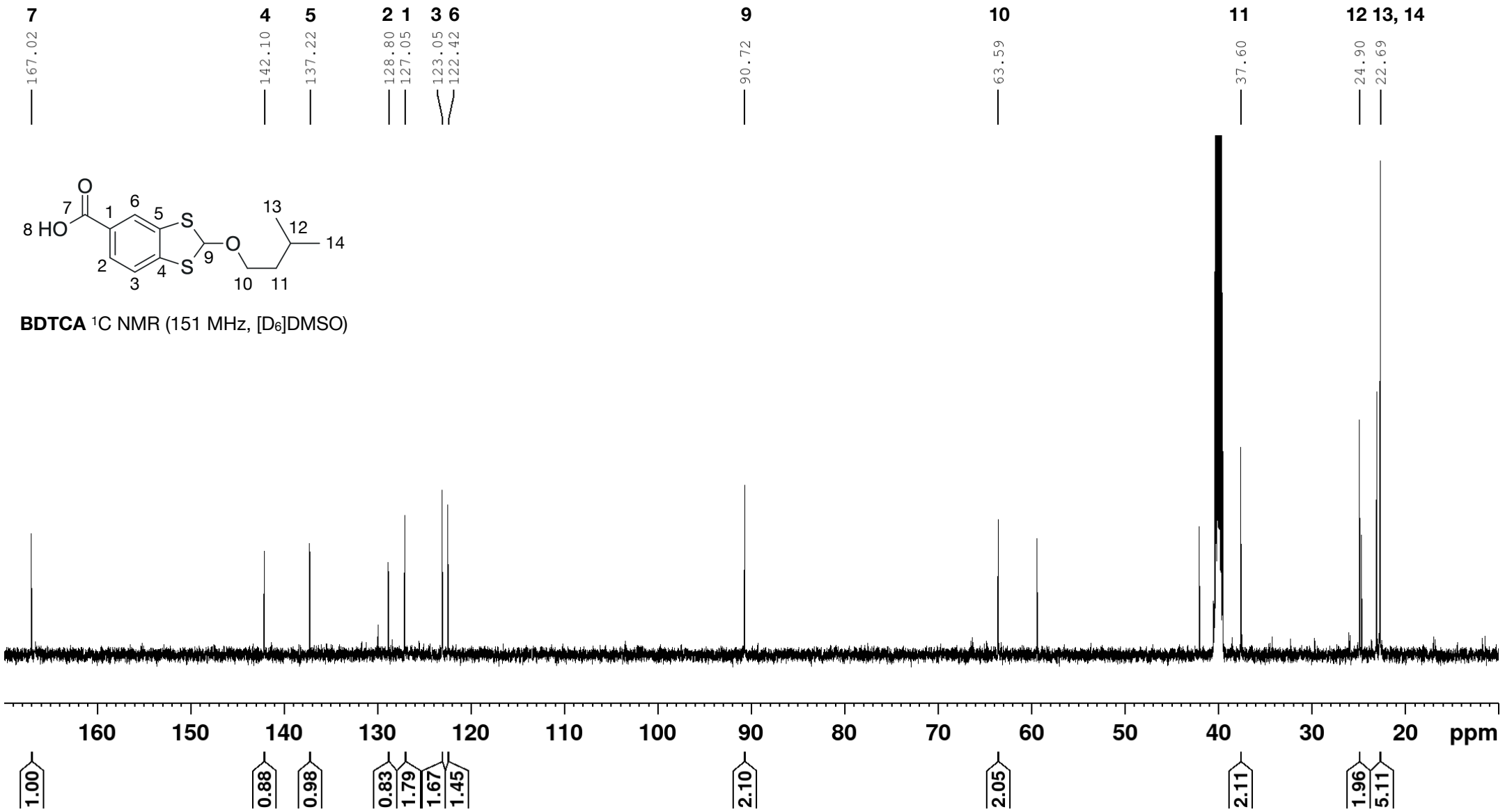

BDTCA ^{1}C NMR (151 MHz, [D$_6$]DMSO)

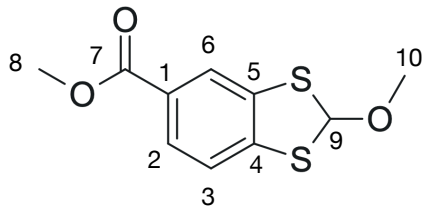

BDTCA-Me ^{1}H NMR (400 MHz, [D$_6$]DMSO)

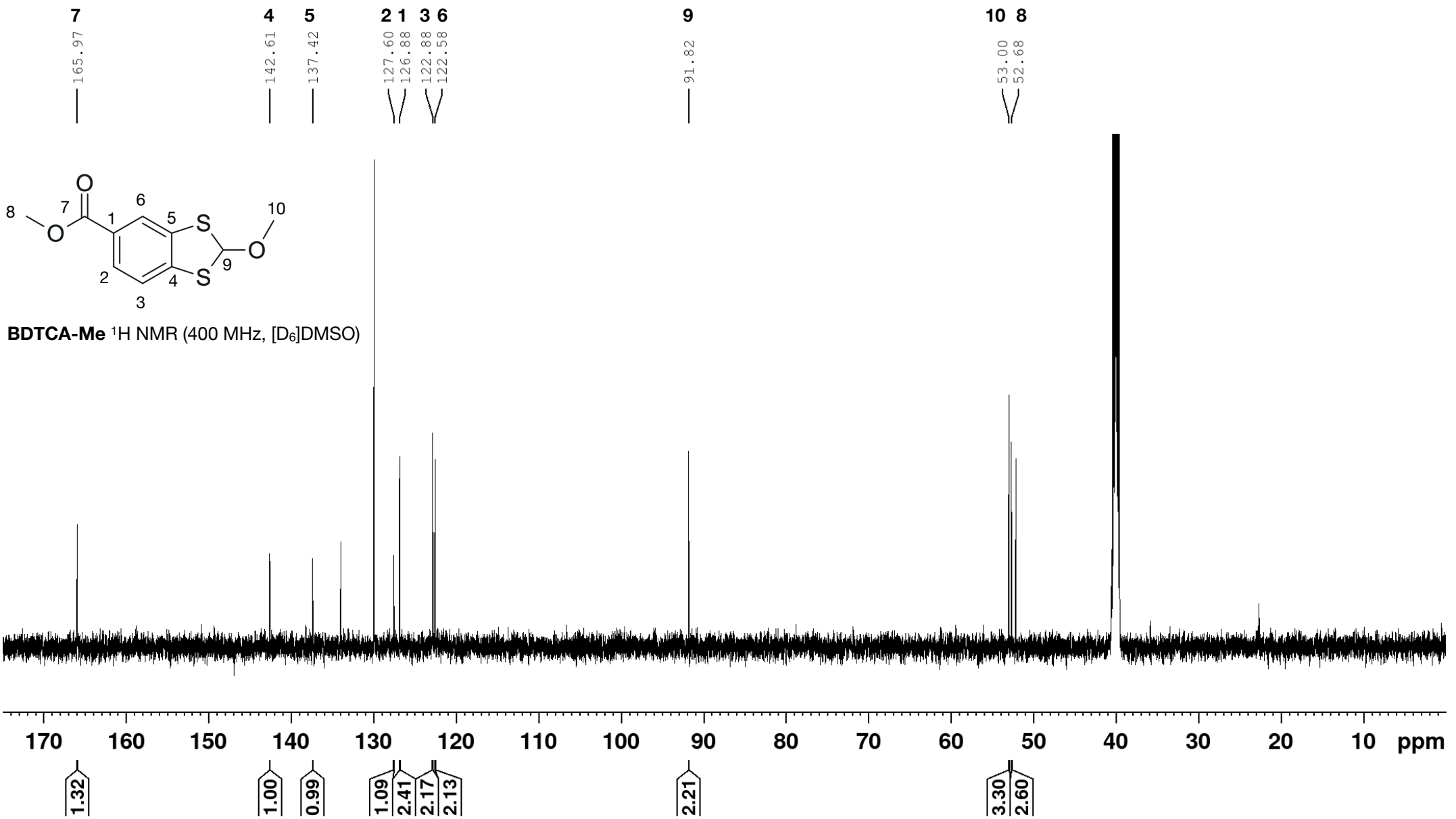
7
4
5
2 1 3 6
9
10 8
165.97
142.61
137.42
127.60
126.88
122.88
122.58
91.82
53.00
52.68
8
7
O
O
1
6
5
S
10
O
9
2
4
S
3
BDTCA-Me 1H NMR (400 MHz, [D6]DMSO)
170
160
150
140
130
120
110
100
90
80
70
60
50
40
30
20
10
ppm
1.32
1.00
0.99
1.09
2.41
2.17
2.13
2.21
3.30
2.60

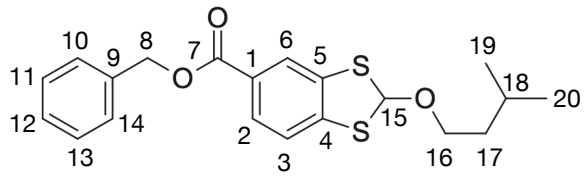

BDTCA-Bn ^{1}H NMR (400 MHz, [D$_6$]DMSO)

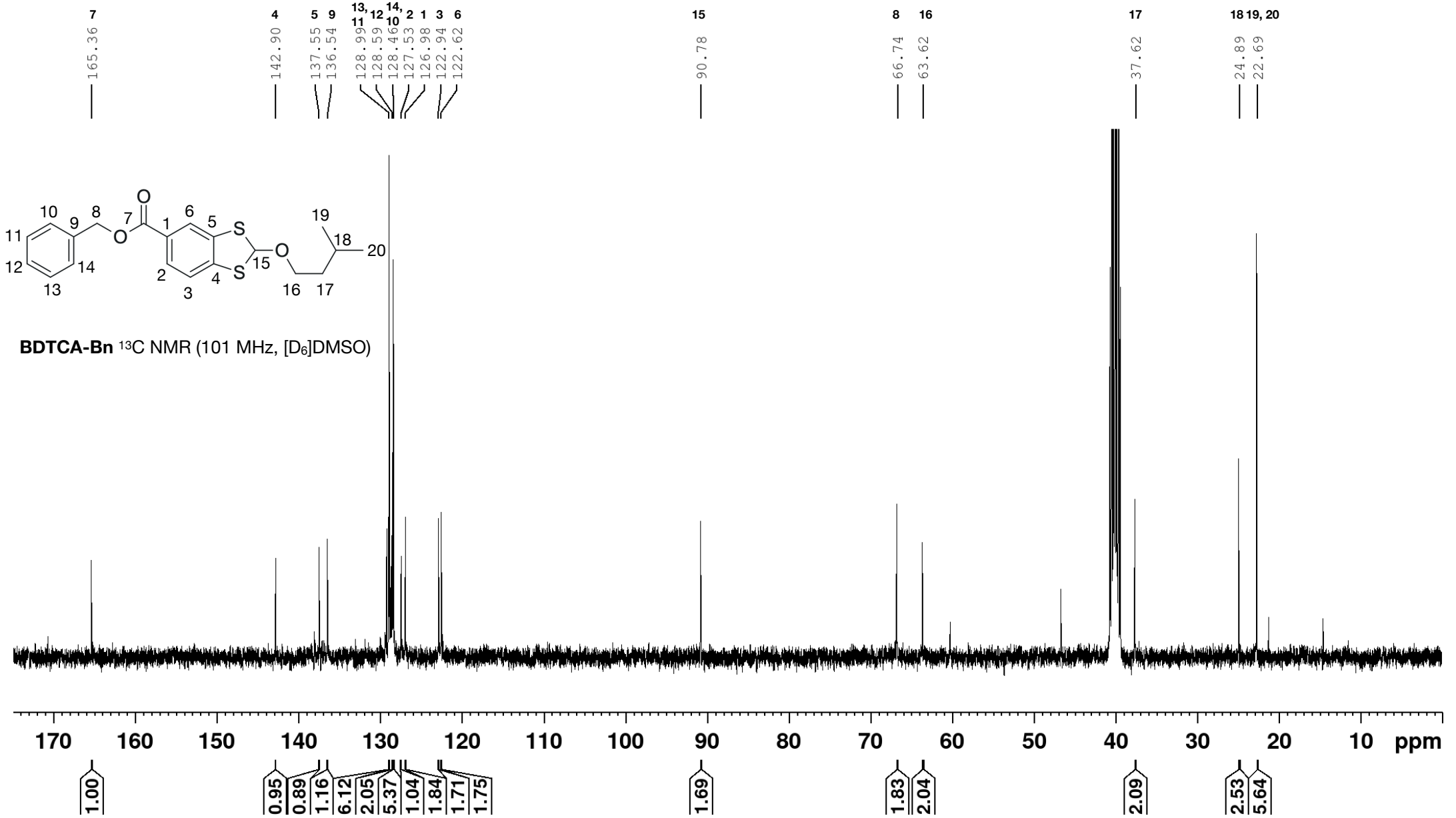
7 4 5 9 13, 11 12 14, 10 2 1 3 6 15 8 16 17 18 19, 20
165.36 142.90 137.55 136.54 128.99 128.59 128.46 127.53 126.98 122.94 122.62 90.78 66.74 63.62 37.62 24.89 22.69
O 7 O 8 10 9 11 12 13 14 1 6 5 S 2 3 4 S 15 O 16 17 18 19 20
BDTCA-Bn 13C NMR (101 MHz, [D6]DMSO)
170 160 150 140 130 120 110 100 90 80 70 60 50 40 30 20 10 ppm
1.00 0.95 0.89 1.16 6.12 2.05 5.37 1.04 1.84 1.71 1.75 1.69 1.83 2.04 2.09 2.53 5.64

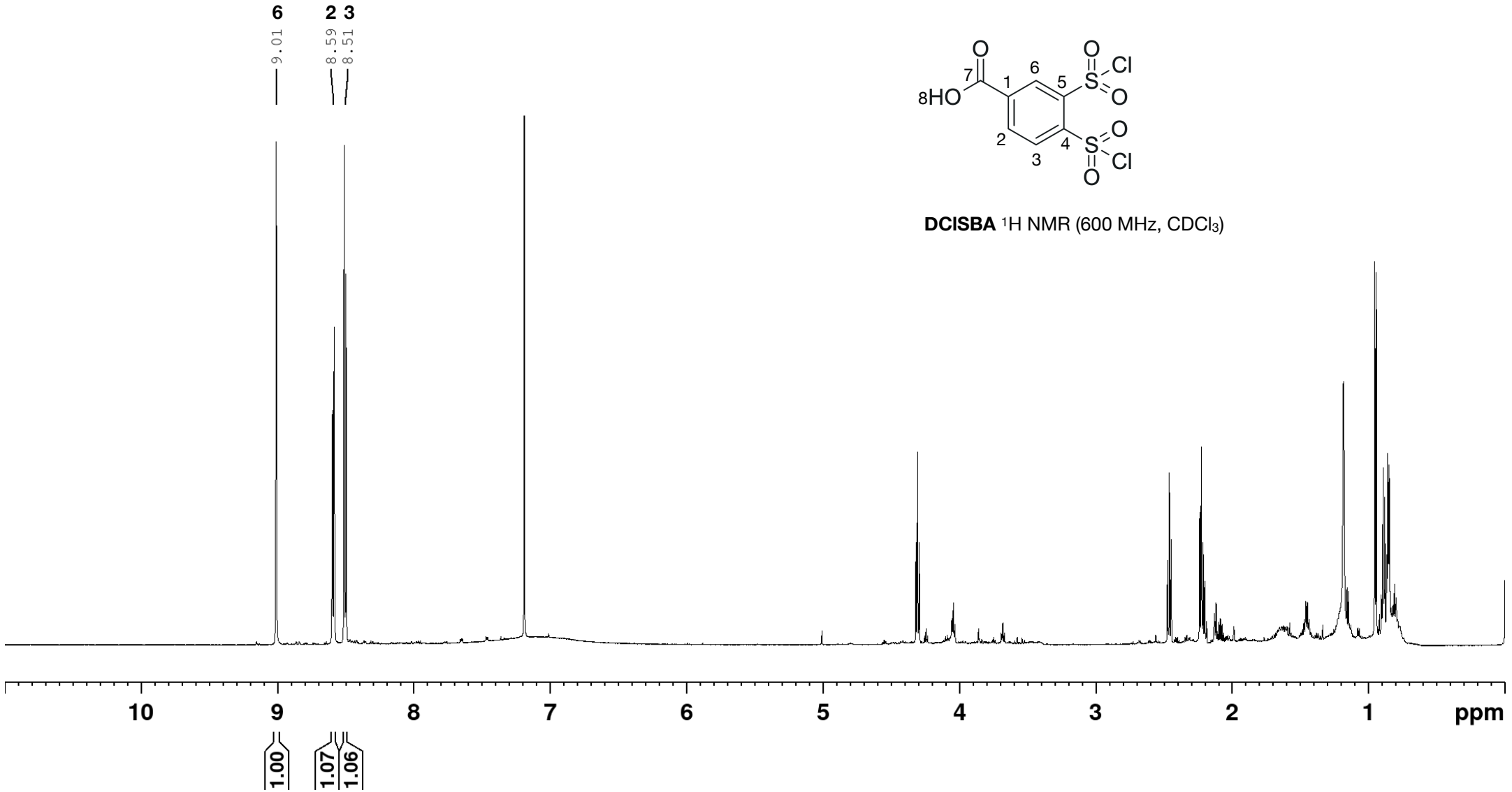

DClSBA ^{1}H NMR (600 MHz, $CDCl_3$)

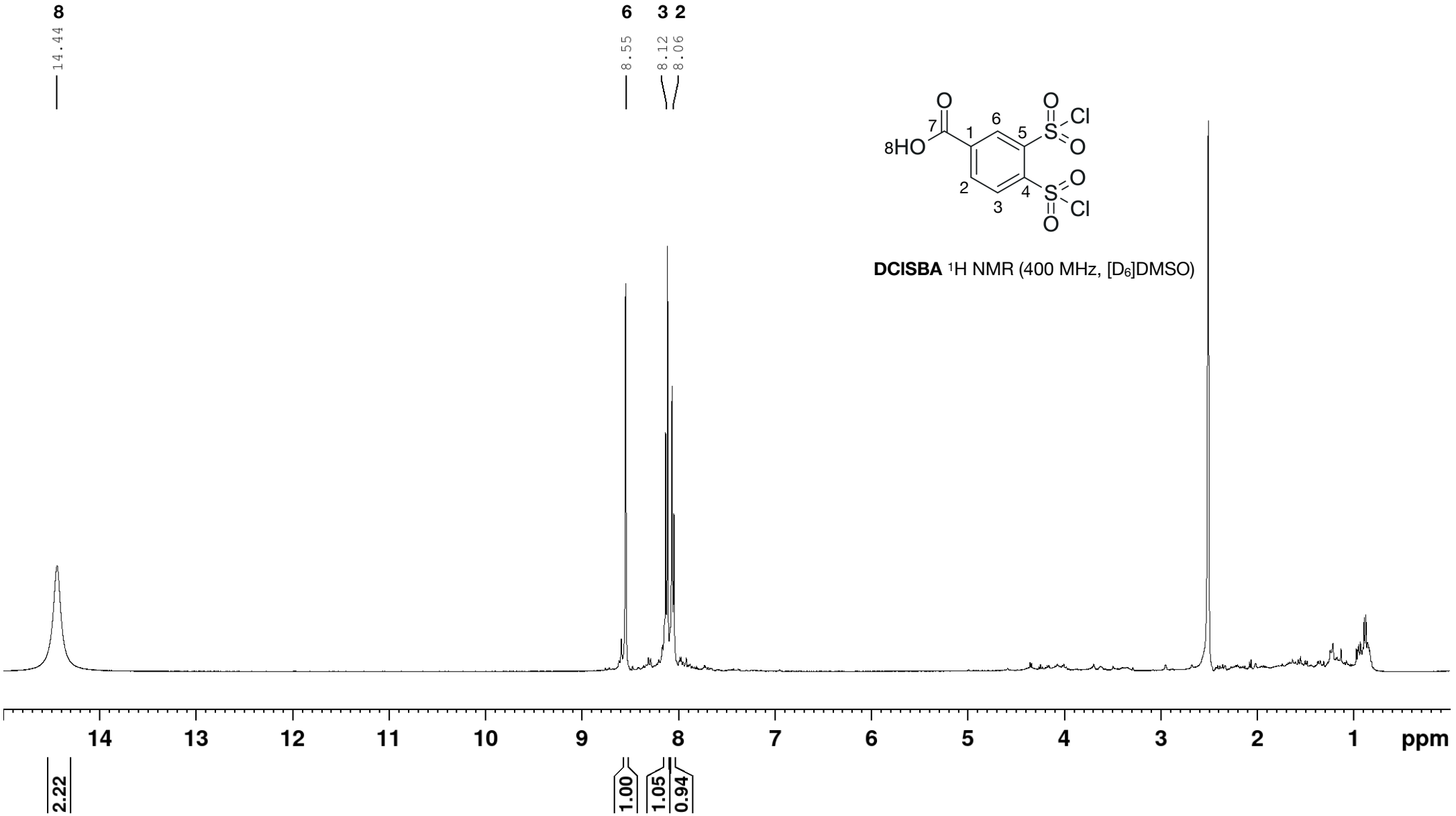
8
14.44
6
8.55
3
8.12
2
8.06
O
7
6
Cl
1
5
S
8HO
O
O
2
4
S
O
3
Cl
O
DCISBA 1H NMR (400 MHz, [D6]DMSO)
14
13
12
11
10
9
8
7
6
5
4
3
2
1
ppm
2.22
1.00
1.05
0.94

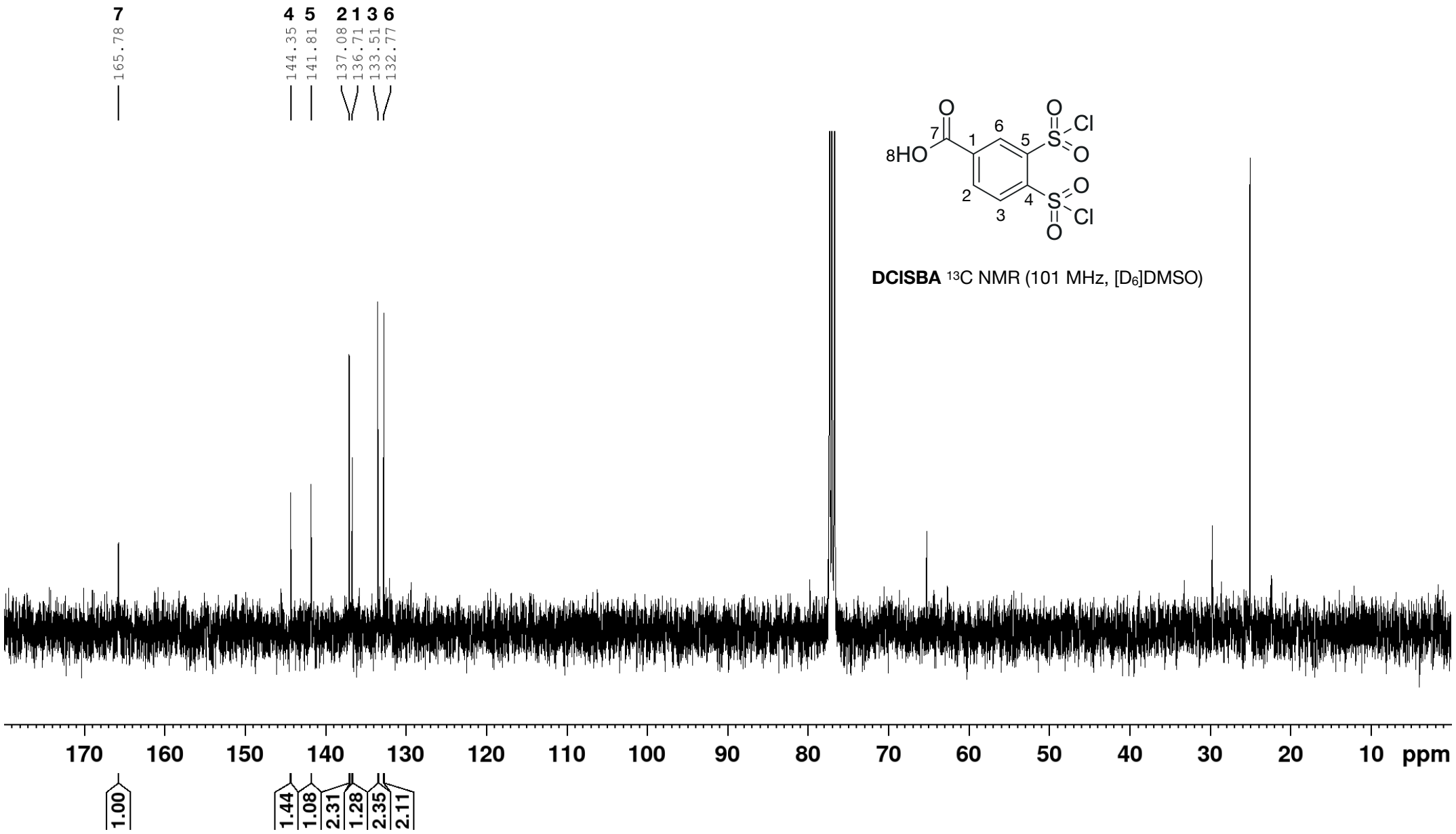
7
165.78
4 5 2 1 3 6
144.35
141.81
137.08
136.71
133.51
132.77
O
O
Cl
7
6
1
5
S
8HO
O
2
4
S
O
3
Cl
O
DClSBA 13C NMR (101 MHz, [D6]DMSO)
170 160 150 140 130 120 110 100 90 80 70 60 50 40 30 20 10 ppm
1.00
1.44
1.08
2.31
1.28
2.35
2.11

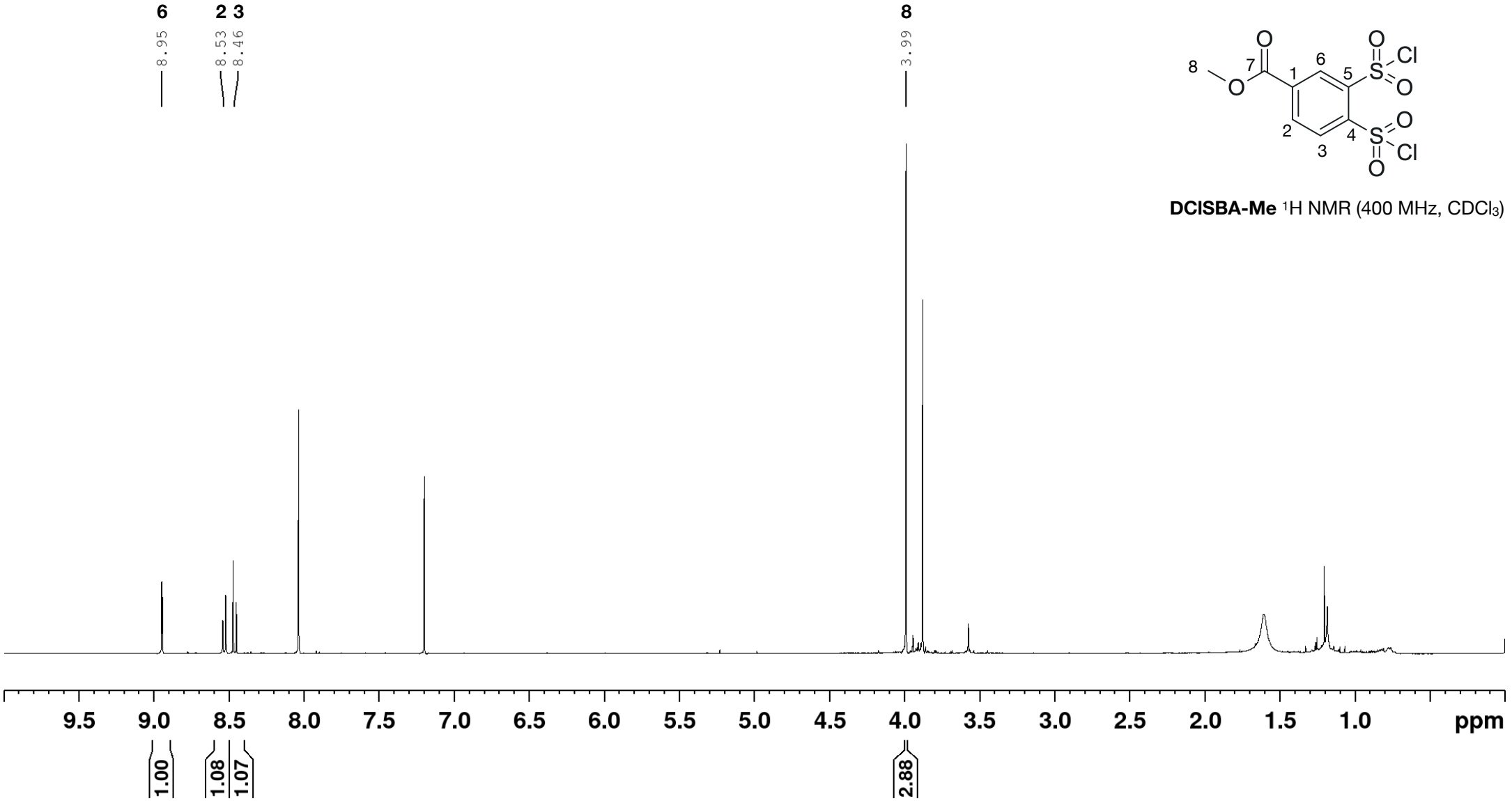

DClSBA-Me ^{1}H NMR (400 MHz, $CDCl_3$)

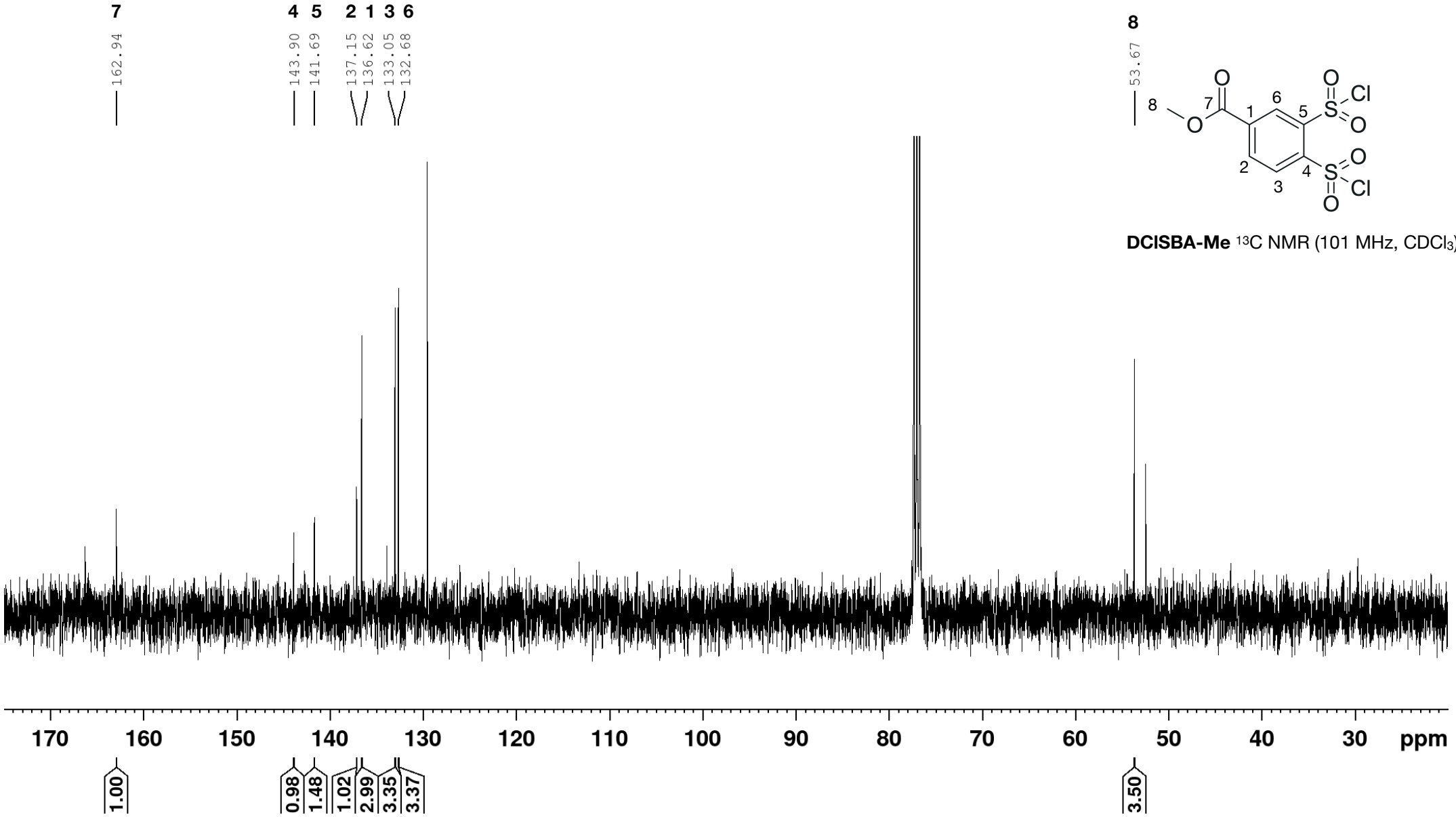

DClSBA-Me ^{13}C NMR (101 MHz, $CDCl_3$)

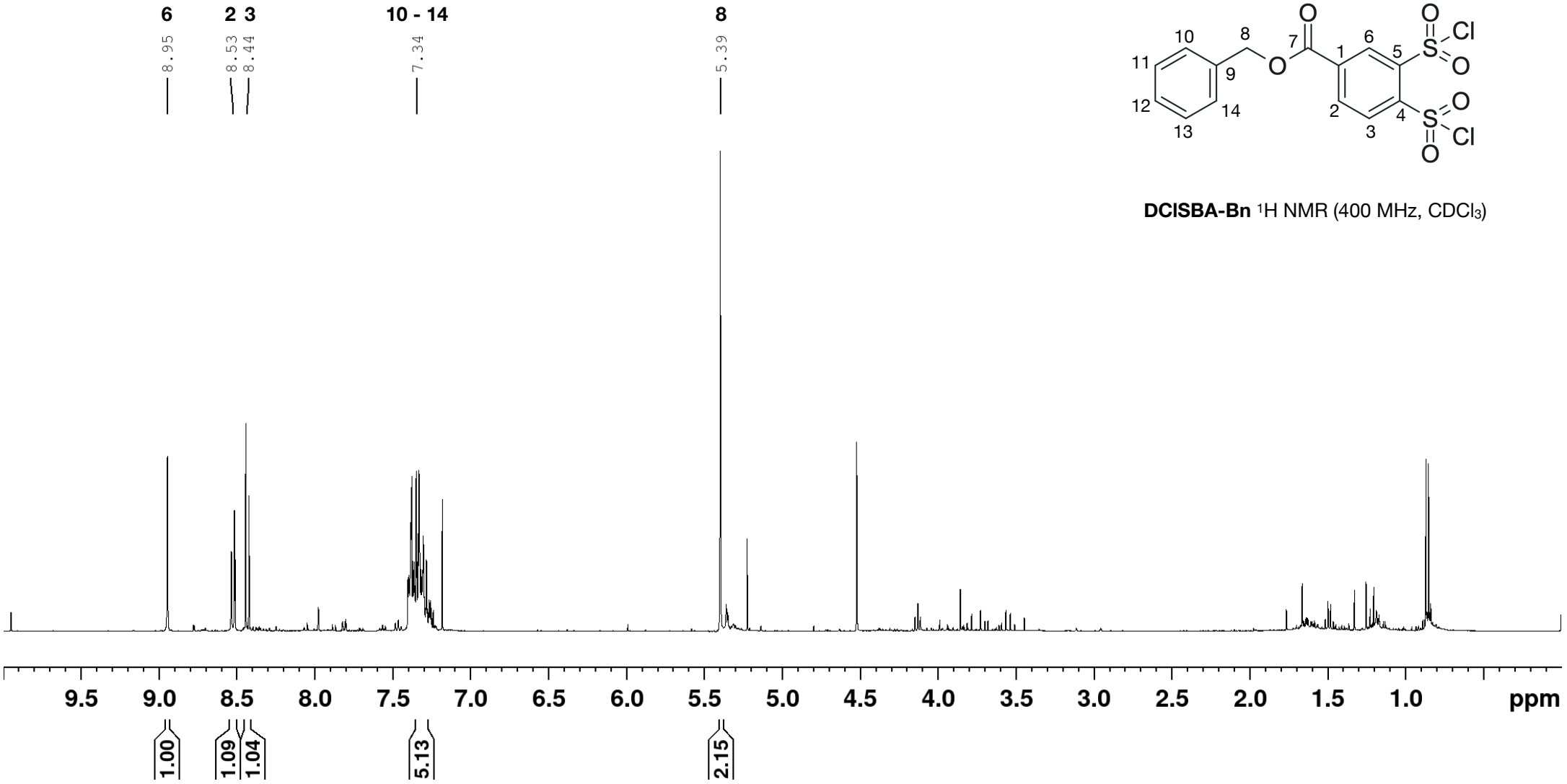

DClSBA-Bn ^{1}H NMR (400 MHz, $CDCl_3$)

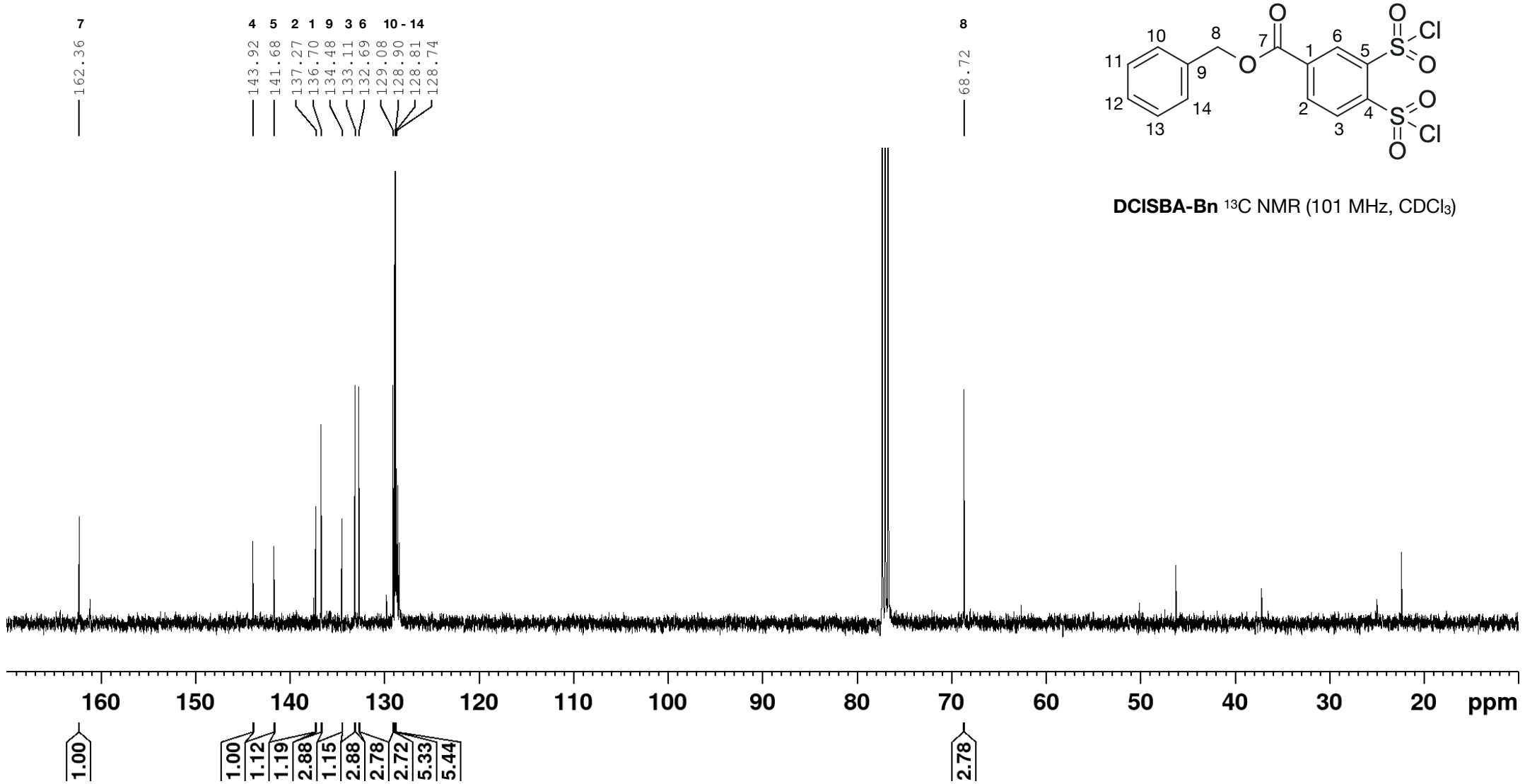

DClSBA-Bn ^{13}C NMR (101 MHz, $CDCl_3$)

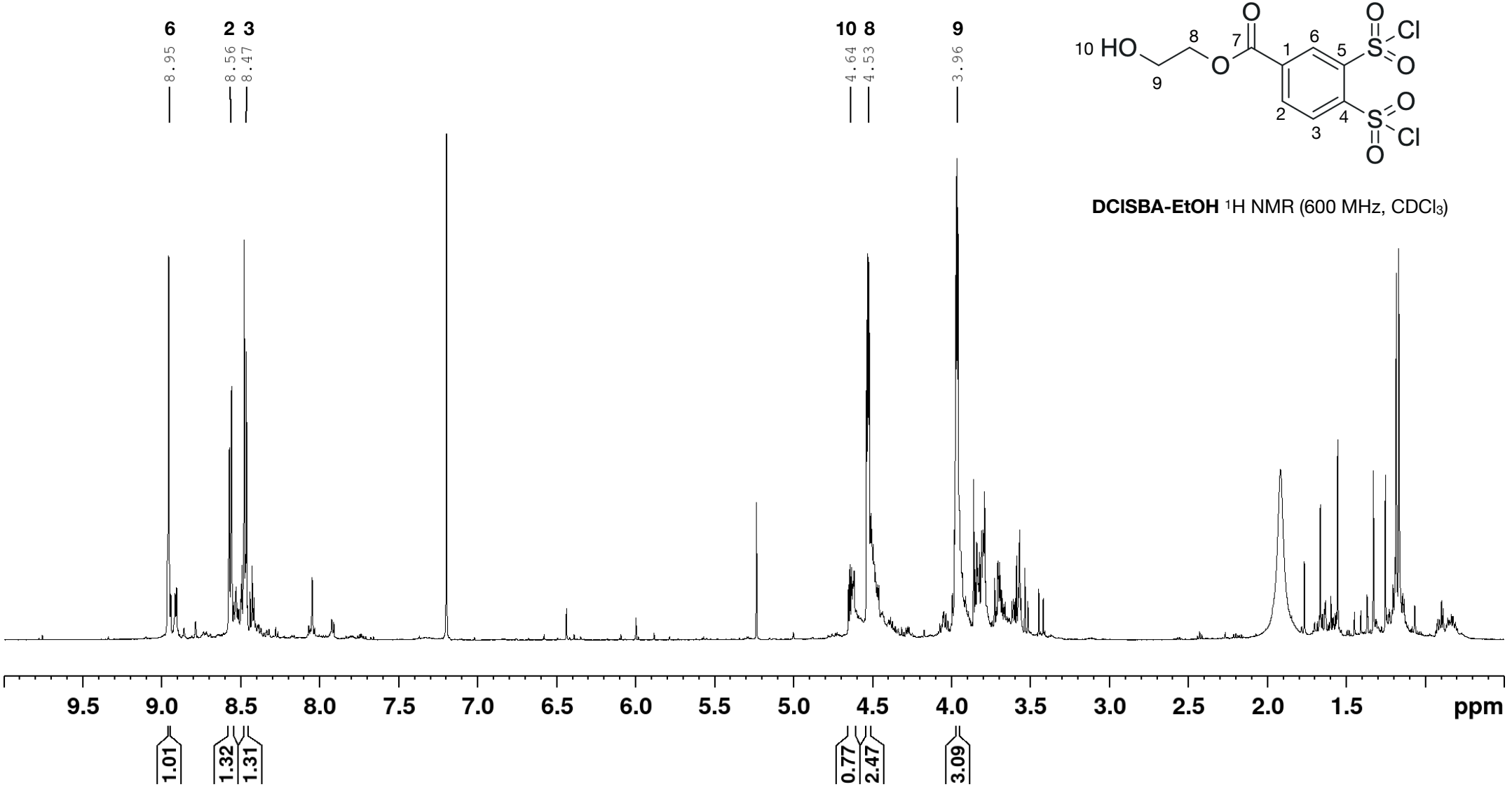

DClSBA-EtOH ^{1}H NMR (600 MHz, $CDCl_3$)

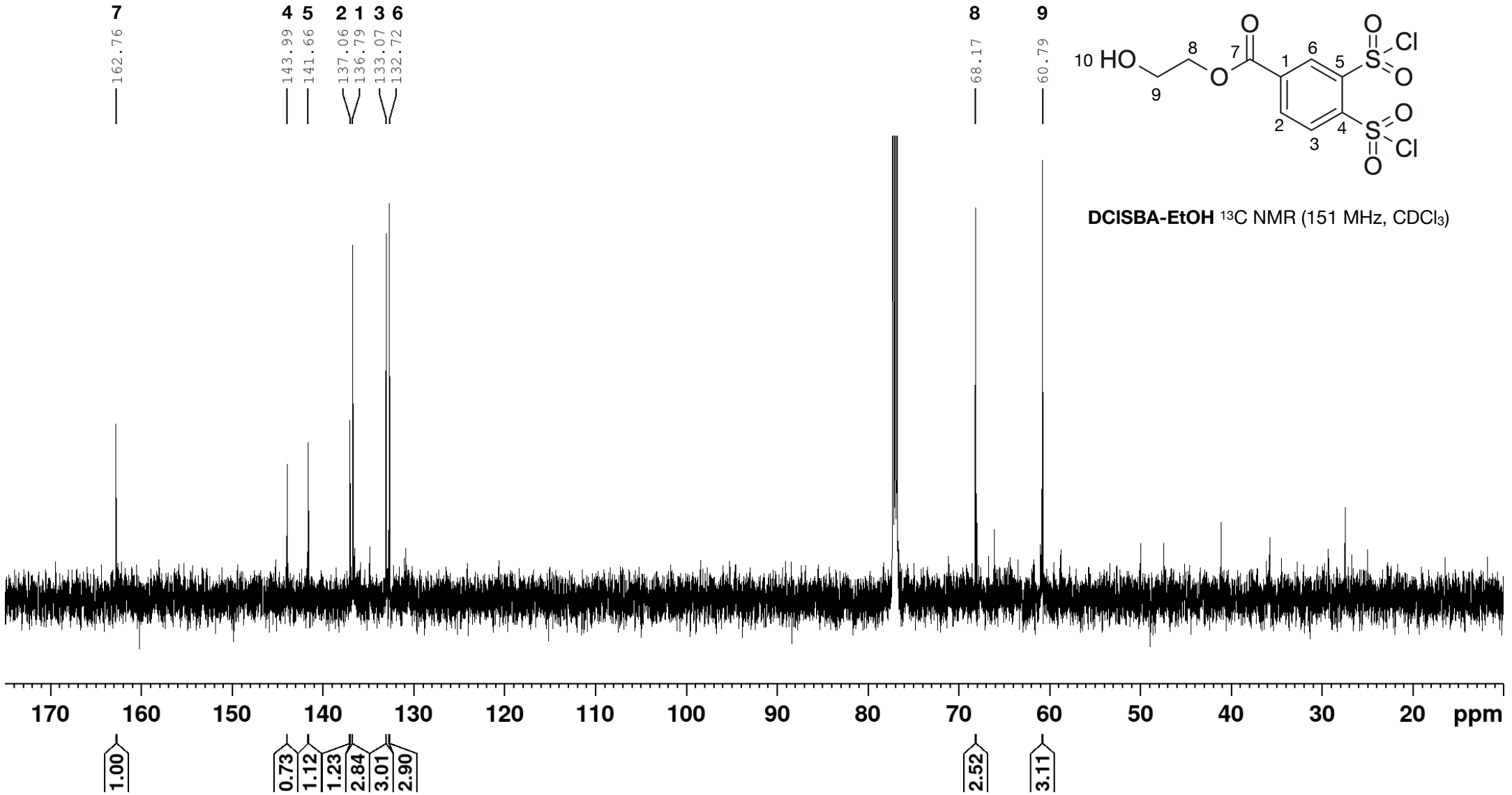

DClSBA-EtOH ^{13}C NMR (151 MHz, $CDCl_3$)

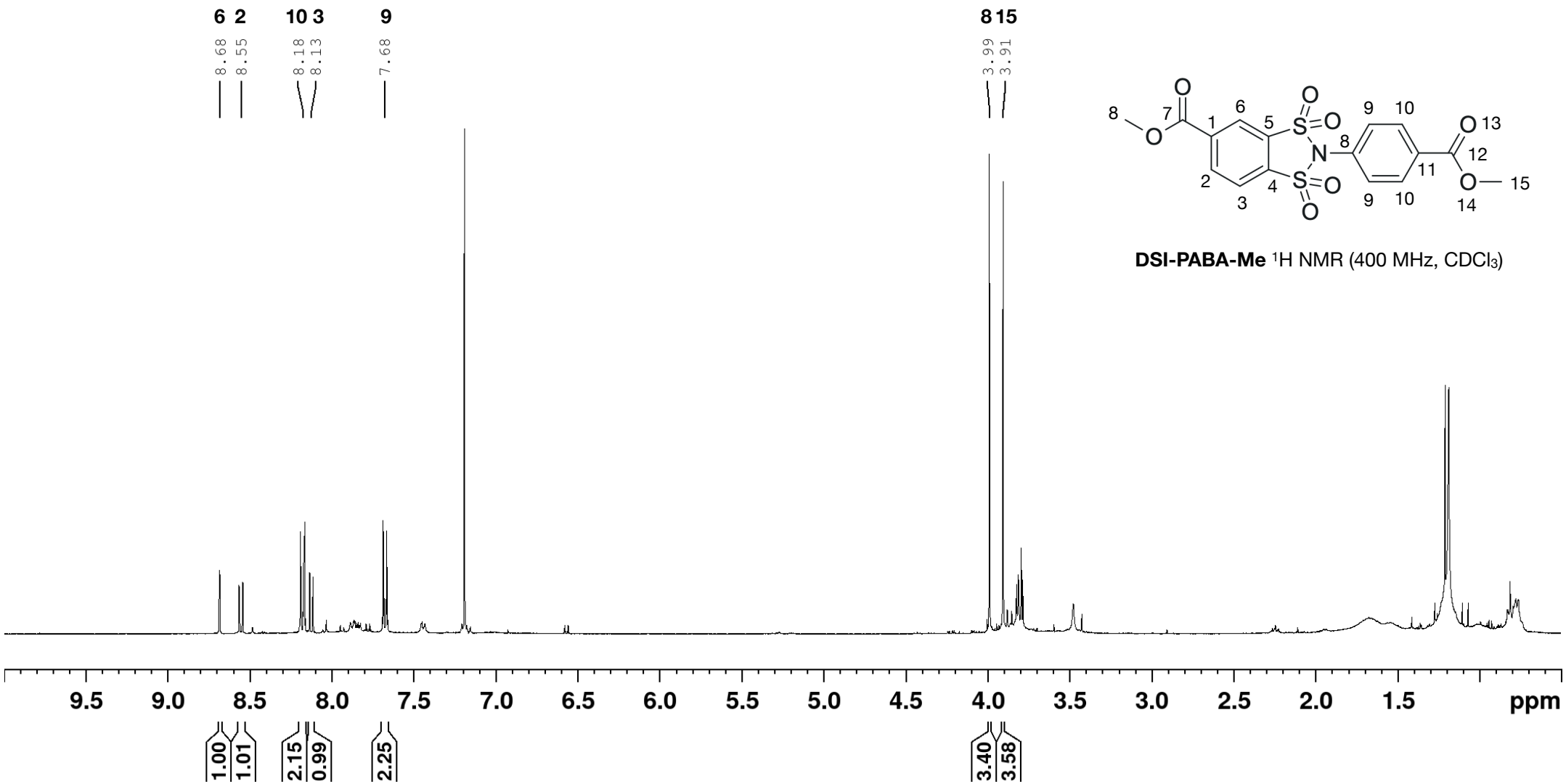

DSI-PABA-Me ^{1}H NMR (400 MHz, $CDCl_3$)

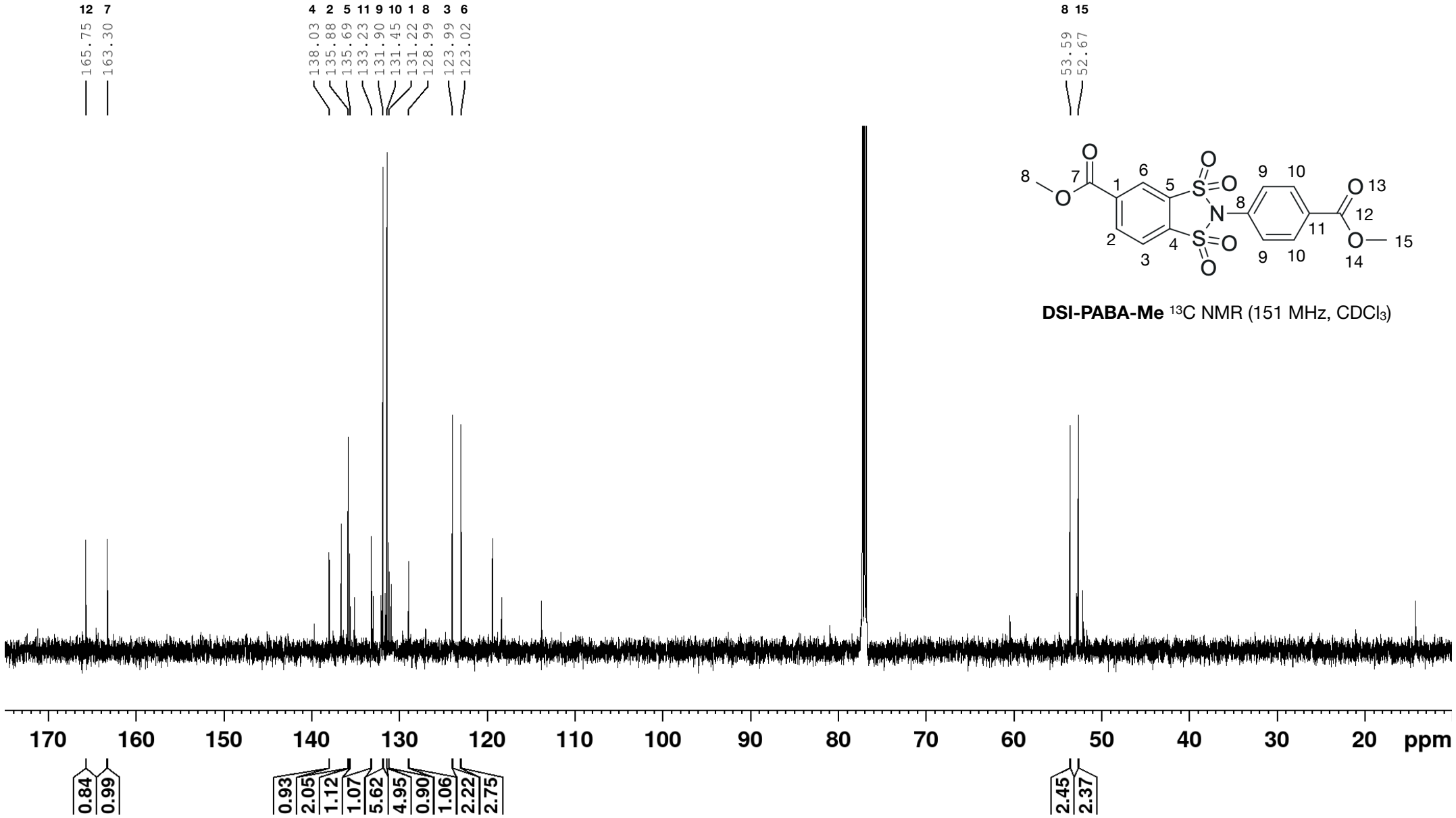

DSI-PABA-Me ^{13}C NMR (151 MHz, $CDCl_3$)

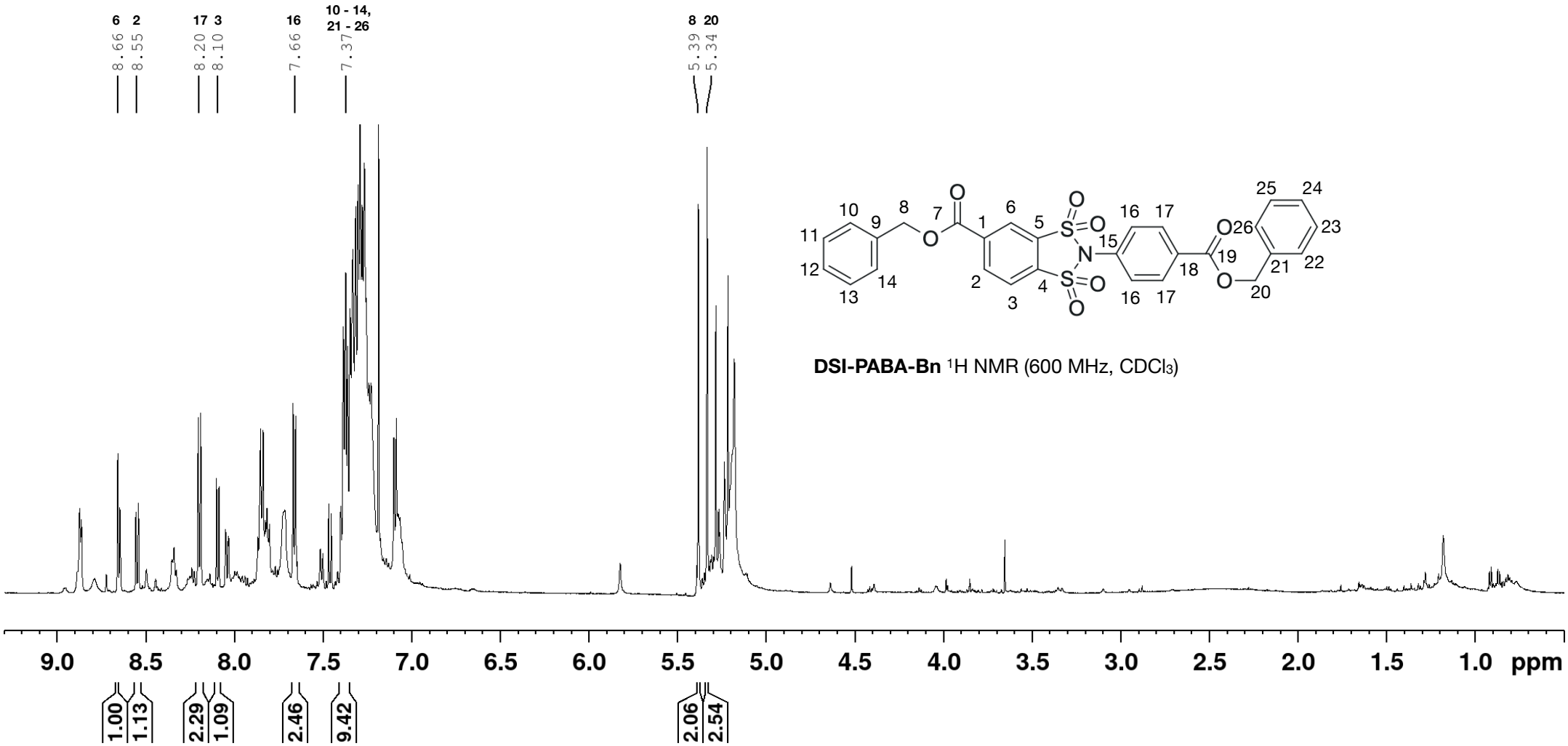

DSI-PABA-Bn ^{1}H NMR (600 MHz, $CDCl_3$)

DSI-PABA-Bn 13C

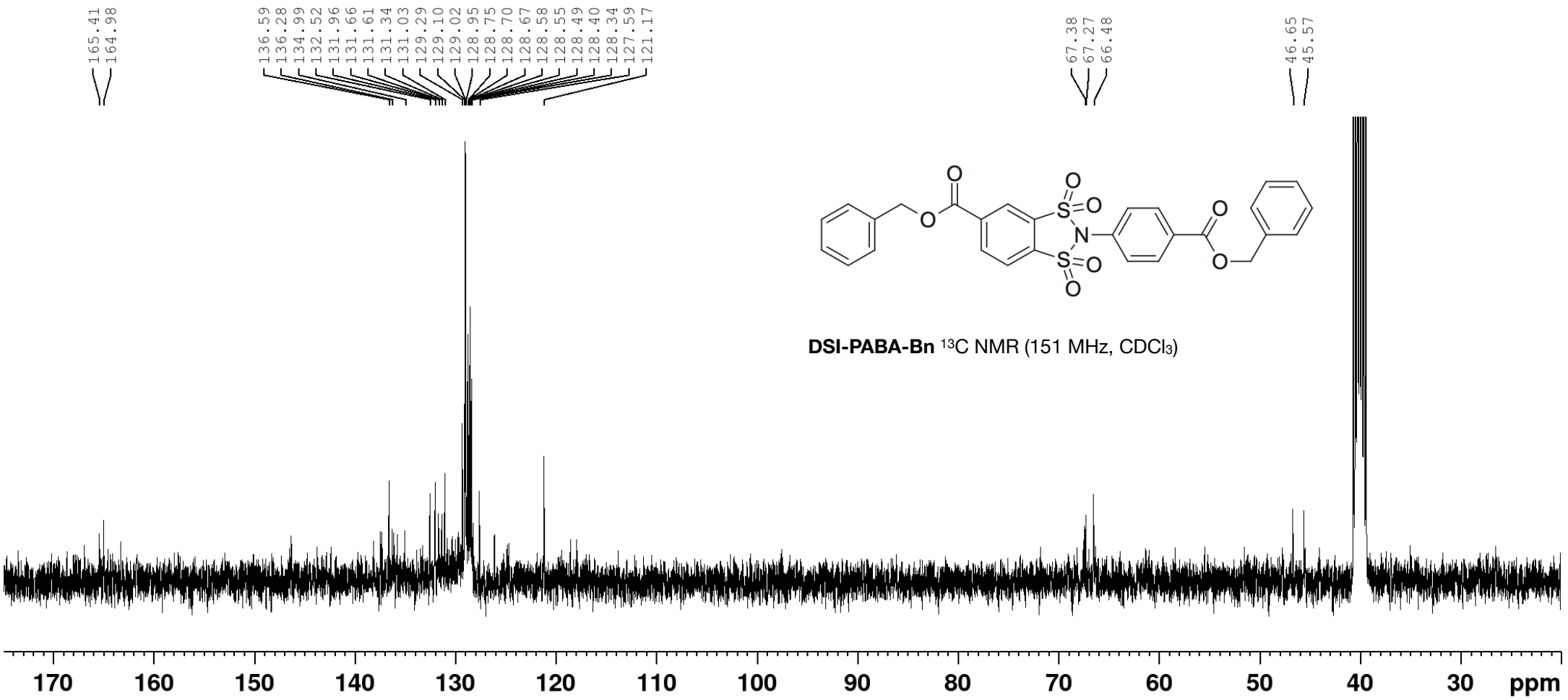

DSI-PABA-Bn ^{13}C NMR (151 MHz, $CDCl_3$)

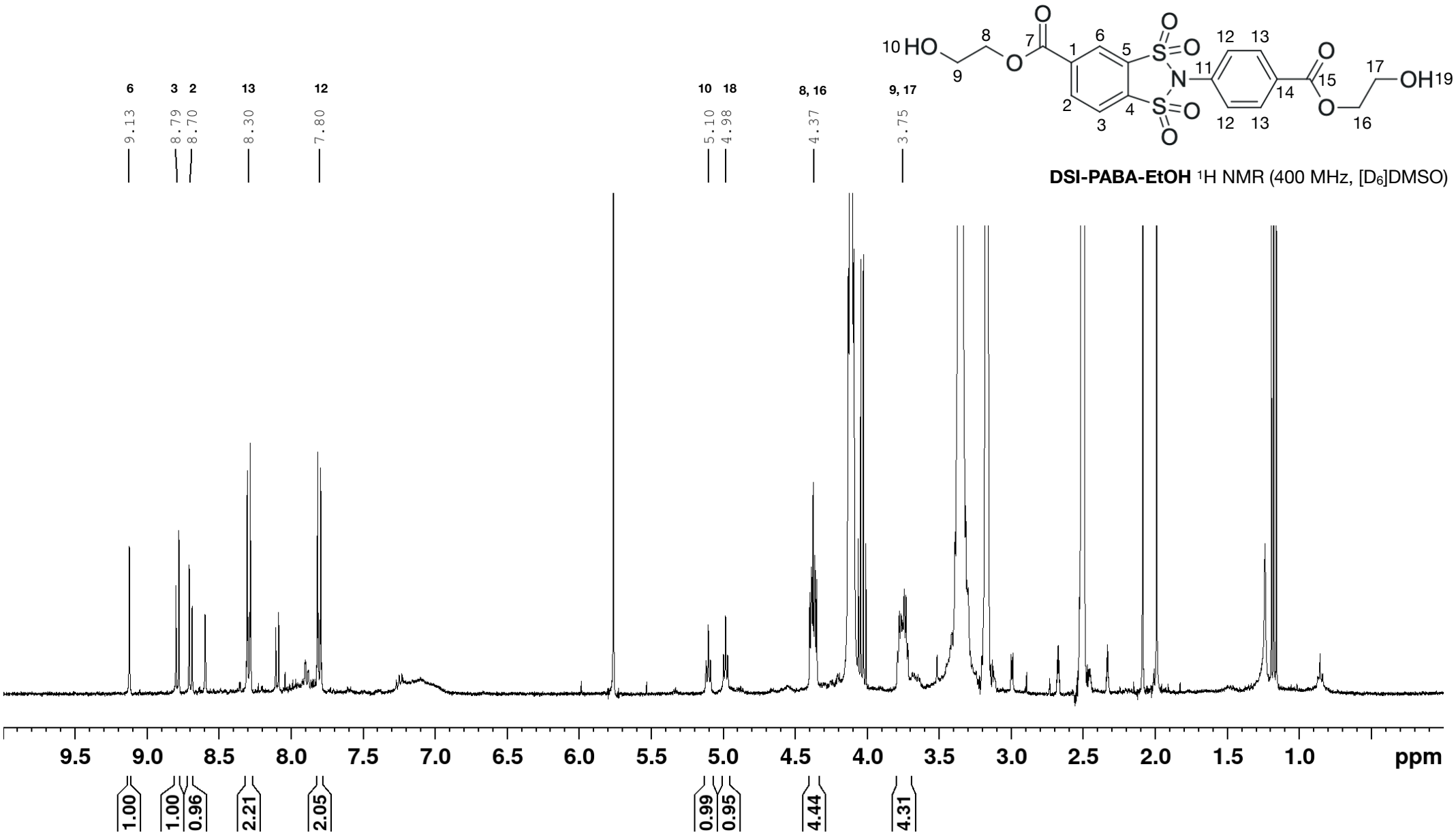

DSI-PABA-EtOH ^{1}H NMR (400 MHz, [D$_6$]DMSO)

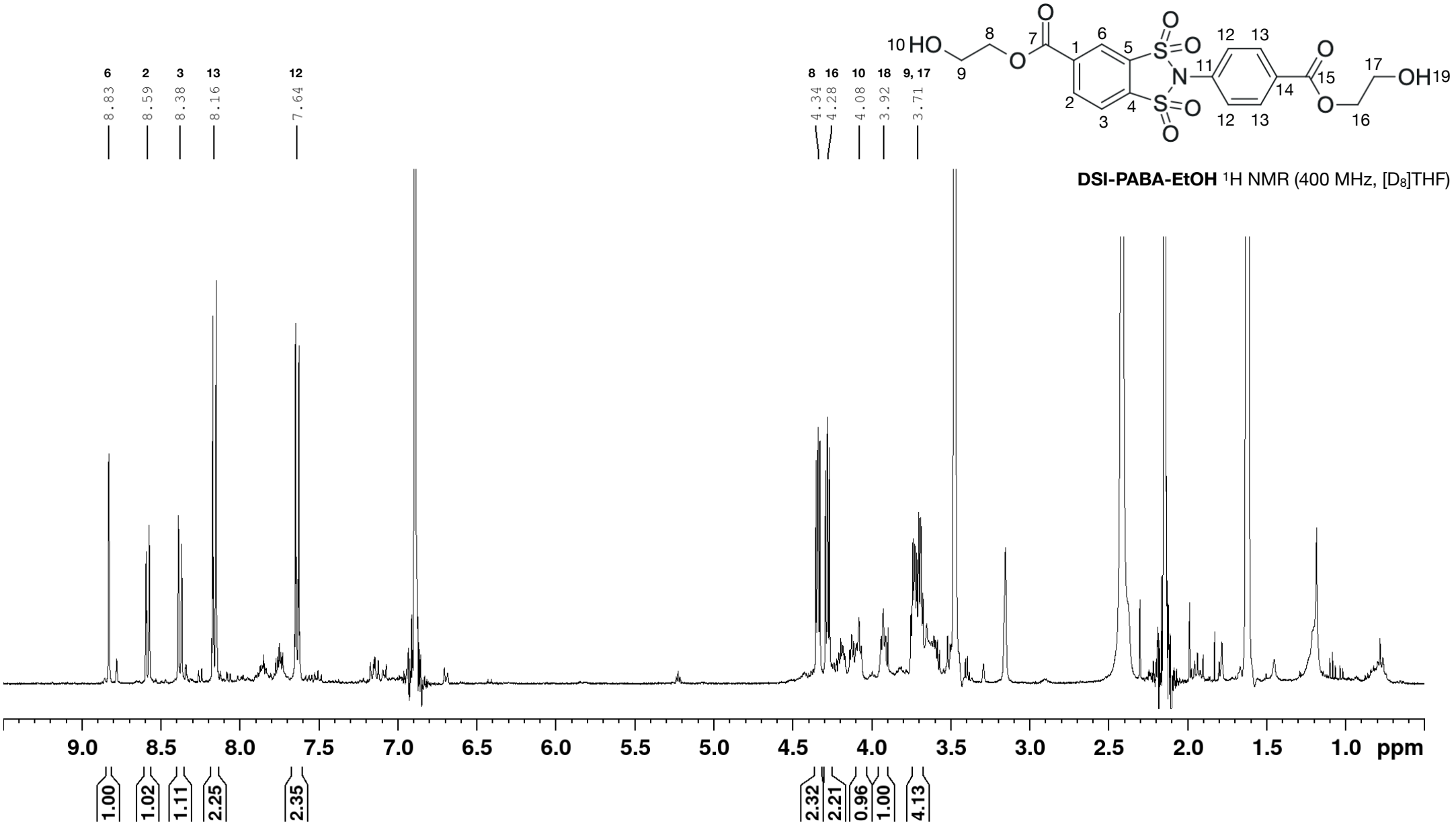
6 2 3 13 12
8.83 8.59 8.38 8.16 7.64
8 16 10 18 9, 17
4.34 4.28 4.08 3.92 3.71
10 HO 8 O 7 O 1 6 5 S O N S O 11 12 13 12 13 14 O 15 O 17 OH 19 2 3 4 O 9 16
DSI-PABA-EtOH 1H NMR (400 MHz, [D8]THF)
9.0 8.5 8.0 7.5 7.0 6.5 6.0 5.5 5.0 4.5 4.0 3.5 3.0 2.5 2.0 1.5 1.0 ppm
1.00 1.02 1.11 2.25 2.35 2.32 2.21 0.96 1.00 4.13

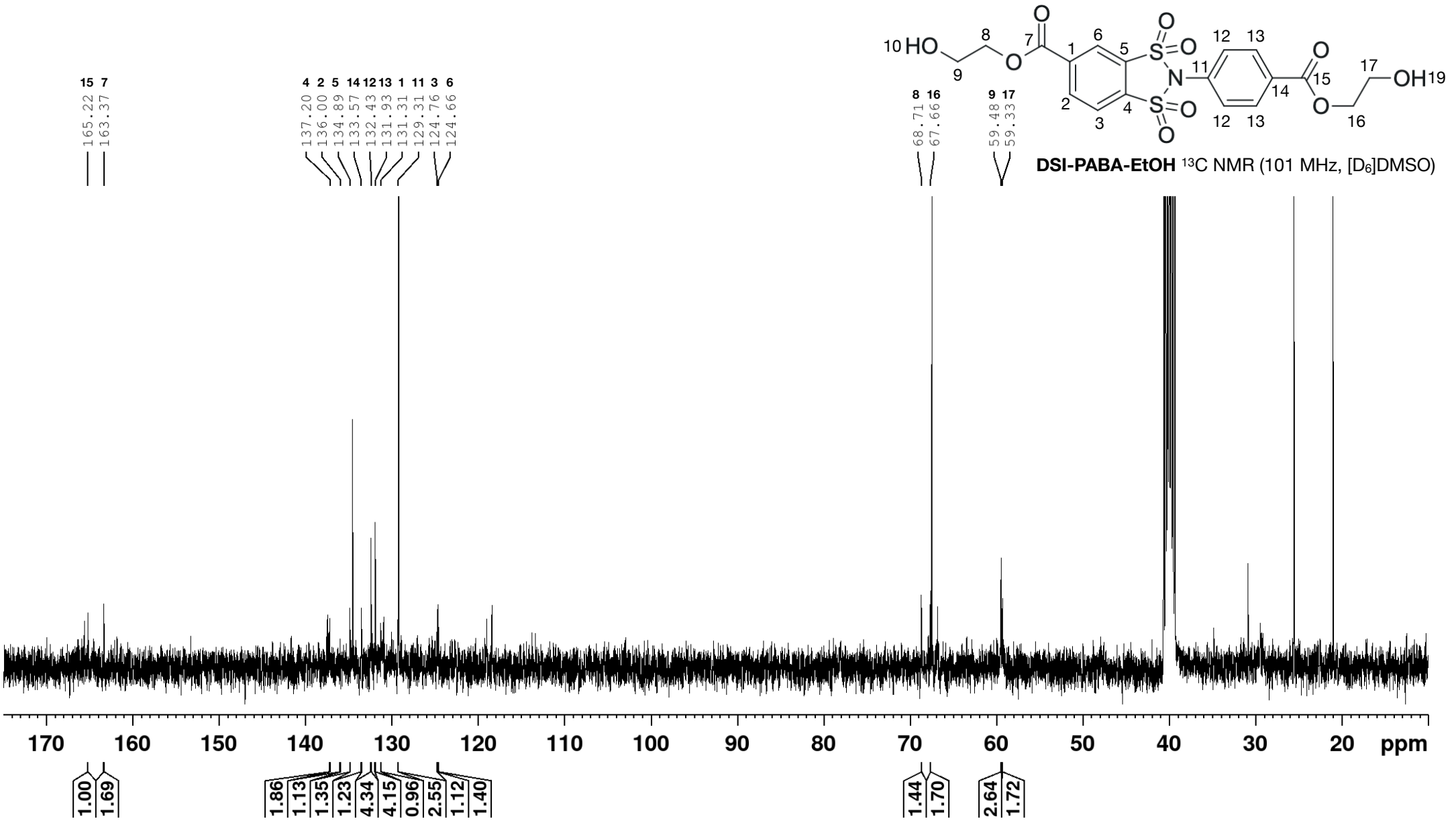
15 7
165.22
163.37
4 2 5 14 12 13 1 11 3 6
137.20
136.00
134.89
133.57
132.43
131.93
131.31
129.31
124.76
124.66
8 16
68.71
67.66
9 17
59.48
59.33
10 HO
OH 19
DSI-PABA-EtOH 13C NMR (101 MHz, [D6]DMSO)
170 160 150 140 130 120 110 100 90 80 70 60 50 40 30 20 ppm
1.00 1.69
1.86 1.13 1.35 1.23 4.34 4.15 0.96 2.55 1.12 1.40
1.44 1.70
2.64 1.72

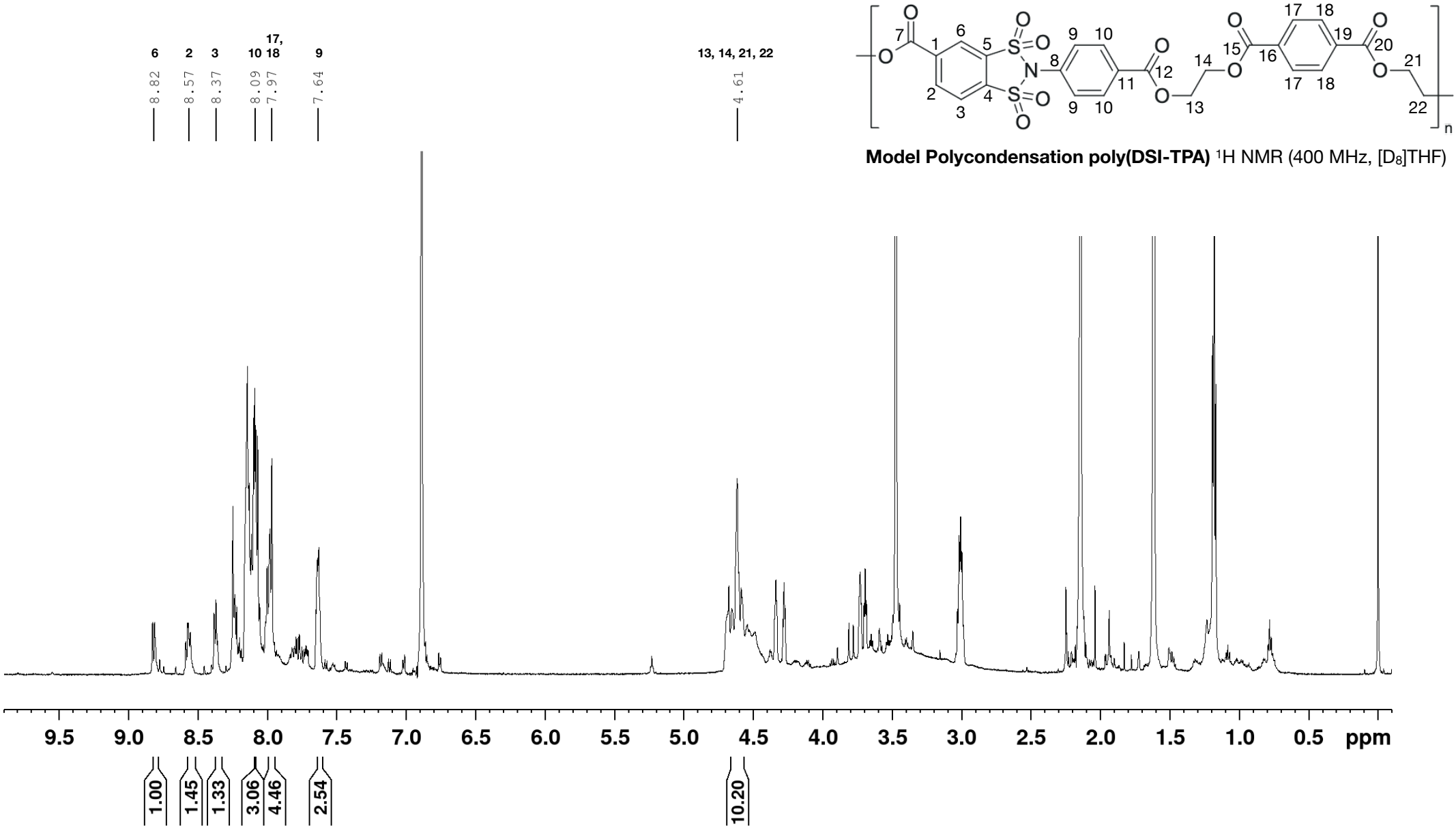

Model Polycondensation poly(DSI-TPA) ^{1}H NMR (400 MHz, [D_8]THF)

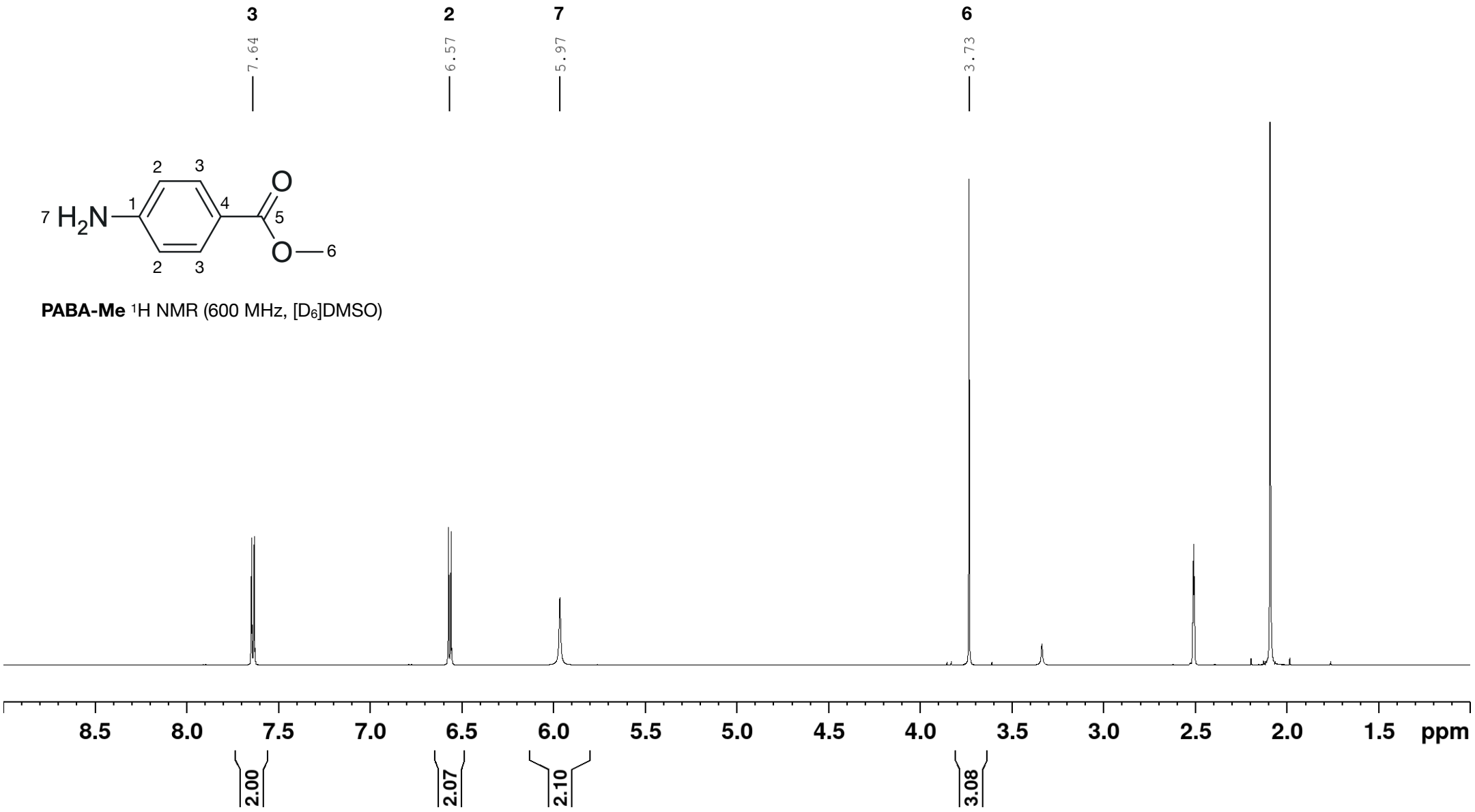

PABA-Me ^{1}H NMR (600 MHz, [D_6]DMSO)

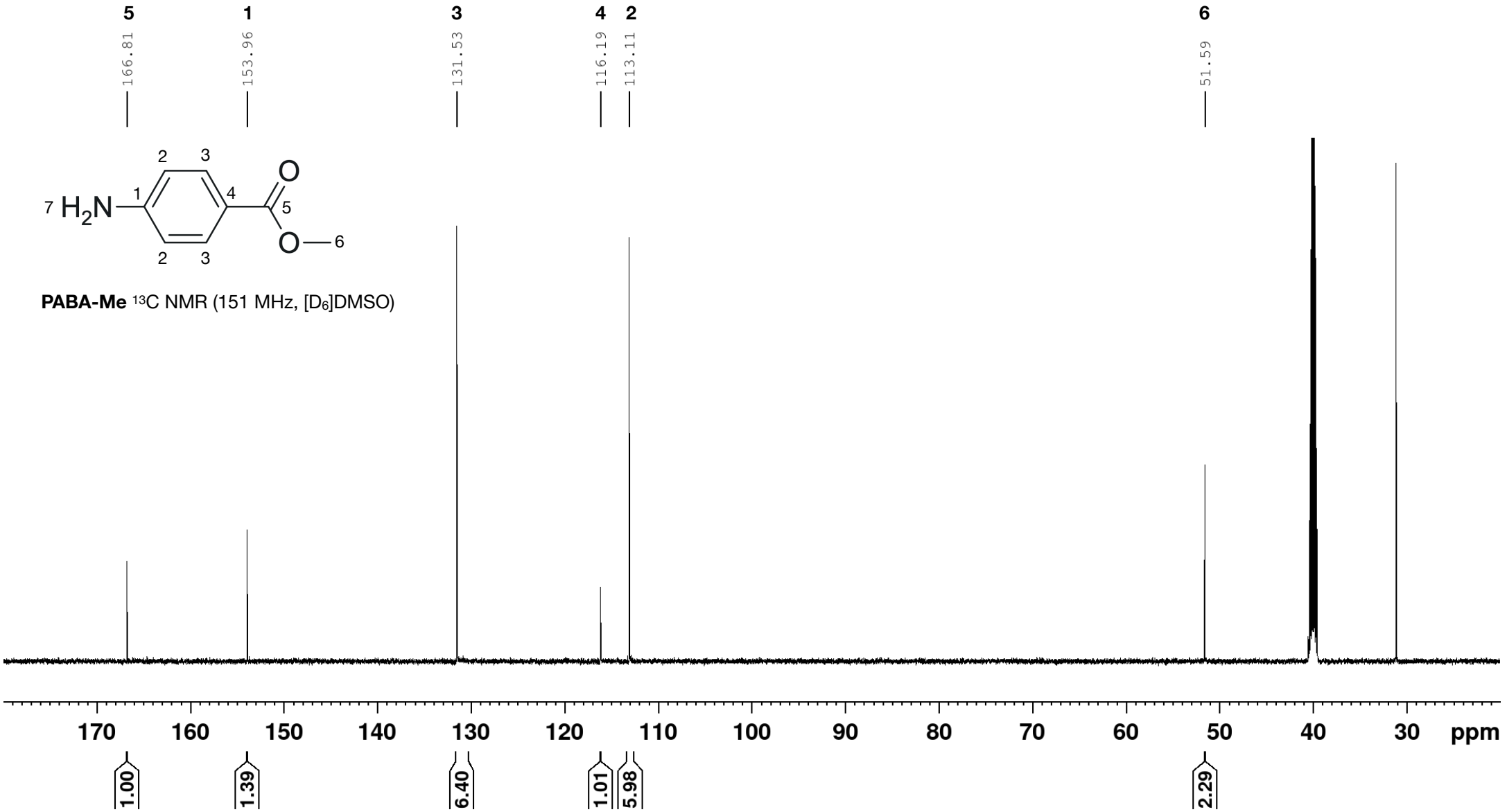

PABA-Me ^{13}C NMR (151 MHz, [D_6]DMSO)

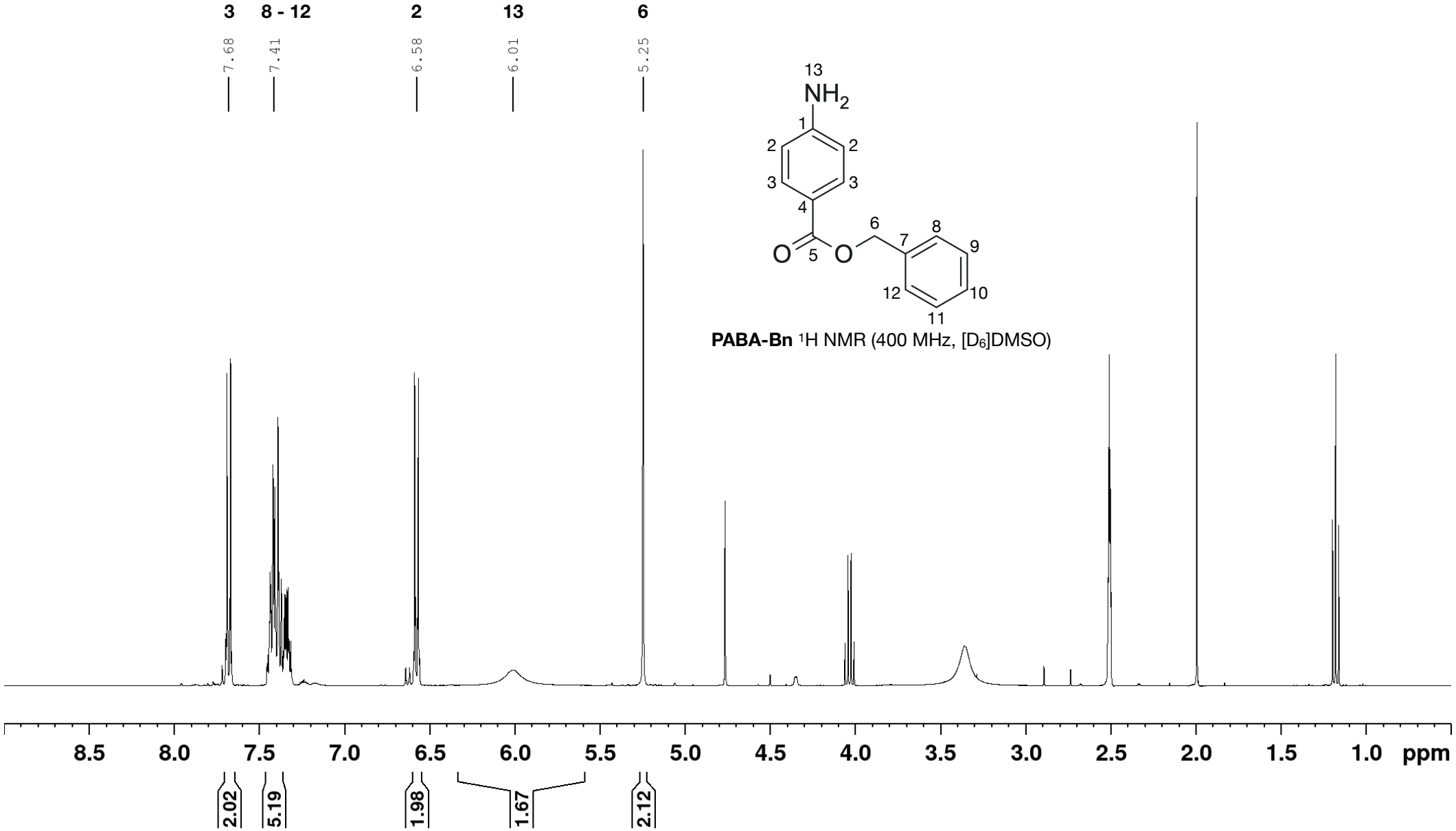

PABA-Bn ^{1}H NMR (400 MHz, [D_6]DMSO)

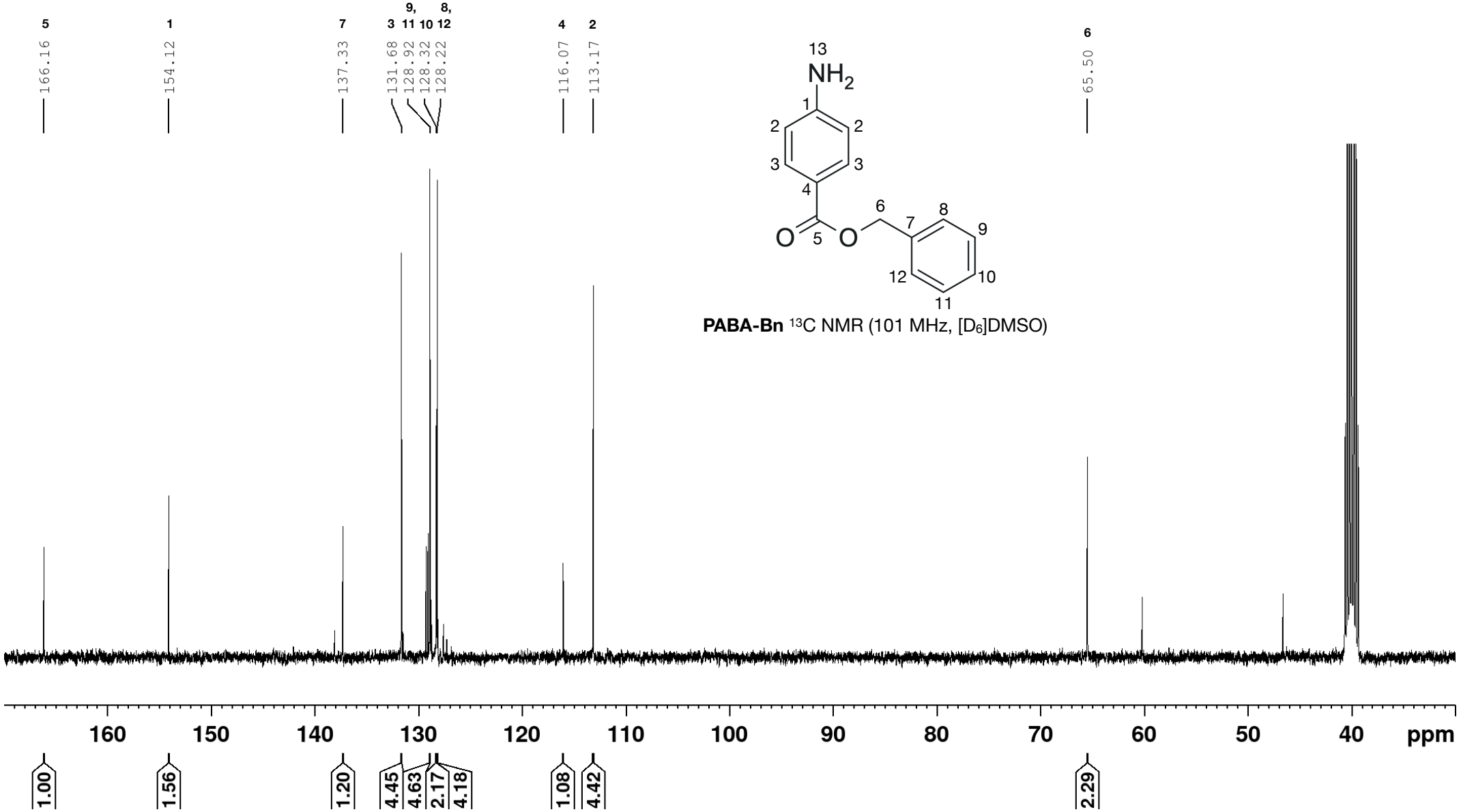

PABA-Bn ^{13}C NMR (101 MHz, [D$_6$]DMSO)

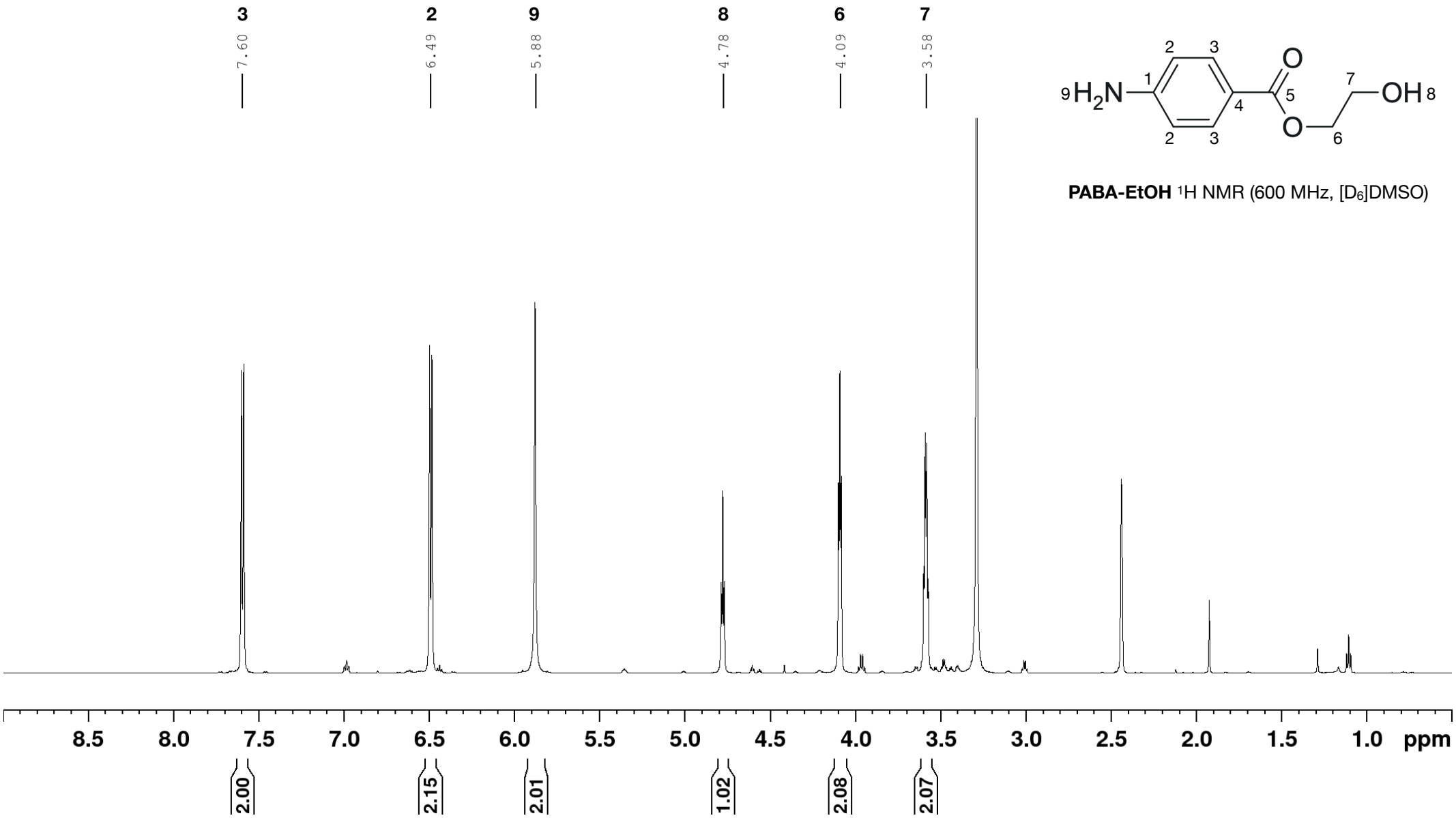

PABA-EtOH ^{1}H NMR (600 MHz, [D_6]DMSO)

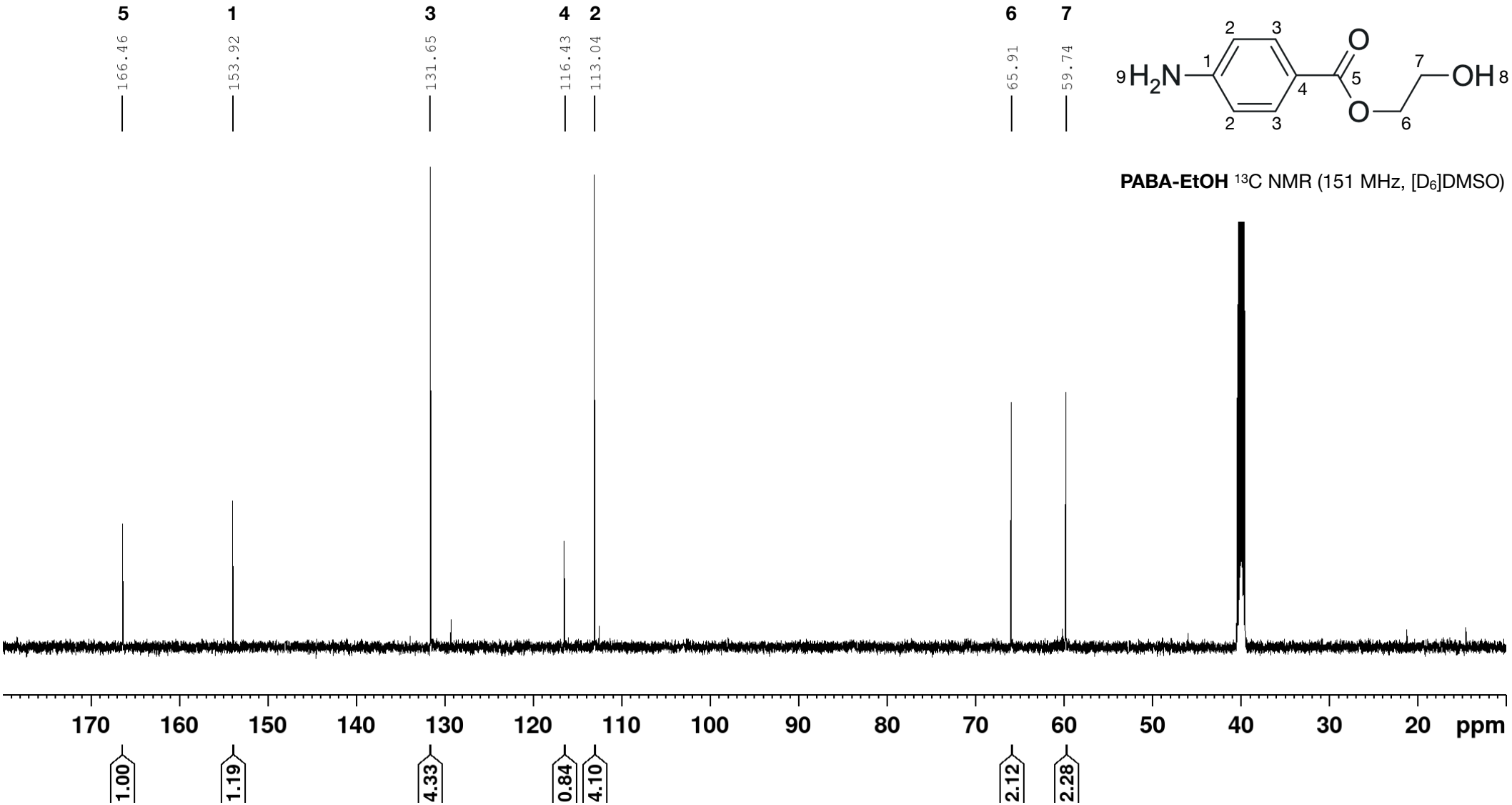
5
166.46
1
153.92
3
131.65
4
116.43
2
113.04
6
65.91
7
59.74
9H2N
OH8
PABA-EtOH 13C NMR (151 MHz, [D6]DMSO)
170
160
150
140
130
120
110
100
90
80
70
60
50
40
30
20
ppm
1.00
1.19
4.33
0.84
4.10
2.12
2.28

BDTCA (^{1}H - ^{13}C HMBC)

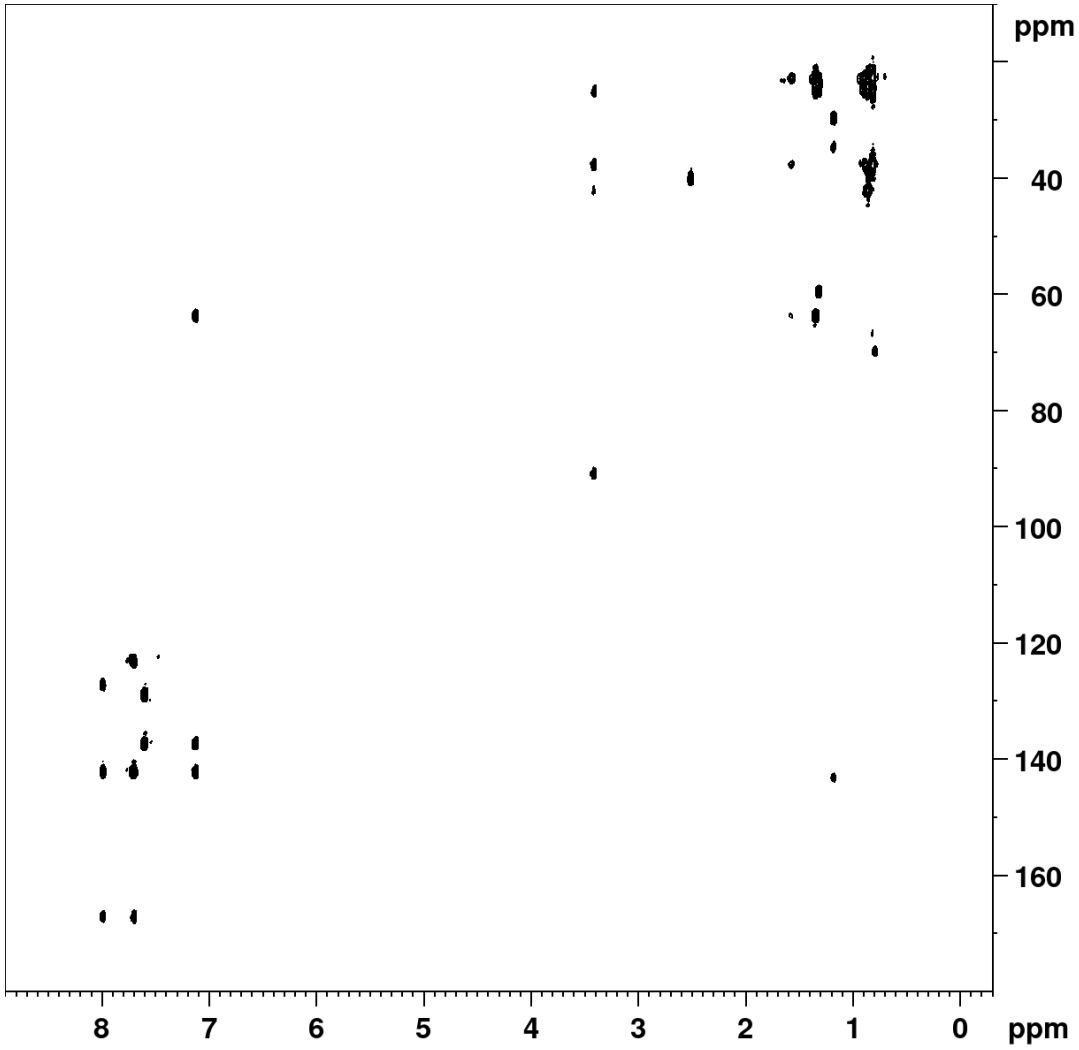

BDTCA (^{1}H - ^{13}C HSQC)

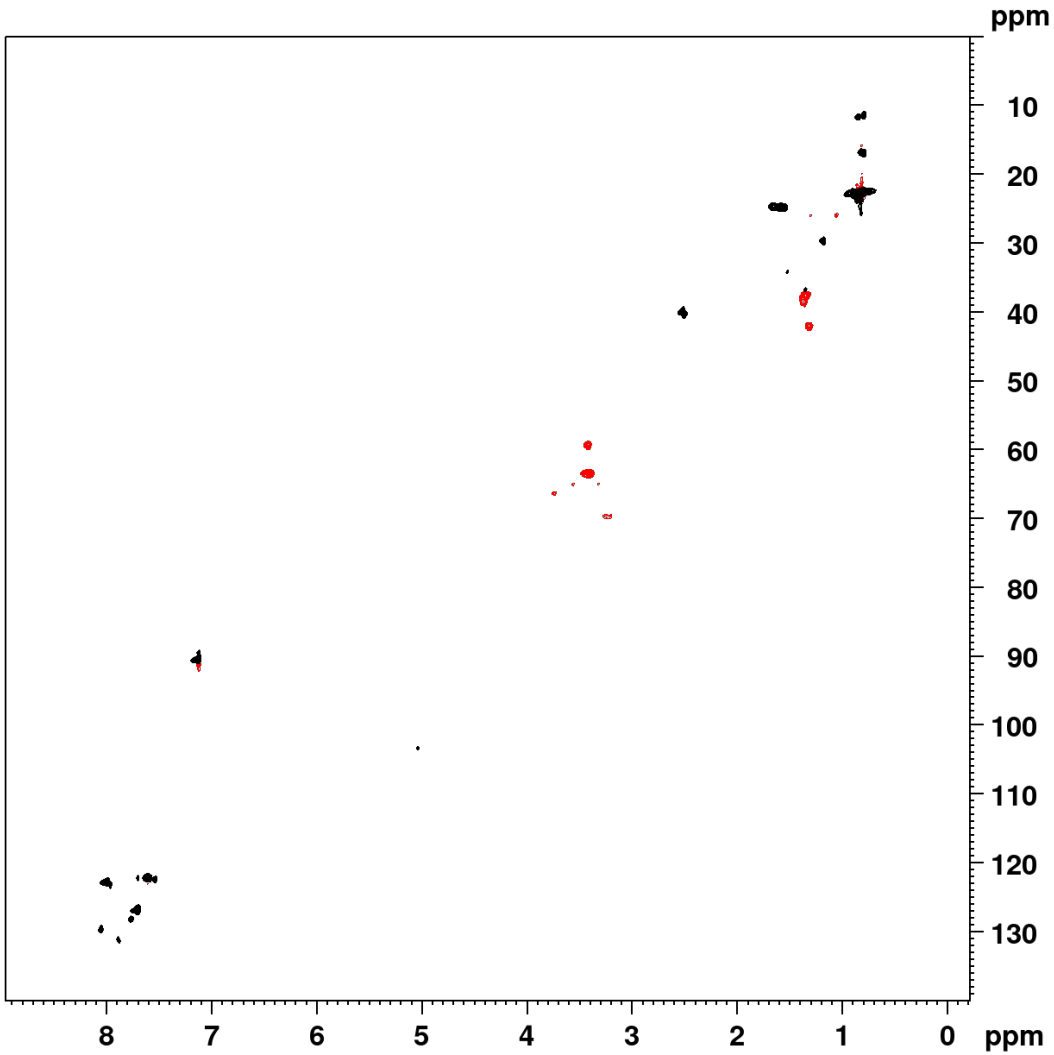

BDTCA-Me (^{1}H - ^{13}C HMBC)

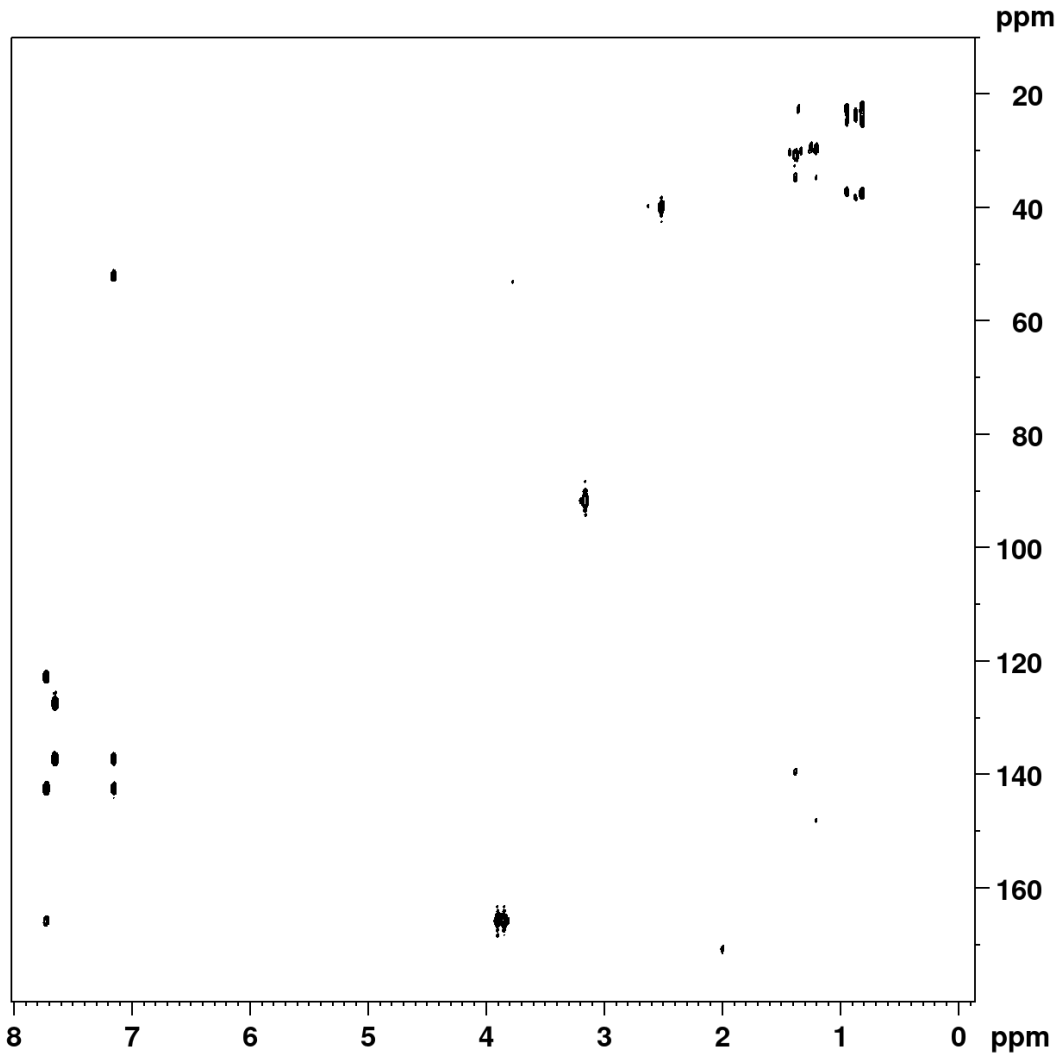

BDTCA-Bn (^{1}H - ^{13}C HMBC)

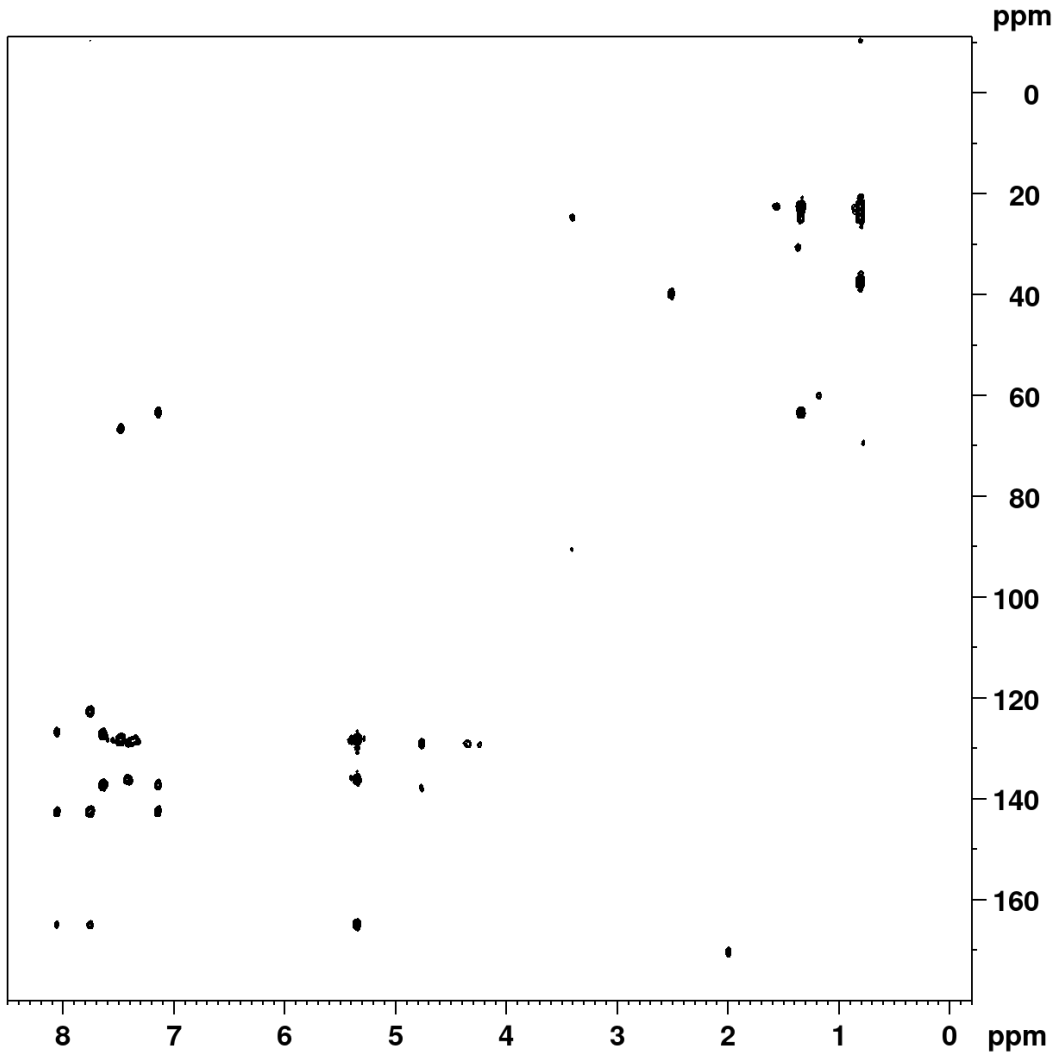

DClSBA-Me (^{1}H - ^{13}C HMBC)

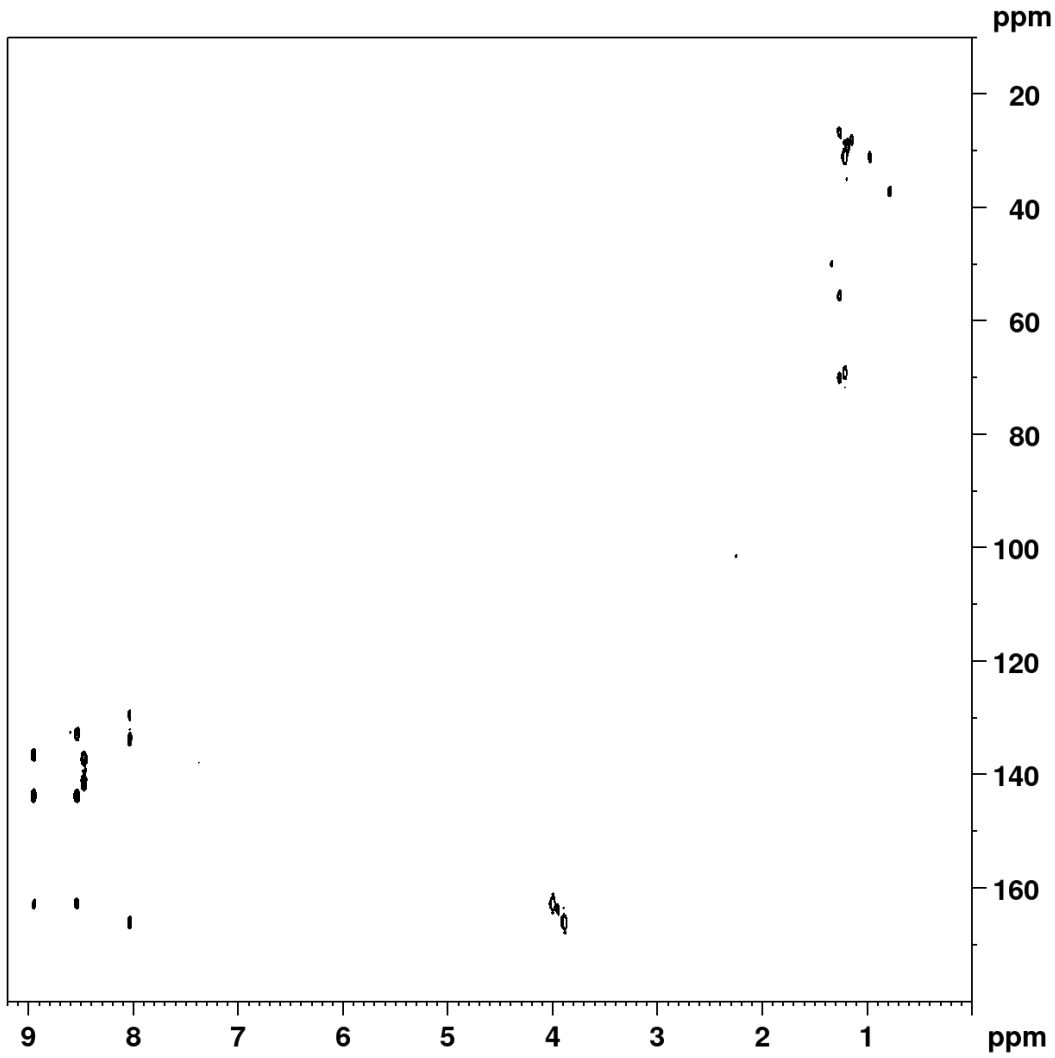

DClSBA-Bn (^{1}H - ^{13}C HMBC)

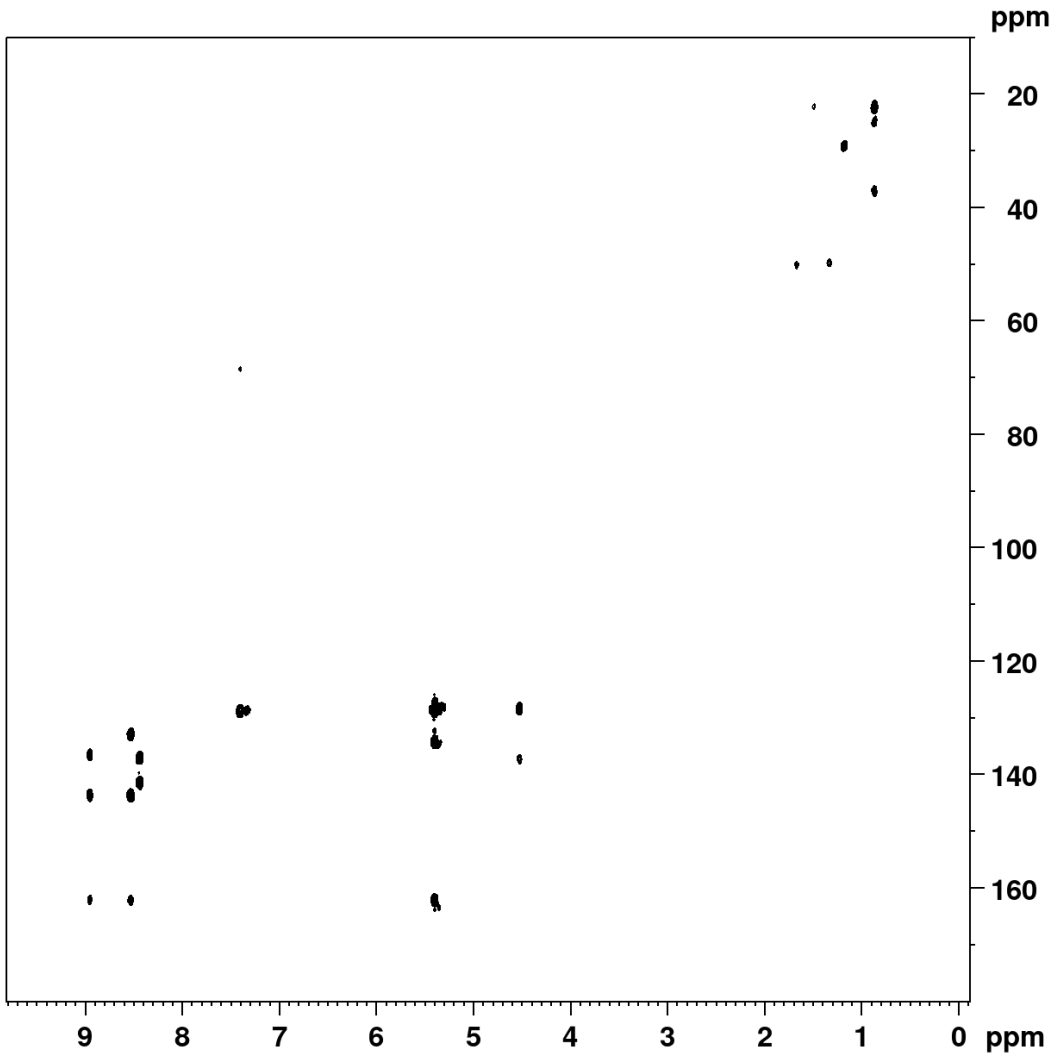

DClSBA-EtOH (^{1}H - ^{13}C HMBC)

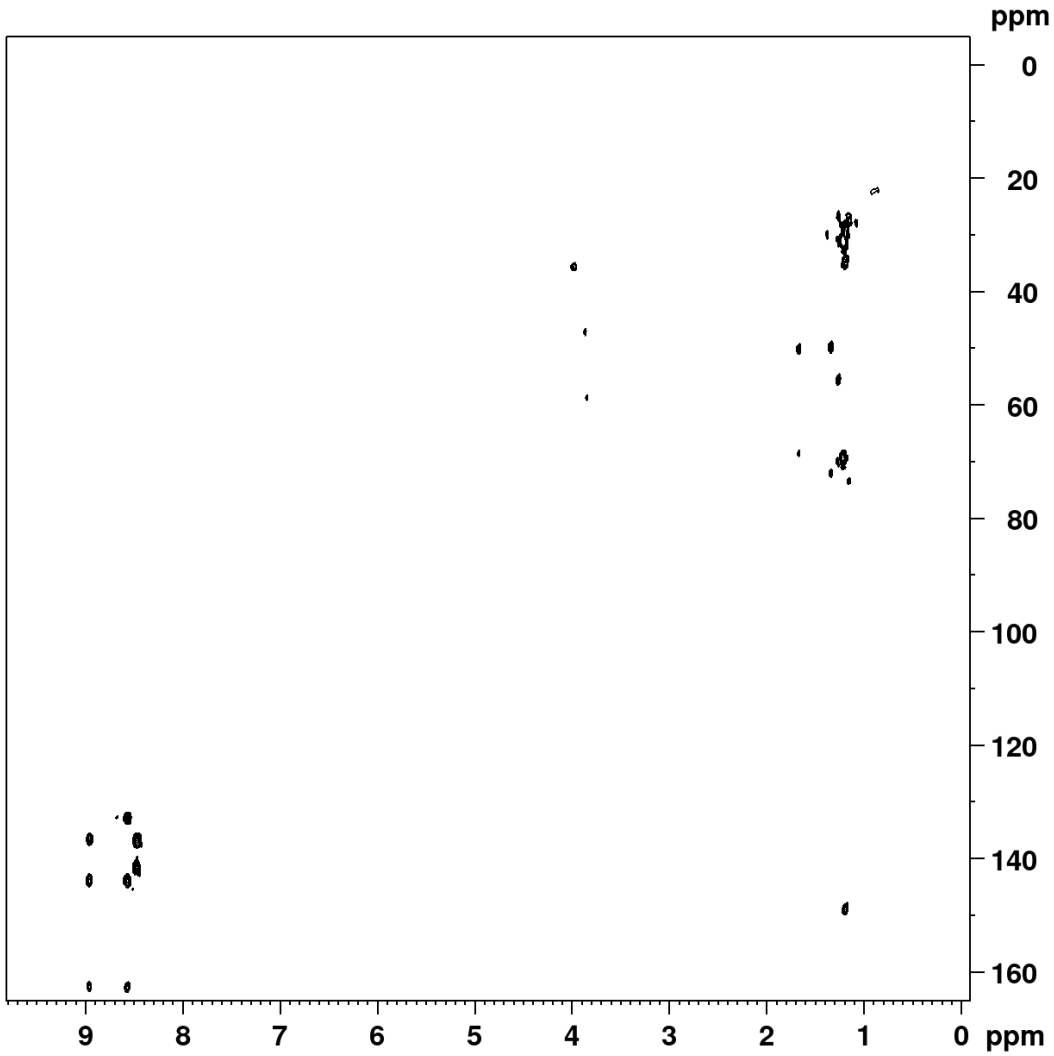

DSI-PABA-Me (^{1}H - ^{13}C HMBC)

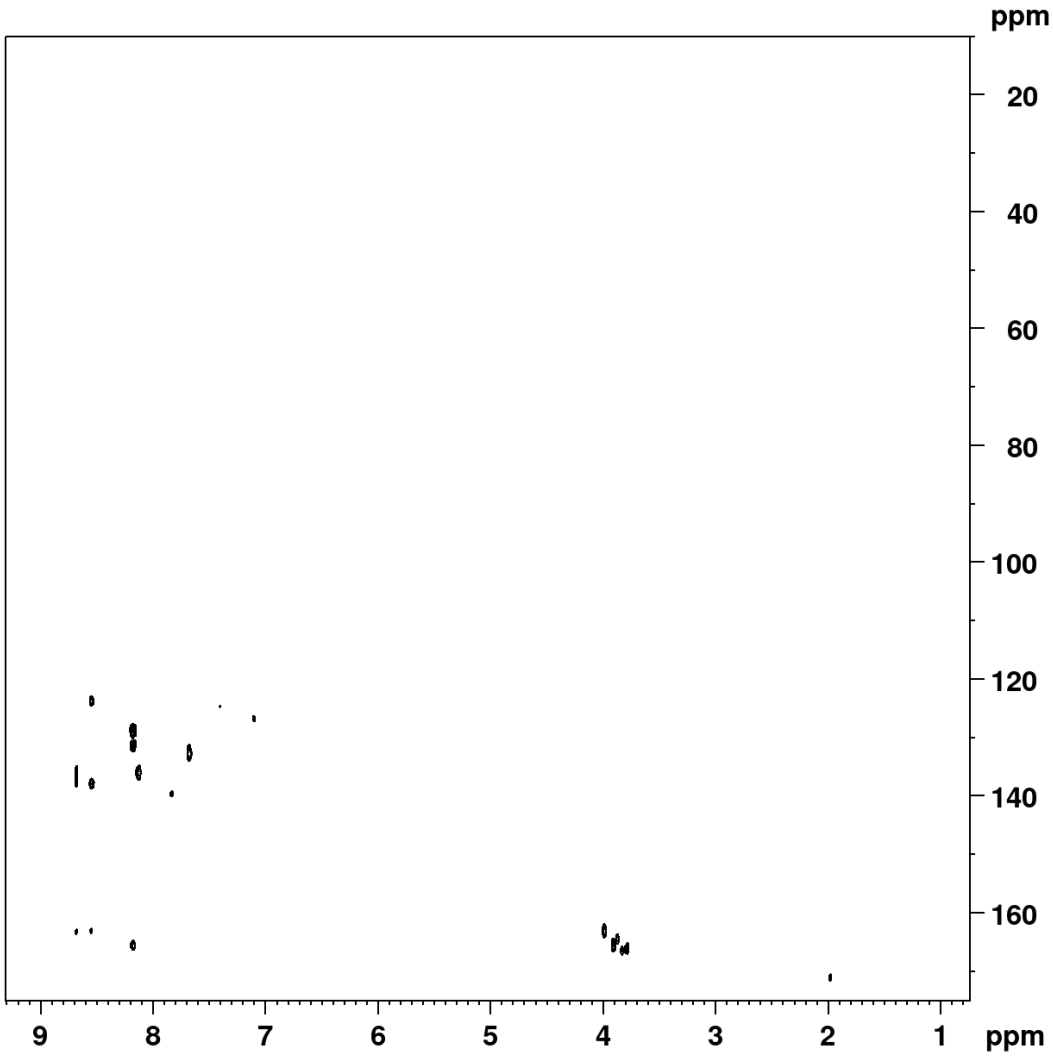

DSI-PABA-Bn (^{1}H - ^{13}C HMBC)

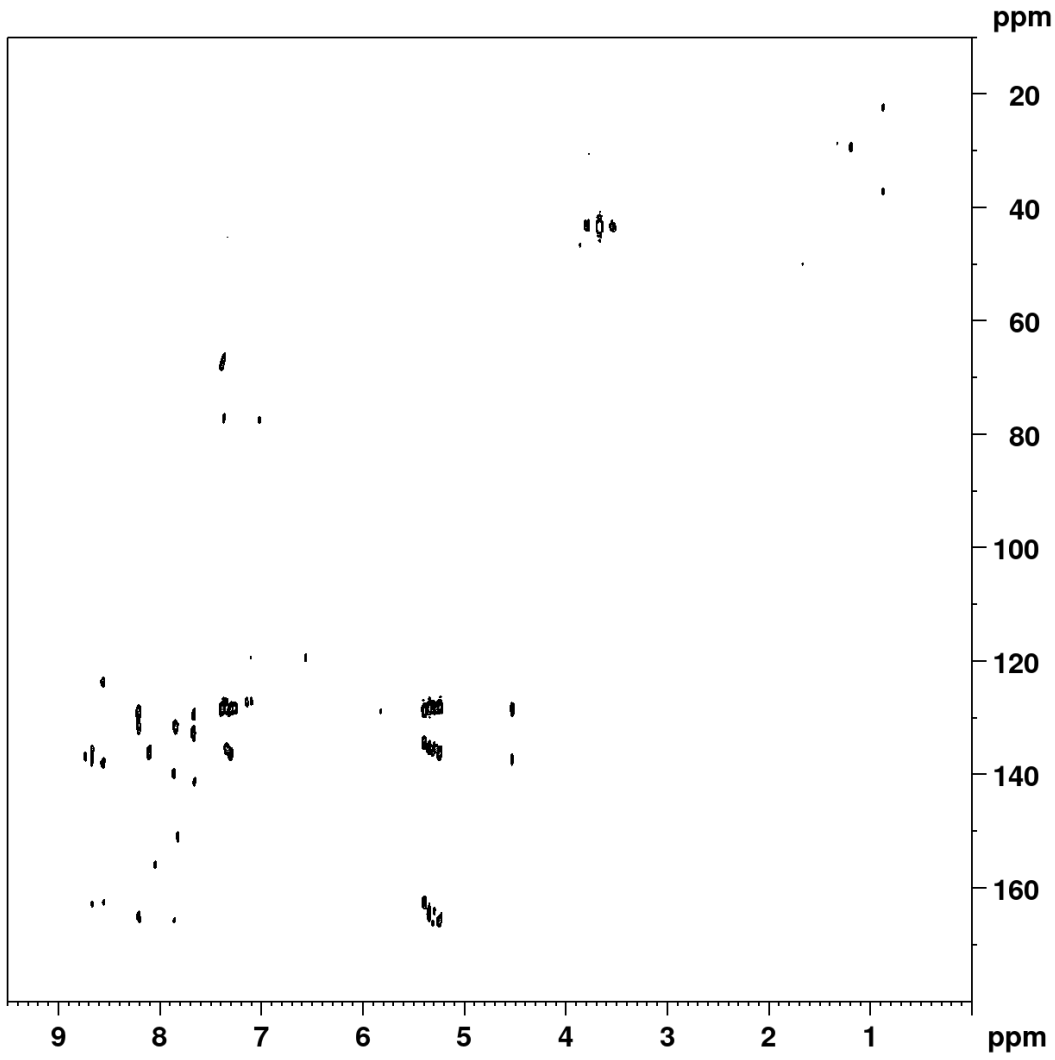

DSI-PABA-EtOH (^{1}H - ^{13}C HMBC)

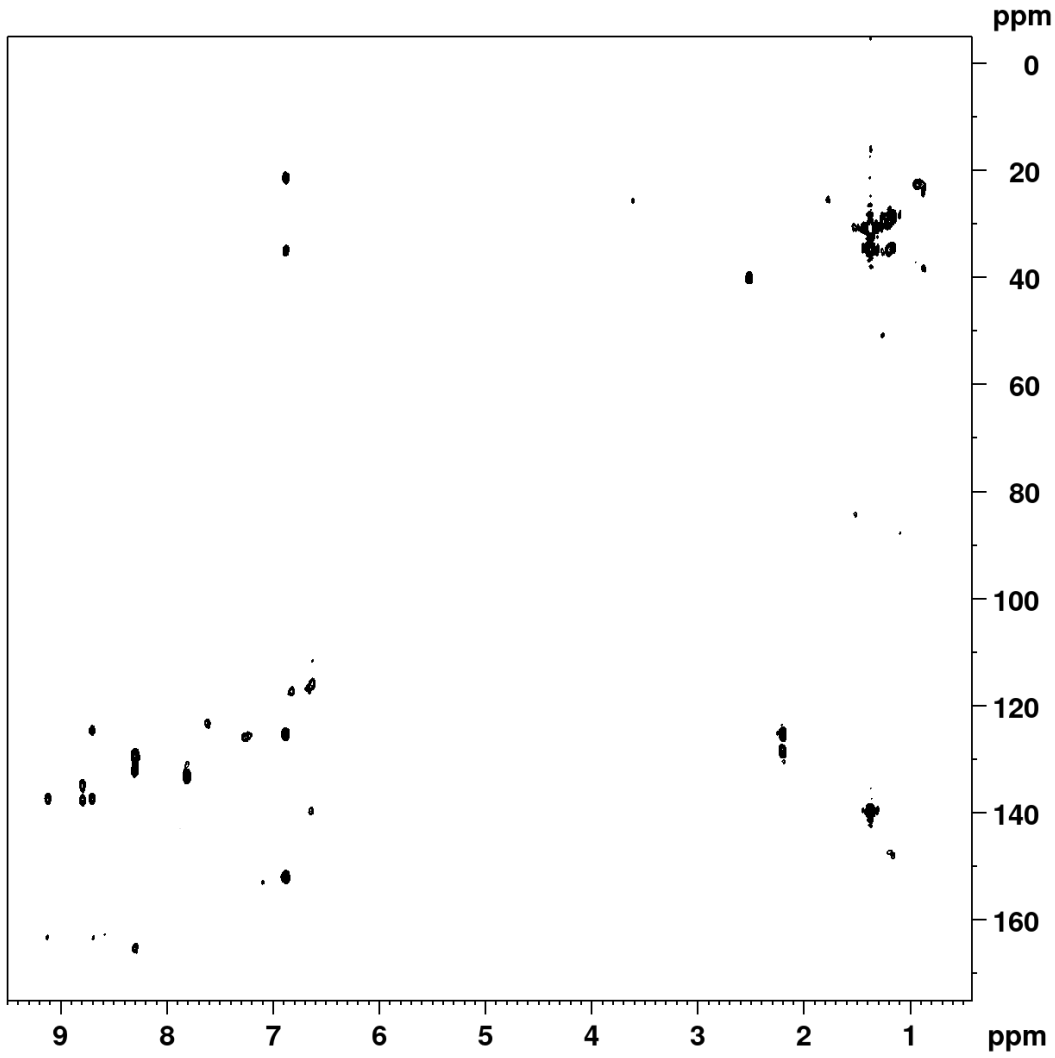

Model Polycondensation poly(DSI-TPA) (^{1}H - ^{13}C HMBC)